



# UNIVERSITÉ DE LILLE

École doctorale  
**Sciences de la Matière, du Rayonnement et de l'Environnement (SMRE)**

Unité de recherche  
**Laboratoire de Physique des Lasers, Atomes et Molécules (PhLAM)**

**Thèse de doctorat**  
**Sensibilité de cellules cancéreuses au stress oxydatif:**  
**Approche systémique pour étudier le couplage**  
**entre le métabolisme et le stress oxydatif**

Mémoire préparé par DANA SIMIUC  
en vue de l'obtention du grade de Docteur en Physique  
Spécialité: Milieux Dilués et Optique Fondamentale

Thèse soutenue le 17 Decembre 2020 devant le jury:

Marie ERARD	Rapporteuse	Université Paris-Sud, France
Miklós GEISZT	Rapporteur	Université Semmelweis, Budapest, Hongrie
Xuefen Le BOURHIS	Examinatrice	Université de Lille, France
Cristian FOCSA	President du jury	Université de Lille, France
Christophe COLLEONI	Examineur	Université de Lille, France
Tudor LUCHIAN	Examineur	Université de Iasi Alexandru Ioan Cuza, Roumanie
Stéphane GUYOT	Examineur	Université de Bourgogne Franche-Comté, France
Emmanuel COURTADE	Directeur de thèse	Université de Lille, France



## UNIVERSITY OF LILLE

Doctoral School  
**Science of Matter, Radiation and Environment (SMRE)**

Research Unit  
**Laboratory of Physics of Lasers, Atoms and Molecules (PhLAM)**

### PHD DISSERTATION

The sensitivity of cancer cells to oxidative stress: systemic approach to study the interplay between metabolic flux and oxidative stress

Manuscript prepared by Dana SIMIUC  
in order to obtain the degree of Doctor of Physics  
Specialty Dilute Media and Fundamental Physics

These defended on 17<sup>th</sup> of December 2020 in front of the jury:

Marie ERARD	Reviewer	Paris-Sud University, France
Miklós GEISZT	Reviewer	Semmelweis University, Budapest, Hungary
Xuefen Le BOURHIS	Examiner	University of Lille, France
Cristian FOCSA	President of the jury	University of Lille, France
Christophe COLLEONI	Examiner	University of Lille, France
Tudor LUCHIAN	Examiner	Alexandru Ioan Cuza University of Iasi, Romania
Stéphane GUYOT	Examiner	University of Burgundy Franche-Comté, France
Emmanuel COURTADE	Director of thesis	University of Lille, France

## Acknowledgments

*Alone, we can do so little;  
together we can do so much.*  
Helen Keller

This work is performed in the biophysics group of stress and many colleagues contributed to it. I take this opportunity to thank to all of them for helping me to start my research career, providing encouragements and helping me to become the person I am today.

I would like to acknowledge to jury members, Marie Erard and Miklós Geiszt for kindly accepting to review my work and to Xuefen Le Bourhis, Stéphane Guyot, Christophe Colleoni, Cristian Focsa, Tudor Luchian for accepting my thesis evaluation.

My team is involved in multidisciplinary research and all members brought significant contribution to my project. Alexandra Pruvost, Raoul Torero carefully introduced me to biochemistry techniques, Quentin Thommen, Benjamin Pfeuty often provided advices and criticism guidance for advancing in this work, Jean Pesez and Anthony Treizebre creatively used their engineer skills to help me building devices in the lab. Working closely with François Anquez, I want to thank him for his contribution in data processing, his interest and implication in my project.

I am grateful to my director of thesis Emmanuel Courtade for adopting me in his team. His passion for science and his didactic character inspired me and helped me to improve my contribution on this project. Thank you for your kindness and patience in supervising my work and for all your time dedicated to my PhD training.

Thank to Gilbert Martinelli for his advices and support provided during my teaching experience. Your trust and encouragements helped me to enjoy being in front of students and to share my passion for science with them.

My office colleagues: Mohamed, Helene, Majid, Darka, Marine, Anna, Tobias, Alexey, Quentin, David, Fatima were in charge of my well-being during my training and I want to thank them for their encouragements and friendly support provided. Your good humor and your nonconformist characters made our office a cozy place. I am grateful to my colleague Sarah for biology discussions and support provided in electrochemistry techniques.

The availability and professionalism of electronic and mechanic departments helped me often to improve the experimental systems I used. I am also thankful to administration departments for their implication during the years, working in the shadow of this project, helping it to rise.

My modest research could not be possible without the support of many people who believed in me or in the potential of this project. Thank to my friends and family who were indirectly involved in this research.

Having my name on the first page of this manuscript is my today success I reached with the everyday patience and confidence of my brave life partner. Your love makes me a better human being.

## Resumé

Les cellules vivantes, lorsqu'elles sont constamment exposées au stress, sont capables de réagir de manière complexe en faisant intervenir divers réseaux de régulation intracellulaire. Leur régulation contrôle par exemple le devenir cellulaire en réponse à un stress oxydatif. Lorsque les mécanismes défensifs parviennent à faire face au stress, une rétroaction négative est impliquée et la cellule survit, sinon la cellule meurt. L'un des principaux mécanismes défensifs repose sur l'interaction entre le flux métabolique et le stress oxydatif, exploitant le rôle dualiste du peroxyde d'hydrogène, agissant à la fois comme une molécule de signalisation et de dommages.

Nos travaux visent à identifier les molécules clés impliquées dans le devenir cellulaire et à suivre leur dynamique au niveau de la cellule unique, à l'aide de la microscopie de fluorescence. Dans un premier temps, nous concevons un système expérimental inspiré des études de chimiotaxie pour contrôler en permanence la dose appliquée de peroxyde d'hydrogène ( $H_2O_2$ ) à la lignée cellulaire du cancer du sein (MCF7). Le choix de la méthode de stimulation joue un rôle important dans notre étude. En effet, afin de délivrer une concentration constante de stimulus aux cellules de mammifères, un milieu de culture cellulaire  $H_2O_2$  non réactif avec  $H_2O_2$  est choisi. En utilisant un système fluïdique, le taux de production intracellulaire de  $H_2O_2$  est contrôlé en faisant varier la concentration externe de  $H_2O_2$ . La délivrance et l'élimination du stimulus sont ainsi effectuées assez rapidement (plus rapidement que la consommation cellulaire) pour étudier les réponses cellulaires dynamiques.

Lors d'une stimulation constante, une dynamique d'adaptation est observée, ce qui suggère que des rétroactions négatives sont impliquées dans la protection cellulaire contre le stress. La variabilité d'une cellule à l'autre est observée et quantifiée à l'aide de paramètres d'adaptation identifiés. Des résultats préliminaires de la dépendance de la modulation du pH par l'état métabolique cellulaire sont discutés. Les caractéristiques d'adaptation ne sont pas représentées lorsque les sources de carbone sont complètement éliminées du milieu externe. Ce résultat souligne le rôle du glucose dans le mécanisme de défense cellulaire. Un autre résultat important est celui de la dynamique de rétroaction qui dépend de la dose de  $H_2O_2$  appliquée aux cellules: une stimulation plus forte implique une réponse plus forte. C'est un premier facteur limitant que nous avons identifié lors de la quantification de la réponse de mort cellulaire au stress  $H_2O_2$ . Les

résultats de la réponse à la dose de mort cellulaire suggèrent que le destin de la cellule (survie ou mort) dépend également à la fois du contrôle du stimulus et de l'état métabolique cellulaire. Afin d'identifier les voies métaboliques impliquées dans la rétroaction négative induite par le stress oxydatif, des molécules clés régulant la voie Phosphate Pentose (PPP) sont modulées. Nous concluons que l'orchestration du réseau moléculaire est plus complexe et que le PPP n'est pas le seul réseau impliqué dans la défense cellulaire. Nous concluons que l'orchestration du réseau moléculaire est plus complexe et que PPP est le réseau principal mais pas le seul impliqué dans la défense cellulaire.

Dans ce manuscrit, une conception expérimentale est présentée afin d'étudier les réponses d'adaptation au stress oxydatif observée en temps réel. Nos expériences confirment la cinétique d'adaptation rapide du NAD(P)H déjà observée dans la littérature. Nous identifions, pour la première fois, un deuxième mécanisme de régulation où le système de glutathion se rétablit en 30 min pendant la stimulation contrôlée par H<sub>2</sub>O<sub>2</sub>. Le métabolisme du glucose soutient la régénération de ce système antioxydant et le réseau PPP est ainsi identifié comme le principal retour négatif dans l'adaptation moléculaire observée ici.

**Mots Clefs:** Dose de stress, dynamique, métabolisme, adaptation, peroxyde d'hydrogène, cellule unique

## Abstract

Living cells, when constantly exposed to stress, are able to respond in a complex manner involving various intracellular regulation networks. Their regulation controls for instance the cellular fate outcome in response to an oxidative stress. When defensive mechanisms manage to cope against stress, a negative feedback is involved and cell survive, otherwise cell dies. One of a key defensive mechanism relies on the interplay between metabolic flux and oxidative stress exploiting the dualistic role of hydrogen peroxide, acting both as signalling and damaging molecule.

Our work aims to identify key molecules involved in cellular fate and to monitor their dynamics at the single cell level, using fluorescent microscopy. In a first step, we design an experimental system inspired by chemotaxis studies to constantly control the dose applied to breast cancer cell line (MCF7). The choice of the stimulation method plays an important role in our study. Indeed, in order to deliver a constant concentration of stimulus to mammalian cells, non-consuming  $\text{H}_2\text{O}_2$  cell culture medium is chosen. Using a fluidic system, the intracellular  $\text{H}_2\text{O}_2$  production rate is controlled by varying the external  $\text{H}_2\text{O}_2$  concentration. Stimulus delivery and removal is thus performed fast enough (faster than cellular consumption) to study the dynamical cellular responses.

During constant stimulation, adaptation dynamics are notified, suggesting that negative feedbacks are involved in the cellular protection against stress. Cell-to-cell variability is observed and can be quantified using identified adaptation parameters. The fluorescent signal is processed and preliminary results of pH modulation dependence by the cellular metabolic state are discussed. The adaptation features are not depicted when the carbon sources are completely removed from external medium. This result underlines the role of glucose in the cellular defensive mechanism. Another important result is that the feedback dynamics is depending by the  $\text{H}_2\text{O}_2$  dose applied to cells: stronger stimulation implies stronger response. It is a first limiting factor we identified while quantifying the cell death response to  $\text{H}_2\text{O}_2$  stress. The results of cell death dose response are suggesting that the cell fate (survival or death) is also depending by both the control of the stimulus and the cellular metabolic state. In order to identify the metabolic pathways involved in the negative feedback induced by the oxidative stress, key molecules regulating the Phosphate Pentose Pathway (PPP) are modulated. We conclude that the

orchestration of molecular network is more complex and PPP is the main but not the only network involved in the cellular defense.

In this manuscript an experimental design is presented in order to study the adaptation responses to oxidative stress in real time. Our experiments are confirming the fast adaptation kinetics of NAD(P)H already observed in literature. We identify, for the first time, a second regulation mechanism where the glutathione system is restoring within 30 min during controlled H<sub>2</sub>O<sub>2</sub> stimulation. The glucose metabolism is supporting the regeneration of this antioxidant system and PPP network is thus identified as the main negative feedback in the molecular adaptation here observed.

**Keywords:** stress dose, dynamics, metabolism, adaptation; hydrogen peroxide, single cell

## Abbreviations and Symbols

1.3Pgli	1,3-bisphosphoglyceric acid
2-Pgli	2-phosphoglyceric acid
3Pgli	3-phosphoglyceric acid
6AN	6aminonicotiamide
6PG	6-phosphogluconate
6PGL	6-phosphogluconolactone
Acetyl-CoA	acetyl coenzyme A
ADP	adenosine diphosphate
ATP	adenosine triphosphate
DNA	deoxyribonucleic acid
E4P	erythrose 4-phosphate
F1,6P	fructose-1,6-diphosphate
F6P	fructose 6-phosphate
FADH	reduced form of flavin adenine dinucleotide
G3P	glyceraldehyde 3-phosphate
G6P	glucose 6-phosphate
G6PD or G6PDH	glucose 6-phosphate dehydrogenase
GAPD or GAPDH	glyceraldehyde 3-phosphate dehydrogenase
GFP	Green Fluorescent Protein
GP	glutathione peroxidase
GR	glutathione reductase
Grx1	Glutaredoxin-1
GSH	glutathione
GSSG	glutathione disulfide
H <sub>2</sub> O <sub>2</sub>	hydrogen peroxide
LDH	lactate dehydrogenase
NAD <sup>+</sup>	oxidized form of nicotinamide adenine dinucleotide
NADH	reduced form of nicotinamide adenine dinucleotide
NADP <sup>+</sup>	oxidized form of nicotinamide adenine dinucleotide phosphate
NADPH	reduced form of nicotinamide adenine dinucleotide phosphate
PPP	Pentose Phosphate Pathway
PPpyr	phosphoenolpyruvic acid
Pyr	pyruvic acid
R5P	ribose 5-phosphate
RI5P	ribulose 5-phosphate
ROS	Reactive Oxygen Species

S7P	sedoheptulose 7-phosphate
TA	transaldolase
TKT	transketolase
X5P	xylulose 5-phosphate
YFP	Yellow Fluorescent Protein

## List of figures

<b>Figure 1.1:</b> Electron structure in the outer layer of main ROS. In green are the paired electrons and in red are the unpaired electrons (reproduction from [18]).....	22
<b>Figure 1.2:</b> Reduction steps of oxygen molecule to reactive oxidative species (reproduction after [17]).....	23
<b>Figure 1.3:</b> Main intracellular ROS production sources (from [25]) .....	25
<b>Figure 1.4.</b> Glucose metabolism in mammalian cells. ....	27
<b>Figure 1.5:</b> H <sub>2</sub> O <sub>2</sub> gradient through cellular plasma membrane (from [68]) .....	35
<b>Figure 1.6:</b> Timeline of the advances in real time molecular dynamics with temporal modulated patterns of H <sub>2</sub> O <sub>2</sub> . Abbreviations: Glutathione Peroxidase (GPrx), Superoxide Dismutase (SOD), Catalase (Cat.), Peroxidase (Prx), Peroxidases (Prox), Glutathione redox potential (E <sub>GSH</sub> ), Nicotinamide adenine dinucleotide (NADH), Nicotinamide adenine dinucleotide phosphate (NADPH), Green Fluorescent Protein (GFP), Electronic Transport Chain (ETC), Fluorescence Lifetime Imaging Microscopy (FLIM), disulfide bounds (ss), hydrogen peroxide (H <sub>2</sub> O <sub>2</sub> ), Real time (RT). ....	39
<b>Figure 2.1:</b> Methods of H <sub>2</sub> O <sub>2</sub> delivery system and the corresponding concentration profiles provided to seeded cells. (A) Bolus or bulk method by mixing H <sub>2</sub> O <sub>2</sub> in cell culture media. (B) The presence of scavengers in medium and the cells are reducing the [H <sub>2</sub> O <sub>2</sub> ] in time. (C) Extracellular reactions often mediated by enzymes E can be initiated in cell culture media as H <sub>2</sub> O <sub>2</sub> generating sources. (D) Extracellular H <sub>2</sub> O <sub>2</sub> continuous generating source presents a logarithmic profile; the enzymatic activity increases the H <sub>2</sub> O <sub>2</sub> production to a certain maximum. Once the substrate of reaction is consumed, the reaction ends. It leads to the decrease of the external stimuli with similar profile as in bolus. (E) Intracellular H <sub>2</sub> O <sub>2</sub> continuous generating sources: exploiting the amino acid oxidase (DAAO) sensitivity to d-alanine allows creation of locally intracellular H <sub>2</sub> O <sub>2</sub> . Once the DAAO transfection is done, the internal [H <sub>2</sub> O <sub>2</sub> ] can be varied by modulating the d-alanine concentration added in medium (top); Similarly, NOX pathway can be used to generate internal H <sub>2</sub> O <sub>2</sub> sources (bottom). ....	44
<b>Figure 2.2:</b> UV-Vis spectrum of complete cellular culture media (DMEM) .....	49
<b>Figure 2.3:</b> HyPerBlu reactions with H <sub>2</sub> O <sub>2</sub> leads to luminescent compound (from [108]). Linear detection range from 10 <sup>-6</sup> to 10 <sup>-4</sup> M of H <sub>2</sub> O <sub>2</sub> using HyPerBlu reagent showing that the H <sub>2</sub> O <sub>2</sub> concentration is proportional with the luminescent signal .....	52
<b>Figure 2.4:</b> Mechanism of extracellular H <sub>2</sub> O <sub>2</sub> quantification using HyPerBlu reagent. ....	53
<b>Figure 2.5:</b> H <sub>2</sub> O <sub>2</sub> stability in various complex cell culture media: Dulbecco's Modified Eagle Medium without Pyruvate, without Glucose (DMEM--), Dulbecco's Modified Eagle Medium	

without Pyruvate, with Glucose (DMEM+-), and very minimal media: Phosphate Buffered Saline 1x with Ca and Mg without glucose (PBS G-), Phosphate Buffered Saline 1x with Ca and Mg with glucose concentration of 4.5 g/L (PBS G+) .....54

**Figure 2.6** Kinetics of H<sub>2</sub>O<sub>2</sub> consumption by MCF7wt cells during 1h incubation in PBS with Ca and Mg and without glucose. Studies are made in duplicates for each cell confluence and each reading is made in triplicates. ....55

**Figure 2.7** Dependence of H<sub>2</sub>O<sub>2</sub> consumption by the number of cells exposed to stress in static system. After 1h of exposing MCF7 wt cells to an initial concentration of 100μM, the concentration diminishes while the number of exposed cells is higher. ....56

**Figure 2.8:** Dose response with cell type as reported in literature: LLC-PK1 [118], HUVEC [119], primary neuronal cells [120] and Hela [121]. The sensitivity of MCF7 wt cells is quantified in our laboratory. ....58

**Figure 2.9:** MCF7wt dose response short (4h) and long (24h) time after stimulation with H<sub>2</sub>O<sub>2</sub>. The stress is applied for 1h using various [H<sub>2</sub>O<sub>2</sub>]. During stress, the cells are kept in minimal medium without glucose, then recovered in their normal growth conditions. Percentage of dead cells is quantified reporting to cell survival observed in bright field images (left) or by using PI marker (right). ....59

**Figure 2.10:** MCF7 wt dose response to various doses of H<sub>2</sub>O<sub>2</sub>. Correcting the dose in the results extracted from literature (top) we observe that the time of stress exposure in static conditions is a key parameter. Here are recalculated the doses of H<sub>2</sub>O<sub>2</sub> stress from publications [115,116,128,129] in in both lack (G-) and presence (G+) of glucose. Significant shift is observed comparing with the original data. The kinetic constants used to correct the results are extracted from literature ( $k_{G+}=1.38 \text{ h}^{-1}$  from [72]) or obtained in our experimental conditions ( $k_{G-}=0.48 \text{ h}^{-1}$ ) .....62

**Figure 2.11:** Dose response of MCF7wt cells to H<sub>2</sub>O<sub>2</sub> stimulus applied in bolus for various durations (30min, 1h, 2h, 3h or 4h). The stimulation is performed in minimal medium (PBS) in two different metabolic conditions: presence (G+) or absence (G-) of glucose. After stress the cells are recovering in their normal growth medium. Cell death is quantified using PI. The survival is observed in brightfield images in unstained cells. Both death and survival are quantified 4h (top graphs) and 24h (lower graphs) after recovery upon stress. ....65

**Figure 2.12:** Dose response of MCF7wt cells to various concentrations of H<sub>2</sub>O<sub>2</sub> applied for 1h, after 4 and 24h of recovery in complete medium, the fraction of dead and living cells are quantified and represented as function of [H<sub>2</sub>O<sub>2</sub>]. In glucose starvation the cell has to use the existing resources to fight against stress. In normal glucose conditions the cell fate is regulated according to stress severity. Inhibiting the PPP the NADPH cytosolic production pool is reduced, another defensive pathways being involved in cell defense. ....67

**Figure 2.13** Fluidic system to create controlled temporal H<sub>2</sub>O<sub>2</sub> stimulus on mammalian adherent cells. ....69

**Figure 2.14:** Flow profile measured in the center of the chamber using Rhodamine 110. ....71

**Figure 2.15:** Cell death in response to hydrogen peroxide: comparing the cellular dose responses observed in static (top) and in continuous external H<sub>2</sub>O<sub>2</sub> delivery systems (bottom). For stimulation in static conditions, cells are seeded in the T25 flask 48h before stimulation. The stress is made by changing the complete medium with the PBS containing H<sub>2</sub>O<sub>2</sub>. After incubation, the stress is stopped by removing it and rinsing the cells with PBS. For recovery the cells are incubated in complete medium (DMEM). They are imaged right after the stress and 24 h later. Cells stimulated in continuous system under flow are seeded 48h in the fluidic channel, in static conditions. Right after stress, cells are recovering in DMEM for 24h. ....72

**Figure 2.16:** Comparing MCF7 wt cell death observed in static and continuous flow systems, upon 1h stimulation at various concentrations of H<sub>2</sub>O<sub>2</sub> (0, 100 μM 250μM). Cell death (upper and lower right plots) and survival (upper and lower left plots) are quantified 4h (triangles) and 24h after stimulation (cercles). The external H<sub>2</sub>O<sub>2</sub> stress is performed in very minimal medium (PBS G+), while the recovery is made in complete DMEM. Experiments in bolus are performed in duplicate, while the ones in fluidic system only once. 73

**Figure 3.1:** Oxidative stress response and cellular fate: upon H<sub>2</sub>O<sub>2</sub> stimulation a cell either adapts to an oxidative stress and thus survive or dies. Death occurs when nucleus cannot be protected by the antioxidants pool (in purple). This behavior is strongly controlled by the cellular ability to restore the ROS-antioxidants balance. The cell is producing internal H<sub>2</sub>O<sub>2</sub> during metabolism at basal rate  $\Gamma_{\text{basal}}$ . External H<sub>2</sub>O<sub>2</sub> is imported *via* passive or active diffusion across the cellular membrane thus varying the total effective production rate  $\Gamma_{\text{total}} = \Gamma_{\text{basal}} + K_{\text{ext}} \cdot [\text{H}_2\text{O}_2]$ , where  $K_{\text{ext}}$  is a constant. ....77

**Figure 3.2:** (A) HyPer construction in reduced and oxidized form (from [153]). (B) Their states are regulated by H<sub>2</sub>O<sub>2</sub> respectively Grx, Trx .In the variations of HyPer fluorescence ratio have to be considered the contribution of each fraction of HyPer in a certain oxidation form at that time (from [154]). (C). Changes in excitation spectrum of HyPer upon oxidation by H<sub>2</sub>O<sub>2</sub> (from [75]). (D) Calibration of SypHer (in situ), reflecting the pH sensitivity of HyPer. In zoom: the variation of fluorescence ratio of sensor at physiologic pH (from [155]).....81

**Figure 3.3:** pH variation during H<sub>2</sub>O<sub>2</sub> stimulation: intracellular HyPer (A-B) and SypHer (C-E) fluorescence are monitored 30 minutes pre-stimulation, 1h during and after stimulation. MCF7 cells are exposed during 1h to 100 μM of external H<sub>2</sub>O<sub>2</sub> solution prepared in DPBS supplemented with glucose (4.5 g/L). Heat maps are corresponding to ratio of the signal observed in single cells (A, C). Suggestive features of single cell responses are extracted (B, D). The absolute SypHer ratio is represented in E, where the black line is the mean of the pH variation in MCF7 cytosol before, after (blue background) and during H<sub>2</sub>O<sub>2</sub> stimulation (pink).83

**Figure 3.4:** Calibration plot of SypHer and HyPer normalized signal as function of pH using data from [126,155].....85

**Figure 3.5:**(A). Molecular mechanism of Grx1-roGFP2 sensor following its reversible conversion. Its regeneration is mediated by GSH; (B): roGFP2 excitation bands depicted in total oxidized (blue) and total reduced (red) forms (from [164]). ....87

**Figure 3.6:**(A)The chemical structure of NADH and NADPH. In blue is highlighted the fluorescent part after light absorption (from [33]). (B) As the fluorescent group is identical in both molecules, their spectral characteristics are overlapping (from [165]). .....88

**Figure 3.7:** Schematic representation of H<sub>2</sub>O<sub>2</sub> scavenging in mammalian cells: in presence of carbon source the cell is able perform normal functions; upon H<sub>2</sub>O<sub>2</sub> stimulation the defense mechanism is perturbed; the molecular dynamics is monitored to observe adaptation dynamics 90

**Figure 3.8:** (A) Scheme of experimental microfluidic chamber in order to create time varying stimulus. (B) Schematic representation of the glucose metabolism highlighting the target molecules imaged by fluorescence microscopy; NAD(P)H is observed by its auto fluorescence, glutathione redox dynamics are monitored with Grx1-roGFP2, while H<sub>2</sub>O<sub>2</sub> and pH variations are targeted with HyPer. Both Grx1roGFP2 and HyPer are ratio metric genetically encoded sensors indicating fold changes of redox homeostasis. ....91

**Figure 3.9:** Parameters characterizing adaptation of cells during and after stimulation: cellular response following 1h of H<sub>2</sub>O<sub>2</sub> stress (upper panels). The adaptation responses are depicted and quantified by different parameters. After stress removal the system readapts to the initial state or close to it (lower panels) .....92

**Figure 3.10:** Molecular dynamics in MCF7 cells upon 100 μM H<sub>2</sub>O<sub>2</sub> stimulation: Grx1-roGFP2 and NAD(P)H cytoplasmic are monitored to observe adaptation features upon addition and removal of continuous 100 μM of H<sub>2</sub>O<sub>2</sub>. Suggestive single cell features are extracted. ....94

**Figure 3.11:** pH estimation *via* SypHer in acidic cytosol. (A) SypHer kinetics: black line represents the mean signal, while the grey area is the variability of the signal corresponding to single cells. The blue background is represented the pre-stimulus and post stimulus SypHer variation, while in pink is highlighted the pH variation during 100 μM H<sub>2</sub>O<sub>2</sub> stimulation. On y axis is plotted  $\Delta R/R_0$  where  $R_0$  is SypHer ratio pre-stimulus and  $\Delta R=R(t)-R_0$ ; (B) Histogram of  $\Delta R_{55}/R_0$  where  $\Delta R_{55}=R_{55min}-R_0$ ; (C) Calibration of SypHer ratio versus pH. Data are fitted with  $R=R_1+R_2/(1+e^{nu(pKa-pH)})$ , where  $R_1=0.1$ ;  $R_2=9.4968$ ;  $pKa=8.4$ ;  $nu=2$ .  $pH_{ref}=7.1$  corresponding to cytosolic pH, thus  $Ref=0.758$  (D) Conversion of data in B with calibration on fig. C.....96

**Figure 3.12 :** Comparison of Grx1-roGFP2 ratio variation upon 100μM H<sub>2</sub>O<sub>2</sub> stimulation and pH variation. (A, B) comparison of Grx1-roGFP2  $\Delta R/R$ : for 100μM H<sub>2</sub>O<sub>2</sub> stimulation  $R=R_{max}$  while after stimulation  $\Delta R = R_{55min}-R_{max}$ ; for pH variation  $R=R_{pH=7.1}$  and  $\Delta R=R_{pH2}-R_{pH=7.1}$ , where  $pH_2$  is 6.9, 6.7 or 6.5; (C,D,E) Comparison of fluorescence variation in each channel at various pH, where the reference is pH=7.1, is plotted the 2D PDF; (F,G,H) Comparison of fluorescence variation in at various time following 100μM stimulation, where the reference is prestimulus, is plotted the 2D PDF .....98

**Figure 3.13:** Effect of [H<sub>2</sub>O<sub>2</sub>] dose on molecular adaptation dynamics in cytosol observed with NAD(P)H fluorescence. Pre-stimulus (blue background A), stimulus (pink background A-B) and post-stimulus (blue background B) fluorescent signals are here averaged over cell population. Normalized NAD(P)H fluorescence kinetics upon various [H<sub>2</sub>O<sub>2</sub>] stimuli are represented: in black solid line 250 μM, in grey solid line 100 μM, grey dashed line 30 μM. ....100

**Figure 3.14:** Effect of  $[H_2O_2]$  dose on molecular adaptation dynamics in cytosol observed with Grx1-roGFP2 – redox potential sensor (A-D) and NAD(P)H fluorescence (E-I). Left panel; schematic definition of parameters characterizing Grx1-roGFP2 and NAD(P)H. The corresponding probability density function (PDF) of each parameter described is depicted in upper panels. (A, E); (B) maximum variation of Grx1-roGFP2 ratio  $\Delta R_{max}$  following  $H_2O_2$  addition; (C) adaptation index  $\alpha_{add} = \Delta R_{55}/\Delta R_{max}$ ; (D) maximum variation of Grx1-roGFP2 ratio ( $\Delta R_{rmv}$ ) following  $H_2O_2$  removal; (F) maximum variation of fluorescence relative to  $F_0$  ( $\delta_{add}$ ) during  $H_2O_2$  stimulation; (G) effective fluorescence recovery rate shortly after  $H_2O_2$  stimulation  $K_{FB}$ ; (H) effective fluorescence drift rate longer after  $H_2O_2$  stimulation  $K_D$ ; (I) NAD(P)H fluorescence gap between pre-stimulus and steady state following  $H_2O_2$  removal  $\delta_{rmv}$ ..... 101

**Figure 3.15:** Schematic representation of metabolic pathways. Adding  $H_2O_2$  external stress performed in lack of external carbon source during stimulation, the cell is limited to use the existing resources to defense against stress..... 104

**Figure 3.16:** Averaged data concerning molecular dynamics upon  $H_2O_2$  stimulation and its removal for starving and glucose importing systems. HyPer (A), NAD(P)H (B) and Grx1-roGFP2 (C); On bottom of each panel are represented the histograms corresponding to the adaptation parameters: initial HyPer ratio ( $H_0$ ), initial NAD(P)H fluorescence level ( $F_0$ ), initial Grx1-roGFP2 ratio ( $G_0$ ) maximum ratio variation ( $\Delta R_{max}$ ), minimum NAD(P)H fluorescence level less than 10 min after stimuli addition ( $F_{max}$ ), HyPer respectively Grx1-roGRP2 ratio variation at 55 min following  $H_2O_2$  addition ( $\Delta R_{55}$ ), fluorescence level at 55 min following  $H_2O_2$  addition ( $F_{55}$ ), minimum HyPer respectively Grx1-roGFP2 ratio variation after  $H_2O_2$  removal ( $\Delta R_{rmv}$ ) and NAD(P)H fluorescence level 55 min after  $H_2O_2$  removal ( $F_{rmv}$ )..... 106

**Figure 3.17:** Schematic representation of the glucose metabolic pathways showing the link between PPP and intracellular ROS quenchers The flux of PPP key molecules will be varied by inhibiting or overexpressing the corresponding enzymes: G6PD and GAPD ..... 108

**Figure 3.18:** Effect of PPP gatekeepers modulation by G6PD over expression and knock down; following the adaptation dynamics after exposing cells to  $100\mu M H_2O_2$  for 1h. The MCF7 cells are maintained in normal glucose conditions (4.5 g/L). The error bars are representing the variation of adaptation parameters corresponding to Grx1-roGFP2 before ( $R_0$ ), during ( $R_{max}$ ,  $\alpha_{add}$ ;) and after stimulation ( $\Delta R_{rmv}$ ). (A) Cumulative Density Function (CDF) where the color code is defined in lower panels (B) initial Grx1-roGFP2 ratio  $R_0$  reflecting the basal redox potential (C) maximum variation of Grx1-roGFP2 ratio  $\Delta R_{max}$  following  $H_2O_2$  addition; (D) adaptation index  $\alpha_{add} = \Delta R_{55}/\Delta R_{max}$ ; (E) maximum variation of Grx1-roGFP2 ratio ( $\Delta R_{rmv}$ ) following  $H_2O_2$  removal..... 110

**Figure 3.19:** NADPH variation during  $100 \mu M H_2O_2$  stimulation on MCF7 cells in various metabolic condition: overexpression (OV) of G6PDH, GAPDH or TKT, knock down (KD) of GAPDH activity. Wild type (WT) is the reference control..... 113

## Contents

Acknowledgments.....	3
Resumé.....	5
Abstract .....	7
Abbreviations and Symbols.....	9
List of figures.....	11
Context of the study .....	18
Chapter 1: Introduction to redox homeostasis .....	20
1.1 Cellular stress response and oxidative stress.....	20
1.2 Reactive Oxygen Species .....	22
1.2.1 Introduction .....	22
1.2 Cellular metabolism of glucose and redox homeostasis .....	26
1.2.1 Glycolysis.....	26
1.2.2 H <sub>2</sub> O <sub>2</sub> quenching in living cells .....	28
1.2.3 Pentose Phosphate Pathway .....	29
1.3 Correlation between oxidative stress response and cell metabolism .....	30
1.4 Oxidative stress response and cellular fate.....	33
1.4.1 Adaptation of cell to stress.....	33
1.4.2 H <sub>2</sub> O <sub>2</sub> dualistic role .....	34
1.4.3 Cell death as non-adaptive response.....	36
1.5 H <sub>2</sub> O <sub>2</sub> as a tool to perturb redox balance .....	38
Chapter 2: How to control the H <sub>2</sub> O <sub>2</sub> stimulus?.....	42
2.1 Introduction.....	42
2.2 Methods of creating H <sub>2</sub> O <sub>2</sub> stress stimuli.....	43
2.3 Creating H <sub>2</sub> O <sub>2</sub> steady state stress pattern using bolus method .....	48
2.3.1 H <sub>2</sub> O <sub>2</sub> degradation by cell culture media.....	48
2.3.2 Kinetics of H <sub>2</sub> O <sub>2</sub> and cell consumption .....	55
2.4 Cell death upon H <sub>2</sub> O <sub>2</sub> stress .....	58
2.4 Role of glucose metabolism in cell death process: stimulus dose approach .....	64
2.4.1 Dose response in different metabolic conditions varying the exposure time .....	64
2.4.2 Dose response in different metabolic conditions varying the stimulus concentration .....	66
2.5 Design fluidic system .....	68
Chapter 3: Cellular adaptation to oxidative stress .....	75

3.1 Introduction.....	75
3.1.1 Background .....	75
3.1.2 Cellular adaptation to oxidative stress .....	76
3.2 Molecular dynamics of oxidative stress .....	79
3.2.1 Monitoring the dynamics of H <sub>2</sub> O <sub>2</sub> .....	79
3.2.2 Methodology of monitoring the intracellular glutathione redox potential.....	86
3.2.3 Monitoring the dynamics of NAD(P)H .....	87
3.3 Intracellular redox balance.....	89
3.3.1 Perturbing the intracellular H <sub>2</sub> O <sub>2</sub> balance .....	89
3.3.2 Materials and methods .....	90
3.3.3 Adaptive dynamics in cellular cytoplasm: results and discussions .....	93
3.4 External H <sub>2</sub> O <sub>2</sub> concentration effect on adaptation dynamics.....	99
3.5 Glucose in adaptation dynamics.....	103
3.6 PPP role in adaptation upon oxidative stress.....	108
3.7 Conclusions and discussions .....	115
Conclusions and Perspectives.....	117
Bibliography .....	123

## Context of the study

Most of living systems, including mammals, are using dioxygen to perform vital functions as respiration and metabolism. During those processes, oxygen radicals can be created and become reactive when interacting with structural parts of the cell. To prevent damages, cells developed an antioxidant system to quench the damaging oxygen species. Metabolism is a complex intracellular process, maintaining their concentration on steady state. While glucose is metabolized in presence of dioxygen to create energy and to perform cellular respiration, it is also used to support the scavenging system which is controlling the redox homeostasis inside the cell to a basal level.

Biological systems as mammalian cells are often exposed to environmental changes, thus the redox potential can be perturbed. Cellular metabolism is constantly regulating to help the cell to survive, dynamically adapting the redox homeostasis to the new condition. For cell division, increased metabolic flux is necessary in order to produce and assembly the structural compounds of the daughter cells. Cancer cells are known to have a particular metabolism, dividing faster than non-cancerous ones. Here we are interested in studying the cellular molecular adaptation to hydrogen peroxide, a side product of metabolism. Our motivation comes from the fact that metabolic changes lead to redox homeostasis perturbation also. The metabolic adaptation can induce functional dysregulations causing diseases as diabetes or cancer progression. In this context we are questioning how is the intracellular metabolism regulation restoring the redox homeostasis and how the oxidative species are controlling the metabolic fluxes in cells? For this purpose, adaptation kinetics process at molecular level are studied under external  $\text{H}_2\text{O}_2$  stimulation as a tool to modulate the intracellular redox pool. This way the oxidant production and antioxidant scavenging balance is perturbed and the dynamics of metabolic reprogramming can be monitored. In order to highlight the adaptive response of the cell to external  $\text{H}_2\text{O}_2$  stimulation, direct enzymatic changes of metabolic dependent detoxification system are targeted. For subtoxic  $\text{H}_2\text{O}_2$  concentrations delivered, direct adaptive signs can be observed on glutathione and thioredoxin antioxidants groups, when conformational enzymatic changes occur during stress exposure, in short timescales ranging from few seconds to minutes [1]. Moreover, metabolic rerouting mechanisms can be mediated by redox changes in the cell. Our intention is

to exploit the mechanism of regulation between cellular cytoplasmic metabolism and redox homeostasis in order to find the cellular vulnerability to oxidative stress. For better understanding how do the cells adapt to oxidative stress, the dynamics of  $\text{H}_2\text{O}_2$  scavenging system dependent by glucose metabolism is monitored. Increase of antioxidants pool activity during stress exposure is the direct sign of cellular defense against  $\text{H}_2\text{O}_2$  stress, process here defined as negative feedback. Thus can be observed how the cells regulate their metabolism to overcome oxidative stress.

In the first chapter, introduction to redox homeostasis and cell death are presented and fundamental biological mechanisms and particularities are discussed. As our purpose is to observe the adaptation kinetics of cells under stress, the second chapter is dedicated to  $\text{H}_2\text{O}_2$  stimulation methods. Using two different stimulation methods, cell death in response to various  $\text{H}_2\text{O}_2$  doses is quantified. The strategy of observing molecular adaptation in mammalian living cells, under controlled  $\text{H}_2\text{O}_2$  stimulation is explained in the third chapter. Adaptation process observed in real time (order of minutes) is showing strong dependence by glucose metabolism. To observe the defensive regulation under stress conditions, key molecules involved in rerouting the glucose metabolism are modulated. We notice that the negative feedback is more complex than anticipated and multiple pathways are involved in defensive mechanism. Finally, preliminary results concerning alternative feedback mechanisms are presented.

## Chapter 1: Introduction to redox homeostasis

### 1.1 Cellular stress response and oxidative stress

Cells are dynamic systems, where the homeostasis is maintained by active mechanisms regulated by feedback loops. Homeostasis represents a dynamic balancing to equilibrium of the variations of internal conditions within narrow limitations [2]. Despite its literally translation (greek: homois = the same, stasis = state) which can denote the unchanging property, homeostasis is in fact defined as a dynamic state of equilibrium.

From the point of view of structure, cells are a bunch of organic and inorganic molecules. The difference between the living and death states is that molecules in living cell are dynamically organized, relieving the cell to act as reactive system, being able to perform functions and to selectively interact with the environment, while dead cell irreversibly lost the ability of maintaining their homeostasis leading to a cellular dysfunctional system. What distinguish the living from dead systems is the ability of performing interactions and active regulations [3]. When environmental conditions change, the cell launches complex process regulated internally by pathways able to fight against damages or to amplify the stressor effect. In particular, we are interested to find tools and trends in the temporal molecular dynamics to predict the cellular fate, as survival or death. The precision of these predictions are of interest also in anticancer therapies. Exploiting the weakness of cancer cells allow the selection of stressor characteristics as nature, intensity and its modulation in time. For example, anticancer therapies are using Reactive Oxidative Species (ROS) to remove the tumor. Normally, ROS exist in cells at basal level, coming mostly as a side effect of oxygen dependent metabolism. The interest in oxidative stimulation comes from its particular behavior too. It has been observed that  $H_2O_2$  has a key role as signaling molecule, being involved in fine tuning of some cellular regulatory mechanisms as inflammation or metabolism [4,5]. It manifests also a damaging power which is exploited in removing the damaged cells or the cancer one [6,7].

Cellular stress can be defined as a process generated by a disturbing factor, leading to the perturbation of cell homeostasis. In 1936 was firstly defined the concept of stress as a response

of a living organism to a damaging source [8]. Then, the author observed that, even after removing the injury, the stress response acts like a syndrome, with different stages. First are observed damages signs, then recovery of the organism takes place with some transformations, depending by the intensity of the dose. Repeating the same injury after a certain time, the organisms could build up resistance by completely returning their structure and functions to normal. If the intensity or the duration of the injury would increase, the organisms would express similar damaging symptoms as observed after the first exposure [8]. After observing that cellular stress can lead to diseases, researchers paid attention to this concept and tried to understand how the cell response is regulated at the molecular level. All living systems suffer at least once a condition that perturbs their homeostasis. Depending by the stress type and its severity, cells can activate pathways to initiate protective or destructive responses. The stress dose, exposure modality and cell history are also factors that can influence the responding mechanisms [9]. The cell ability of reacting by adapting to the new environment insures their survival. For example, cancer cells experience different stress conditions as starvation, hypoxia, anticancer therapies and others [10]. The capability of surviving in these conditions promotes the cancer proliferation. The ability of stress source to create irreversible intracellular damages can lead to cell death, thus removal of the tumor cell.

Oxidative species are intra and inter-cellular signaling molecules governing cellular functions as division, cellular respiration, circadian clock and processes as inflammation or host defense mechanisms (immune cells), their regulation maintaining the cellular functions. Elevated levels of ROS bioavailability overtaking antioxidant defensive capacity can have destructive effects as oxidation of proteins, lipids or DNA [11–13]. In particular, oxidative stress occurs when the intracellular balance between ROS and antioxidants is perturbed, being defined as a disruption of redox control [13,14]. Oxidative stress is a pathophysiological situation of cellular redox alteration as a result of intracellular ROS overproduction. The Encyclopedia of stress presents an improved definition of oxidative stress as *“an imbalance between oxidants and antioxidants in favor of the oxidants, leading to a disruption of redox signaling and control and/or molecular damage”* [15,16]. Maintaining redox homeostasis can thus underlies the disease/health condition of the cell.

## 1.2 Reactive Oxygen Species

### 1.2.1 Introduction

Reactive Oxygen Species (ROS) are often defined as reactive chemical species containing oxygen (**Figure 1.1**). Depending by their electronic structure the ROS exist in two forms. Free radicals as oxygen, singlet oxygen, superoxide, peroxide, hydroxyl radical are highly reactive species, containing at least one unpaired electrons on the outer orbital of the molecule. For example, the oxygen atom contains 8 electrons. Together two oxygen atoms form an oxygen molecule with the unpaired electrons on the last orbital. On the triplet sigma state, known also as the ground state acts as radical. The singlet form of oxygen is also a free radical, having the two last electrons in antiparallel spin [17]. Non-free radicals as Hydroxyl ion and Hydrogen peroxide are more stable having all electrons of outer orbital paired. To become reactive, they are converted as free radicals [6].

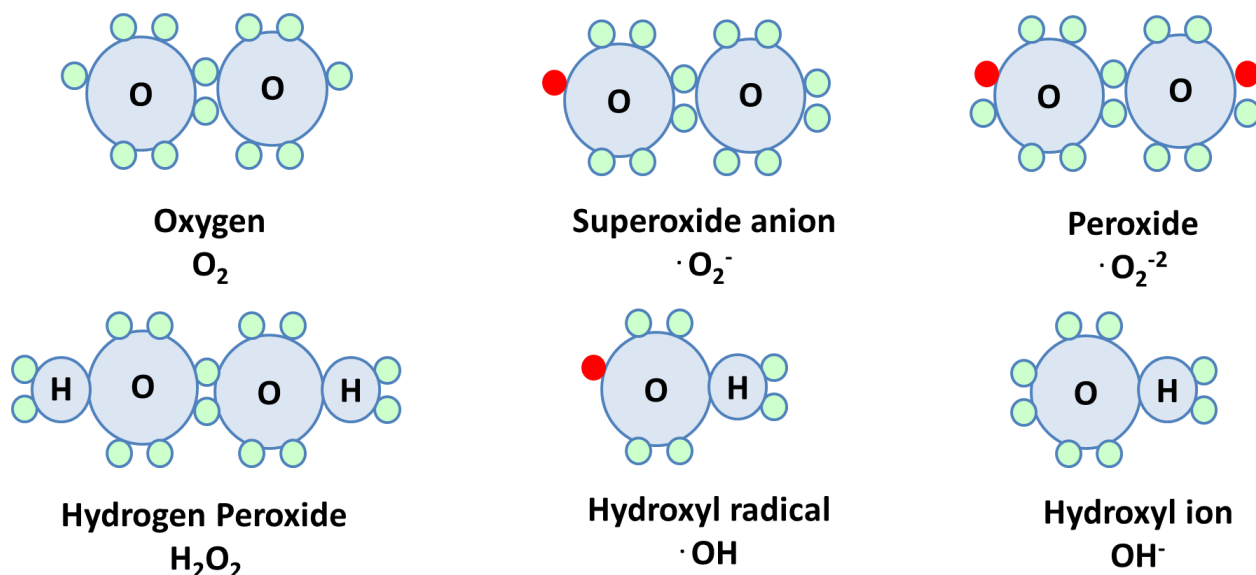


**Figure 1.1:** Electron structure in the outer layer of main ROS. In green are the paired electrons and in red are the unpaired electrons (reproduction from [18]).

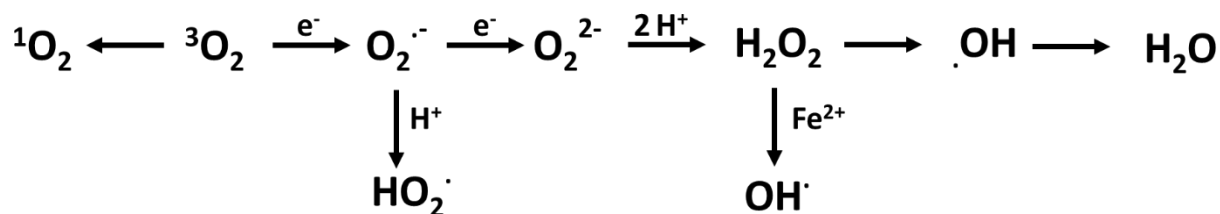
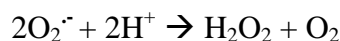


**Figure 1.2:** Reduction steps of oxygen molecule to reactive oxidative species (reproduction after [17]).

ROS can be interconverted between them in physiological circumstances (**Figure 1.2**). In its ground state, the oxygen molecule is a weak oxidant due to the parallel electron spin which blocks the direct insertion of the electron pair to a molecule [17]. In the process of forming the water as bio-product in cellular respiration, oxygen is reduced to superoxide anion, a precursor of most reactive oxidative species. Once converted into hydrogen peroxide, it can be quenched by iron containing antioxidants, thus becoming nonreactive. However,  $\text{H}_2\text{O}_2$  decomposition can lead back to free radicals, as has been described by the Fenton reaction or Haber Weiss mechanism [19]:



Various ROS producing and scavenging systems are found in different cellular compartments and their complex interplay is still not well understood. The unlimited accumulation of ROS can perturb the cellular functions, leading to irreversible damages [20]. To neutralize the harmful effect of ROS, they can be quenched by the specific enzymatic system existing inside the cell (**Table 1.1**). Each ROS type has a particular mode of action, creating specific damages in the cell. Given the short life time of microseconds order, free radicals as singlet oxygen, superoxide and hydroxyl radical are very reactive, creating damages at their production site. The non-reacted ones can be converted to a non-free radical with longer lifetime, as  $\text{H}_2\text{O}_2$ .

**Table 1.1:** Properties of reactive oxidative species exploited in living cells (reproduction from [21]).

ROS	$T_{1/2}$	Migration distance	Scavenging systems	Mode of action	Cell damages
Singlet oxygen	1-4 $\mu$ s	30-100 nm [22]	Carotenoids $\alpha$ -tocopherol	Oxidizes DNA, proteins and fatty acids	Proteins with Trp, His, Met, Cys and Tyr residues; DNA
Superoxide	1-4 $\mu$ s	30 nm	SOD	Reacts with iron containing proteins	<i>via</i> Fe center
Hydroxyl radical	1 $\mu$ s	1 nm	Flavonoids Proline	Very reactive with all biomolecules	Proteins DNA Lipids
H <sub>2</sub> O <sub>2</sub>	1 ms	1 $\mu$ m	Catalase Peroxidase Peroxiredoxins Flavonoids	Oxidizes proteins and creates O <sup>•</sup> <i>via</i> O <sub>2</sub> <sup>•-</sup>	Proteins with cys residue

Oxidative processes are the result of normal physiology of the cell. Reactive Oxidative Species (ROS) can be created in oxygen dependent reactions required for cellular processes [23,24]. They can exist in two forms: free radicals, able to trigger cascade reactions thus magnifying their damaging effects, or non-free radicals. The second one possesses different roles in cellular redox homeostasis. Due to their stability and longer lifetime non-free oxygen radicals can travel longer distances, diffusing through cell compartments, acting not only as destructive elements but also as secondary messengers [25,26]. It has been shown to control cell fate, signal transduction pathways, regulating cellular processes as inflammation [4], cell differentiation [27,28], cell proliferation [29], aging [30], neurodegenerative diseases [31] or metabolic diseases as diabetes [32] or cancer [6]. Our interest on this peculiar oxidant is given by the H<sub>2</sub>O<sub>2</sub> connection with the intracellular metabolic pathways and its propriety of being regulated by enzymatic system dependent of the cell metabolism [33,34].

Almost 100 years ago were observed the hydrogen peroxide effects on cells and became of interest in cellular biology [35]. Nowadays the H<sub>2</sub>O<sub>2</sub> intracellular regulation still remained unclear. Its dualistic role have been exploited during the years for highlighting the orchestration of different pathways by monitoring its intracellular dynamics and its correlation with key molecules involved in metabolic pathways or programmed death [4,36,37].

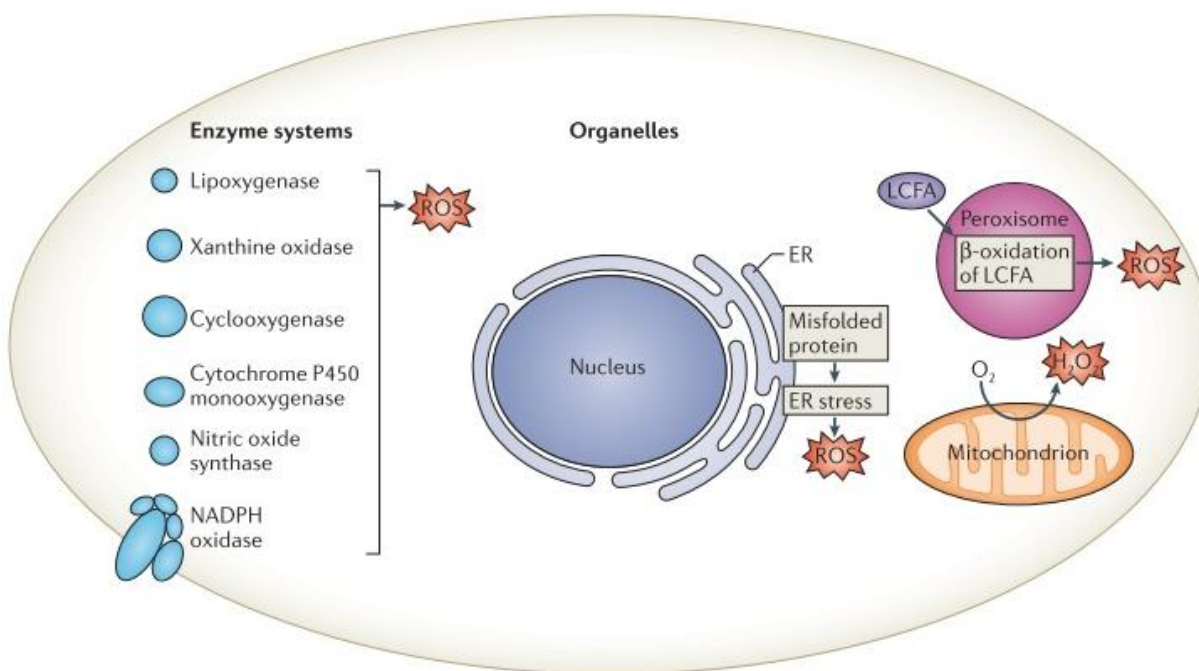


**Figure 1.3:** Main intracellular ROS production sources (from [25])

ROS can be produced inside the cell as byproducts in normal functions (**Figure 1.3**). The main cellular compartments producing ROS are the mitochondria, during the respiratory chain, the endoplasmic reticulum in the process of protein folding produce a stressful effect, thus creating ROS and the peroxisome, during the metabolic oxidation of long chain fatty acids. ROS can be created also by the enzymatic system existing notably in the cell cytoplasm, as nitric oxide synthase, cytochrome P450 monooxygenase, cyclooxygenase, xanthine oxidase or lipoxygenase. The NADPH oxidases founded in the cell membrane are part of Nox family and are remarkable for their role in immune system cells which creates ROS as defensive mechanism against pathogens [25]. Constant balancing of ROS generation allows achieving redox balance under physiological conditions. As metabolism is the main ROS source production site and the main scavenging supporting process in the cell, it will be further deeply described.

## 1.2 Cellular metabolism of glucose and redox homeostasis

Glucose is the main fuel required for almost all processes that a cell needs to survive. It enters inside the cell by an active mechanism, each cellular membrane containing glucose channels, internally controlled [38]. Once inside, glucose decomposes, process called metabolism, to create building blocks and energy required for their assembly (**Figure 1.4**).

### 1.2.1 Glycolysis

Glycolysis is the metabolic pathway which leads to the creation of energy. It takes place in two cellular compartments: it starts in cytosol and it ends in mitochondria. In this process, one molecule of glucose leads in the creation of 32 adenosine triphosphate (ATP) molecules. In cytosol, one glucose molecule breaks in two pyruvate molecules. This process is initiated by two ATP molecules and catalyzed by specific enzymes whose roles are to reduce the activation energy necessary to decompose the glucose molecule. The pyruvate is then metabolized in mitochondria and reduced to 3 molecules of nicotinamide dihydrogenase (NADH) and 1 molecule of flavin adenine dinucleotide (FADH) in a process known as Krebs cycle or citric acid cycle. They are used in the creation of ATP in the final step of glycolysis, the respiratory process, which takes place in the inner mitochondrial membrane in presence of oxygen.

The electron transport chain consists of a series of five protein complexes: NADH dehydrogenase (complex I), succinate dehydrogenase (complex II), ubiquinol-cytochrome c reductase (complex III), cytochrome c oxidase (complex IV), ATP synthase (complex V) and two mobile carriers: ubiquinone and cytochrome c. They are involved in the transport of electrons received from donor molecules, NADH and FADH. The respiratory process starts when the two electrons from NADH are released in the first complex, and two hydrogen ions are transferred between the two mitochondrial membranes. In a similar way, FADH donates its electrons to succinate dehydrogenase. The first mobile carrier transports the electrons to the third complex. They are then transferred by cytochrome c, one by one to the next complex. Each time when one electron is transferred, one hydrogen ion is pumped through the complex III. The second mobile carrier releases the electrons to the cytochrome oxidase. When 4 electrons, 8 hydrogen ions and molecular oxygen are into the complex two water molecules are assembled and are released inside the mitochondria. The rest of 4 hydrogen ions are pumped across the

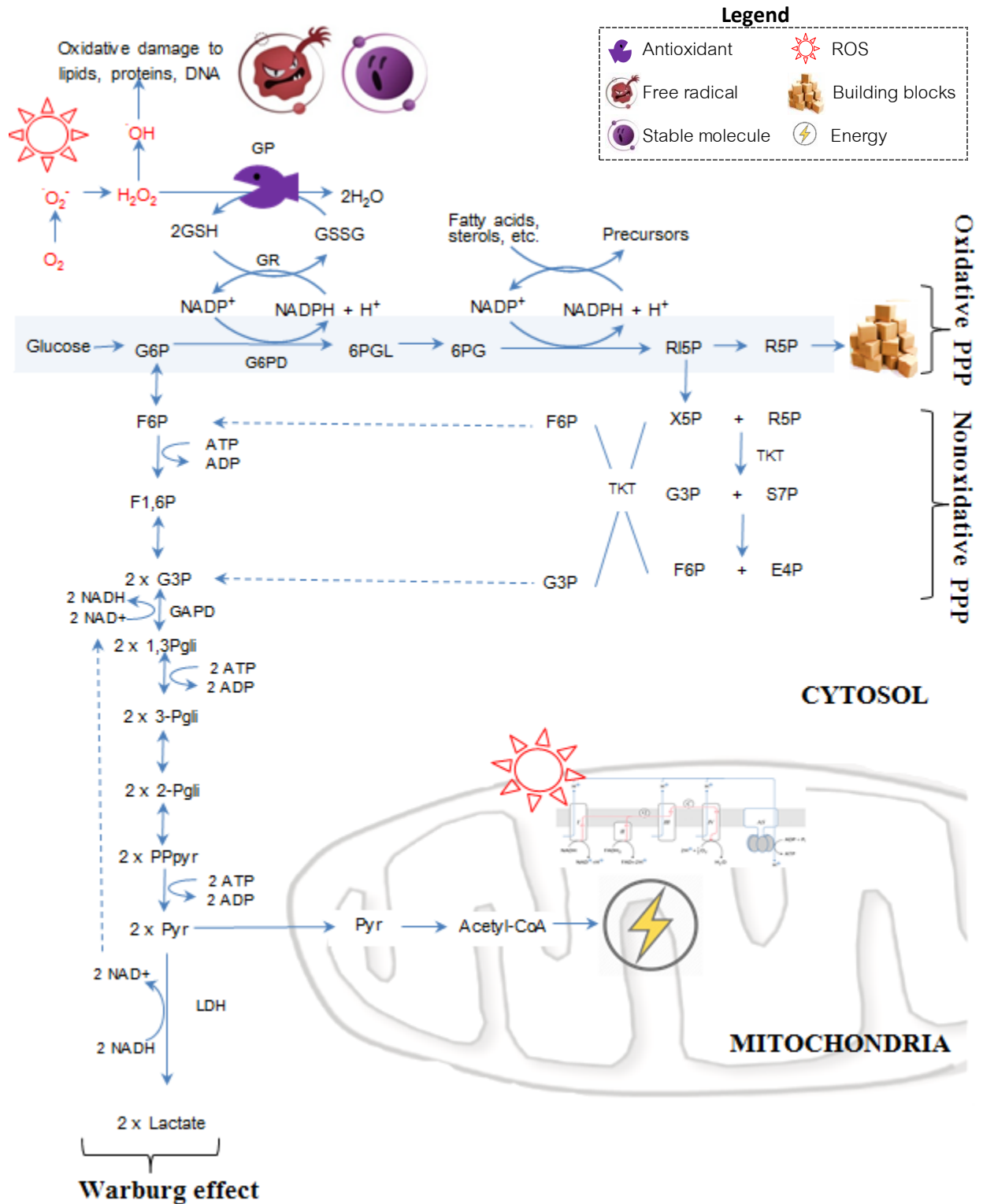


Figure 1.4. Glucose metabolism in mammalian cells.

inner membrane. During the electron transport process, protons are pumped in the inter-membrane space, increasing the number of negative remaining charges in the mitochondria, thus creating a gradient. The potential energy created in this gradient is necessary in the last complex of the respiratory chain, ATP synthesis. It will allow binding of inorganic phosphate by ADP to create ATP, while protons will be transferred back in the mitochondrial matrix *via* complex V.

The inner mitochondrial membrane is the main site of energy release but also the main ROS generator of cell. The electron transfer through complexes is not perfect. Electron leakage often happens on complex I and complex III, molecular oxygen being reduced to superoxide [25,39]. It can become a more stable ROS specie, being converted as H<sub>2</sub>O<sub>2</sub>, thus diffusing in cytosol. Here, the H<sub>2</sub>O<sub>2</sub> activity can be reduced or even stopped by antioxidant enzymes.

### 1.2.2 H<sub>2</sub>O<sub>2</sub> quenching in living cells

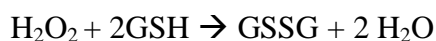
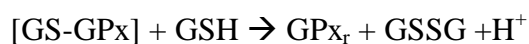
Two main catalytic mechanisms of antioxidant enzymes have been described. The H<sub>2</sub>O<sub>2</sub> conversion can be directly realized through an active locus metal ion or *via* pathways implying the electron transfer in regenerating redox couples containing sulfide bridges, as is the case for glutathione and thioredoxin systems [20]. The H<sub>2</sub>O<sub>2</sub> decomposition by heme group is one of the first observations of biological interest. The **catalase** binds to hydrogen peroxide molecules and decompose them into nontoxic elements as water and oxygen. This process takes part in two steps. Firstly, one molecule of H<sub>2</sub>O<sub>2</sub> links by catalase. In this process the hydrogen atom interacts with histidine amino acid contained in catalase structure and deprotonates it, making an electrostatic interaction between the anionic peroxide and iron Fe<sup>3+</sup>. One oxygen molecule remains covalently linked by the iron Fe<sup>5+</sup> containing catalase. Once the first water molecule is produced and regenerates the deprotonated histidine in the active site, the second H<sub>2</sub>O<sub>2</sub> molecule binds by the enzyme. It is spited in a similar way, thus resulting the first O<sub>2</sub> molecule and the second water compound. The catalase rate constant is estimated as  $2 \times 10^7 \text{M}^{-1} \text{s}^{-1}$  [40].

The oxido-reduction process of **peroxidase** is realized in a similar way as catalase, both enzymes containing heme groups with iron atom in the active center [41].

**Peroxiredoxin** is an enzymatic family characterized by the presence of cysteine residues in their active site. In mammalian cells 6 peroxiredoxin types are identified, all having similar

antioxidant role. In presence of a catalyst as  $\text{H}_2\text{O}_2$ , the thiol group is converted to sulfenic acid, then disulfide bounds are formed and the protein changes/switches its conformation. What distinguishes the different types of peroxiredoxins is the recycling back of sulfenic acid to a thiol [42–44].

**Glutathione peroxidase** (GPx) is an enzyme containing selenocysteine in the active site. It reacts in a similar way with  $\text{H}_2\text{O}_2$  with the particularity that the sulfur from thiol group is replaced by selenium [45]. In the process of  $\text{H}_2\text{O}_2$  decomposition, GSH plays a cofactor role to recycle the glutathione peroxidase, as can be observed in the following reactions [46]:



where  $\text{GPx}_r$ : reduced glutathione peroxidase,  $\text{GPx}_0$ : oxidized glutathione peroxidase,  $\text{GS-GPx}$ : glutathione-enzyme complex,  $\text{GSSG}$ : glutathione disulphide,  $\text{GSH}$ : glutathione.

The antioxidants previously described have a direct action on  $\text{H}_2\text{O}_2$ . They are maintained by their corresponding pathways and are all together involved in the regulation of redox homeostasis [47]. However, the main scavenging activity is performed by glutathione and peroxiredoxins enzymes [48]. Their activity is directly depending by glucose metabolic flux on Pentose Phosphate Pathway, being restored by NADPH produced here, after reacting with  $\text{H}_2\text{O}_2$ .

### 1.2.3 Pentose Phosphate Pathway

We previously describe the mechanism of creating energy from glucose. Glucose is necessary also to create building blocks. It is suggested by the name of the pathway itself being called pentose phosphate. This means that five carbon molecules and a phosphate group will result in a single compound. We find those elements in the DNA structure, the genetic code of

entire cell. Pentose Phosphate Pathway (PPP) is oxygen and ATP independent glucose metabolism.

In PPP are distinguished two distinct phases: one oxidative, the other non-oxidative. The first phase starts from G6P compound created in the glycolysis process. After enzymatic catalysis, ribose 5 pentose, CO<sub>2</sub> and NADPH are created.

NADPH is necessary due to the donor role required in the oxido-reduction of antioxidants. It is the way how the cell provides the scavenging power against oxidative species created as side products during electron transport chain in mitochondrial membrane. Under the activity of glutathione peroxidase, H<sub>2</sub>O<sub>2</sub> is converted in water by reduced glutathione. NADPH created after glucose 6-phosphate dehydrogenase catalysis, will be the electron donor involved together with glutathione reductase in the regeneration of GSH from its oxidized form GSSG [49]. When the cell need to produce more NADPH, ribose 5 pentose is recycled back into glucose 6 phosphate *via* non-oxidative phase. If the cell has to divide, the rate production of ribose 5 phosphate will increase. It will be necessary to produce nucleotides and nucleic acids for DNA synthesis.

### 1.3 Correlation between oxidative stress response and cell metabolism

ROS are created as byproducts during glycolysis. The energy synthesis is realized in presence of oxygen which can lose electrons and becomes a free radical. To overcome this issue, the cell develops its protection system dependent by glucose metabolism too. Antioxidants are regulated *via* pentose phosphate pathway, the main NADPH producer. It was observed that the ratio of NADP<sup>+</sup>:NADPH in cytosol is low,  $3 \times 10^{-7} / 3 \times 10^{-5} = 10^{-2}$  [47], comparing with NAD<sup>+</sup>:NADH (700 in cytosol; 7-8 in mitochondria [50–53]). The previews ratios quantification were determined via endpoint measurements, on lysed cells, 50 years ago. Their values are still used in modeling, because of the lack of recent determination in real time data. Real time experimental data are still on troubleshooting, due to the existing detector limitations. The known NAD<sup>+</sup>:NADH ratios are quantified between 100-850 using Sonar probe in various mammalian cells [54] while free NADPH:NADP<sup>+</sup> has been recently determined in cytosol,

nucleus and mitochondria as 55-80, 40-67 respectively 175-325 using time-correlated single photon counting TCSPC FLIM and FRET NAD(P)-Snifits sensor in mammalian cells [55].

$\text{NAD}^+$  is the main product generated during glycolysis; it accepts electrons leading to the glucose breakdown by oxidation, while NADPH is the electron donor necessary to regenerate the oxidized form of antioxidants back to their reduced form for instance to regenerate GSH/GSSG system.

Both NADH and NADPH are electron carriers soluble in water that can be reversibly oxidized. The pools of NADH and NADPH are maintained with different redox potentials in cells. NADH is an electron carrier for catabolic reactions in glucose metabolism while NADPH transfers electrons required in anabolic reactions. The ratios of [oxidized form]/[reduced form] are high for NADH and low for NADPH [49].

When cells have enough oxygen, one glucose molecule can be oxidized in order to generate 30 ATP *via* oxidative phosphorylation and only 2 ATP in glycolysis. It is obvious that most energy is produced in presence of oxygen, in the respiratory chain, leading also to reactive oxidative species as side products. In the late 19<sup>th</sup> century it was observed that, when the  $\text{O}_2$  levels decrease, cell shifts the energy production from oxidative phosphorylation *via* glycolysis: this phenomenon is called Pasteur Effect [49]. Later on, Otto Warburg noted that even when the oxygen levels are adequate, the rate of energy production in anaerobic glycolysis increases in cancer cells [56]. Anaerobic glycolysis is used with the purpose to create energy by converting the pyruvate into lactate, thus creating  $\text{NAD}^+$  necessary in catabolic reaction with Glyceraldehyde-3-phosphate [57]. Even if this mechanism leads to generation of much less ATP molecules, the lack of oxygen dependent reactions in glucose metabolism seems to have a crucial role in cancer development [56].

Since Warburg effect defines cancer disease as an injury of cellular respiration [58], it was exploited in anticancer therapies and it still remained one viable theory. Studies on mammalian cells are confirming metabolic advantages of cancer cells by increasing rate of anaerobic glycolysis as energy generation strategy. In cancer cells the ATP concentrations are lower, the mitochondrial membrane potential is decreased and the  $\text{NAD}^+:\text{NADH}$  and  $\text{NADP}^+:\text{NADPH}$  ratios are 5, respectively 10 times higher comparing with normal cells [59].

This suggests that cancer cells are maintaining a particular redox homeostasis, regulating the glucose metabolism in a specific way. Cancer cells developing tumors are experiencing specific metabolic conditions. They have to adapt in extreme situations as nutrient limitations or hypoxia which justify their necessity of surviving in metabolic stressful condition.

The glycolytic pathways are strongly interconnected, the key junctions biomolecules between PPP and glycolysis being G6P, pyruvate and acetyl CoA. (Figure 1.4) The glucose flux entering the PPP *via* G6P depends on cell type role and varies between 5-30% [60]. The basal rate of PPP is regulated by a key controller, G6PD, an enzyme highly expressed in cancer cells [60,61], with strong specificity for NADP<sup>+</sup>. NADPH is produced while G6PD oxidize G6P into 6PG. Even if the two glucose pathways are dividing at G6P, they remain tightly connected. The metabolic necessities of cell are regulated by reversible enzymatic reactions in the non-oxidative part of PPP.

The non-oxidative phase depends by the availability of enzyme substrates. The PPP or glycolysis will use G6P depending by the cell needs. In a simple manner we could say that, if ATP is necessary, glycolysis will be the main route of G6P. When NADPH is needed, PPP will be in favor to use G6P. It is a logic scenario, but in reality, the regulation of the glucose metabolism is not so simple. Indeed, when the cell is in the division phase, it requires making nucleic acids. R5P will be produced *via* non-oxidative phase of PPP. The biosynthesis is not a priority and NADPH is not going to be produced with an increased rate. If equal amounts of R5P and NADPH are necessary, they will be produced *via* oxidative phase of PPP. Liver cells, neurons or fat tissue are using much more NADPH than R5P to make fatty acids. Both oxidative and non-oxidative phases of PPP will be used, and a specific metabolic branch called gluconeogenesis. If both NADPH and ATP are needed, they will be produced *via* oxidative phase of PPP respectively glycolysis. F6P and G3P will enter glycolysis *via* pyruvate junction. It can be further used in biosynthesis or oxidized to produce more ATP in mitochondria [49].

Depending on metabolic requirements cancer cells activate PPP flux *via* specific mechanisms. NADPH is produced in PPP not only for biosynthesis, it is also the main reducing power used to protect biomolecules by oxidants [62].

We describe how PPP flux is regulated towards glycolysis. One standing question remained: how are aerobic and anaerobic glycolysis regulated? The anaerobic glycolysis is realized in cytoplasm, when glucose is split in two pyruvate molecules. Pyruvate will be metabolized then in mitochondria where the aerobic glycolysis takes place to generate energy and ROS as side products. Cancer cells are often exposed in extreme conditions, having limited access to oxygen. It was observed that in hypoxic conditions, cells generate superoxide anion. An increased production of superoxide leads to activation of aerobic glycolysis, by pH alkalization which increases the PFK activity in F6P – F1.6P catalysis. Superoxide is converted by superoxide dismutase into a more stable ROS, H<sub>2</sub>O<sub>2</sub>, whose longer lifetime provides an important role in signaling. Increased H<sub>2</sub>O<sub>2</sub> promotes the activation of HIF1 which stimulates the lactate production and decrease the oxidative phosphorylation rate. This is one of the proposed mechanisms of Warburg effect regulation in cancer cells.

## 1.4 Oxidative stress response and cellular fate

### 1.4.1 Adaptation of cell to stress

Adaptation of any life form is a required condition to survive, due to the dynamically changes of the environment. Specific receptors are integrated in their structure, constantly tracking the environmental changes. To adapt, the systems (cells, organisms) are regulating different functions, pathways or gene expression, according to the changes [63]. When damages encounter, repairing pathways will be regulated and defensive mechanisms will be activated. For example, when glucose is sensed by a cell, it will produce proteins involved in the trans-membrane transport to internalize it, then to metabolize it [64].

A system exposed to a stimulus, able to sense and respond to it, is considered adapted if it can return to steady state or near to it, after certain time duration. Limiting the duration response, the homeostasis of the system is involved in maintaining the basal activity. The process of reaching the basal level after stimulation is defined as perfect adaptation. When the system returns close to basal level without reaching it, one can consider near perfect adaptation [65].

Homeostasis is constantly maintained in cells by negative feedback loops. It manifests when a stress source occurs and the cell will initiate a protection mechanism to fight against

damages by reducing/inhibiting it, bringing the cell back to equilibrium. There are also situations when opposite effect can be preferred, when the system has to move farther away from the normal range. This is the positive feedback that intensifies the modification in the physiology of the system to a definite end point [66]. In the context of redox homeostasis, the adaptation is the ability of a cell to sense and to regulate a stimulus in order to reach back its homeostasis.

Homeostasis imbalance persistence occurs due to irreversible damages *via* positive feedback mechanisms or overwhelmed negative feedbacks. If the internal balance cannot be controlled and properly regulated, it can lead to diseases [2]. In perfect adaptation process, even if the signaling pathway is transiently responding to stimulation the response is independent of input stimuli. In this case, reaching the steady state after stimulation should not depend on the input [65,67].

#### 1.4.2 H<sub>2</sub>O<sub>2</sub> dualistic role

H<sub>2</sub>O<sub>2</sub> is known as a crucial redox metabolite controlling redox signaling, sensing and regulation processes [68]. It presents **signaling molecule** characteristics, observed since the 70's and proved during time [40]. H<sub>2</sub>O<sub>2</sub> is a small inorganic molecule playing a particular role in living systems, being able to travel from its production site to the action place. H<sub>2</sub>O<sub>2</sub> is an uncharged molecule with a neutral oxidation number (the oxidation number of hydrogen is +1, while the one of oxygen in a peroxide compound is -1). Its long lifetime of milliseconds provides an ability to diffuse through membranes, from one compartment to another or from one cell to another [69]. Its intracellular production is controlled according to the cellular needs, so its removal.

The hydrogen peroxide sensing phenomenon is an oxidation process of a specific macromolecule (proteins containing cys residues, iron, which are often antioxidant enzymes) which conducts to later modifications in the activity of the signaling pathway [70]. The H<sub>2</sub>O<sub>2</sub> molecule is reduced to water and oxygen most often by an enzymatic system produced by the cell itself.

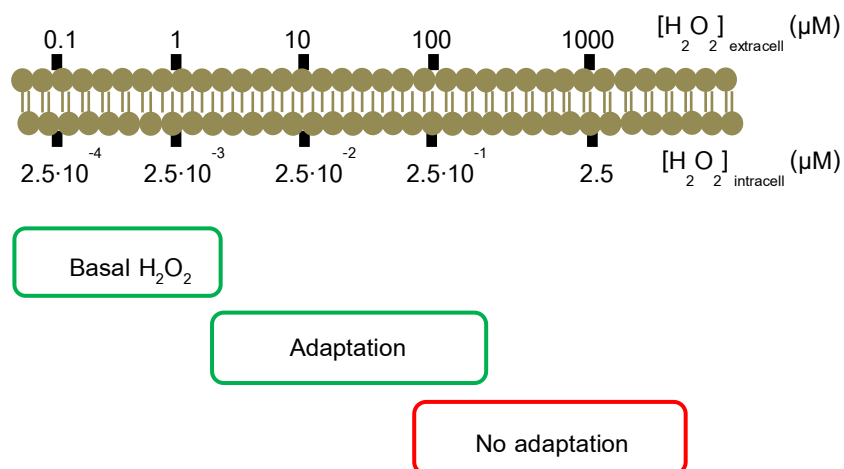


**Figure 1.5:** H<sub>2</sub>O<sub>2</sub> gradient through cellular plasma membrane (from [68])

The ability of a cell to adapt to oxidative stress is depending by the type of stimulus, the stimulation method and the dose received. Predicting the cellular adaptation by exploiting the H<sub>2</sub>O<sub>2</sub> dualistic role in cell involves finding the dose parameters. In pharmacology, the dose is simply considering by the stimulus concentration and the time of exposing the system to it. Despite biological particularities of cells as membrane permeability, metabolic activity, etc, concentrations leading to cellular adaptation to stress have been suggested (**Figure 1.5**). However, the temporal patterns of its appliance are difficult to define. Gradual stimulation and fractional stress could lead to better adaptation of the system [1] but their adjustments are unclear.

H<sub>2</sub>O<sub>2</sub> diffusion through cellular plasma membrane is not a classical diffusion process. H<sub>2</sub>O<sub>2</sub> is a small inorganic molecule that can freely cross the membrane. Once it is inside the cell, the homeostatic processes interplay the internal H<sub>2</sub>O<sub>2</sub> regulation. Recent studies lead to a mediated diffusion via peroxiporins aquaporins [71]. The H<sub>2</sub>O<sub>2</sub> gradient was estimated, in a simplified mammalian system, taking into account the main H<sub>2</sub>O<sub>2</sub> antioxidants activity, as 10 [72]. Once the system becomes more complex, and more quenchers are considered, the gradient between extracellular and intracellular H<sub>2</sub>O<sub>2</sub> levels are estimated between 200 - 650 [73,74]. Recent experimental data [75] are showing that the inter-membrane gradient established under extracellular stimulation with μM of H<sub>2</sub>O<sub>2</sub> is 390±40. However, it is a limited quenching power of the cell against external H<sub>2</sub>O<sub>2</sub> sources. Once they are overpassed, the cell is injured leading

from reversible processes that we call adaptation to irreversible damages as tumor-genesis or death [76].

### 1.4.3 Cell death as non-adaptive response

Death is naturally occurring in all living systems. *Via* this process the systems that can perform their function are selected and the ones whose activity have been damaged or represent a damage risk are removed. Regulatory genes are constantly controlling mechanisms of cell division, identification of cellular abnormalities and activate programmed cell death when necessary. This way the homeostatic balance is maintained in multicellular organisms. Uncontrolled cellular death can lead to degenerative diseases as Parkinson or Alzheimer, while excessive proliferation conducts to diseases as cancer which can provoke the death of the entire organism. The obstruction of programmed death mechanisms can influence the selectivity process, favoring the anticancer therapy resistance. Understanding how cells can lose their viability and in which conditions they die is necessary in the context of finding anticancer strategies of therapy [77].

Cell death is defined as a process when a cell loses its viability. Under stress conditions, death is an effect of non-adaptation to the changes, when the system reaches to the “point of no return” and the irreversible process of death starts. In the last years many cell death types have been identified. They can be classified in 3 main categories of cell death, based on their molecular regulations and their morphological criteria [77,78]:

- apoptosis: programmed cell death, characterized by apoptotic bodies formation;
- autophagy: self-eating process culminating with lysosomal degradation;
- necrosis: uncontrolled cell death, culminating with cell corpses as terminal effect.

The different cell death types are interconnected each cell death manner presenting different interconnectivities degrees. In reality, it is difficult to constraint complex systems as living cells to behave on the assumption that each death pathway would operate individually, even if from the therapeutic perspective drugs have been developed on this premise [78].

The molecular mechanisms involved in programmed cell death are also responsible of non-lethal processes as senescence, mitotic catastrophe and terminal differentiation that occur to stop the activity of damaged cell [78].

Regulated cell death mechanisms can occur in two different scenarios. The first is known as programmed cell death and it acts as a built-in effector, in the absence of any external perturbation. The other one is activated in presence of a prolonged or intense external or internal perturbation of internal homeostasis, when adaptation processes to restore the internal balance of cell cannot be restored anymore [78].

Concerning cell death induced by ROS, it has been observed intrinsic apoptosis, ferroptosis, lysosome dependent cell death, netotic cell death and necrosis [78]. Intrinsic apoptosis is initiated by different perturbations existent in the environment as: ROS overabundance, DNA damages, mitotic errors and alterations leading to ROS producing intracellular compartments.

Apoptosis distinguishes by the changes made in different cell compartments during the process: phosphatidylserine translocations in the cellular lipid bilayer, chromatin condensation in nucleus and pro-apoptotic molecules activation as caspase family in cytosol and mitochondria [79]. Ferroptosis occurs at severe lipid peroxidation process leading in ROS and iron generation. Lysosome dependent cell death ROS are responsible of lysosome membrane permeability. Netotic cell death type is specific for neutrophils being particularly ROS mediated.

Necrosis is a process, occurring accidentally. It depends by the concentration of ROS and the time of stimulation [79].

As each ROS species present specific reactive proprieties, we are asking if they could be able to mediate in a specific way a particular type of death processes. Suggestions were made about the role of hydrogen peroxide of acting as regulator in pathways where caspases and pro-apoptotic molecules are implied. It has been observed that  $H_2O_2$  induced more severe damages than another ROS as superoxide or singlet oxygen [79].

Pentose Phosphate Pathway is the main antioxidant regulator in cytosol. Intracellular ROS and GSH are mediators in cell death and apoptosis processes. Increased G6PD activity

producing reducing equivalents (power) has anti-apoptotic and pro-survival role. Cell death induced by  $\text{H}_2\text{O}_2$  is more efficient when G6PD activity is inhibited (by DHEA and 6AN); contrary, the over expression of G6PD favors the cell survival (resistance to apoptosis). However, higher PPP flux leads to increased levels of NADPH providing apoptosis resistance.

In experimental models, overexpressing PPP gatekeepers enzymes as G6PD, TKT or TA are showing cell survival due to PPP hyper activation. On the other hand, instead of inhibiting a certain enzyme, the alternation between the oxidative and non-oxidative PPP branches seems to promote cell survival and apoptosis resistance. The pathological meaning of PPP and its role in cell transformation in carcinogenesis has still to be experimentally proven [60].

## 1.5 $\text{H}_2\text{O}_2$ as a tool to perturb redox balance

Our study comes in the context of molecular detection techniques development in living cells. Intracellular regulation pathways of different cellular functions have been identified in the last 100 years and their regulation has been explained mostly based on endpoint measurements that have been performed on populations of lysed cells. The chemical advances in synthesizing, decomposing and stabilizing peroxide molecules are the starting point in observing the  $\text{H}_2\text{O}_2$  role in biology. Its contribution has been observed in parallel with the intracellular antioxidants discovery and the detection of internal production sources as electron transport chain in presence of oxygen.

The progressing in the development of the genetically encoded fluorescent proteins probes made in the last 20 years allows us to track a specific protein in living cells and to monitor  $\text{H}_2\text{O}_2$  dynamics in real time, with minimal perturbation of the system. Once the GFP have been discovered, various genetically encoded probes have been developed. Our interest is focusing on metabolic related sensitive probes targeting  $\text{H}_2\text{O}_2$  (Grx1-roGFP2, HyPer), NAD(P)H cofactors (Frex, iNAP) or the ratio NAD(P)H/NAD(P)<sup>+</sup> (Perox, Sonar, Apollo). Using the intracellular sensors allow us monitoring the molecular dynamics in real time and to address cellular adaptation to oxidative stress.

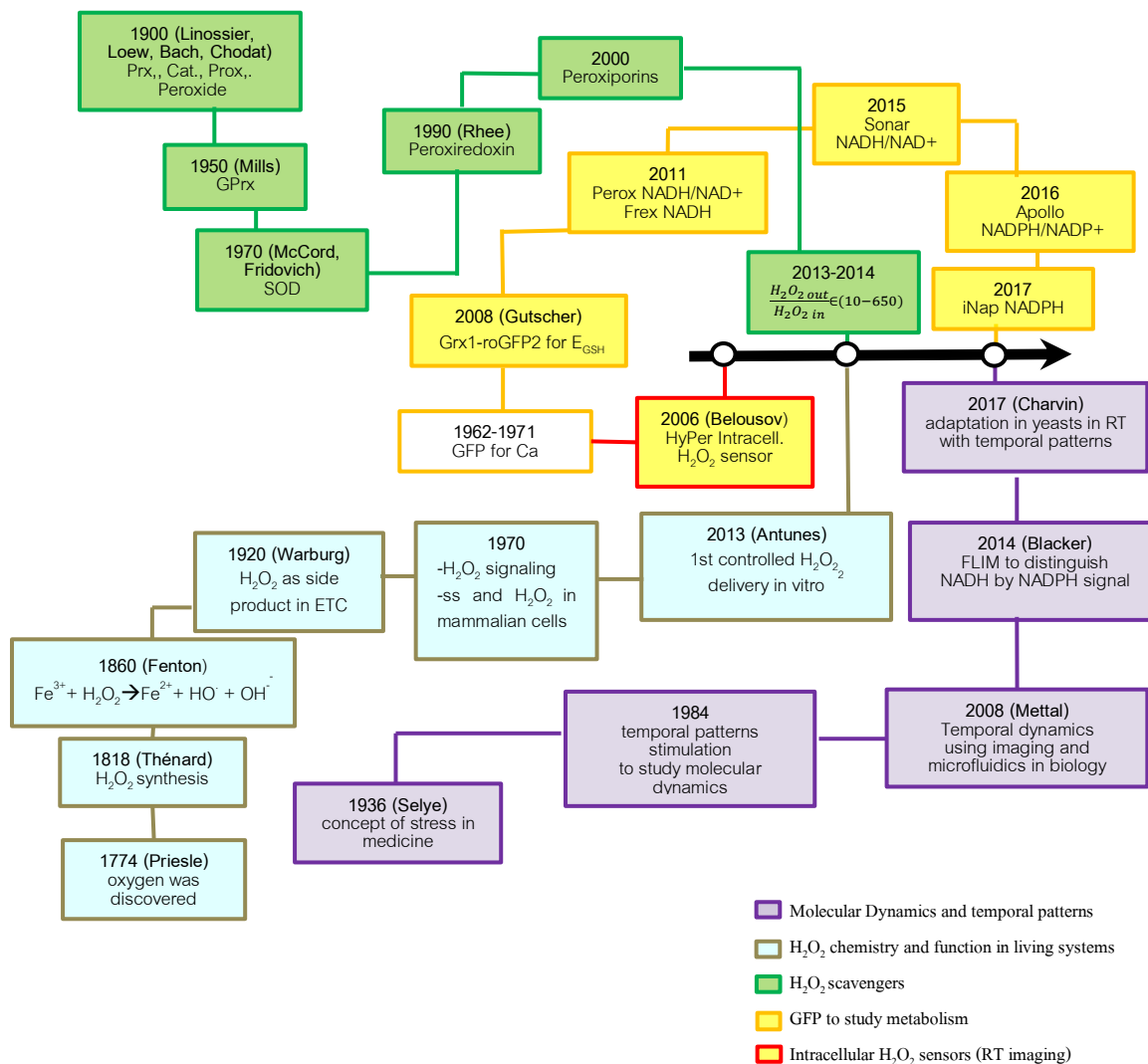


**Figure 1.6:** Timeline of the advances in real time molecular dynamics with temporal modulated patterns of  $H_2O_2$ . Abbreviations: Glutathione Peroxidase (GPrx), Superoxide Dismutase (SOD), Catalase (Cat.), Peroxidase (Prx), Peroxidases (Prox), Glutathione redox potential ( $E_{GSH}$ ), Nicotinamide adenine dinucleotide (NADH), Nicotinamide adenine dinucleotide phosphate (NADPH), Green Fluorescent Protein (GFP), Electronic Transport Chain (ETC), Fluorescence Lifetime Imaging Microscopy (FLIM), disulfide bonds (ss), hydrogen peroxide ( $H_2O_2$ ), Real time (RT).

Given the dualistic role that  $\text{H}_2\text{O}_2$  can play in living cells, it becomes an interest to quantify its dynamics in time and space. Deregulation in metabolic state of the cell leads to different responses in oxidative stress conditions. Tools for studying the dynamics of molecular adaptation under stress conditions have been developed (**Figure 1.6**).

The experimental systems usually preferred in microscopy are unicellular organisms as bacteria or yeasts because they can mimic an independent organism. They, are small and complex, easy to culture and to follow their generations in a few hours experiment. In a basal study of medical interest for understanding human metabolic diseases, bio-mimetic systems populations of mammalian cells cultured *in vitro* are of interest. The commercially available cell lines are well characterized in different growing conditions and are accessible for every lab working in the field. This allows us to compare the obtained results and to build the puzzle of a certain topic we are involved in. In the context of cell-to-cell variability, recent *in vitro* studies focus on single cell and the classification of different behaviors according to defined characteristics [80–84].

Time varying chemical patters have been observed naturally, for example in circadian rhythmicity [85]. They allow the system to adapt to the environmental changes. To create experimentally time-controlled stress patterns, fluidic systems have been developed. In time, they have been designed from macro to micro level, providing better flow profile control and smaller stimulation volumes to be used. As *in vitro* cultures are sensitive to changes, seeding them in micro environments would add a supplementary perturbation to the system. In our study we will present a custom macrochamber connected to fluidic system. The parallel plates are maintaining a laminar flow, controlling the delivery of the external  $\text{H}_2\text{O}_2$  stimulation to the seeded/bottom adherent cells.

The necessity of our study is justified by the fact that, during the time, the techniques of following the intracellular  $\text{H}_2\text{O}_2$  in cells evolved, so the *in vitro* cell culture maintenance and detection reagents of targeted molecules involved in oxidative processes in living cells or out of cells. Once with the development of genetically encoded fluorescent proteins it becomes possible to monitor specific proteins in living cells. Nowadays most studies focus on their spatial and temporal localization, using time lapse imaging.

Our study is focusing on monitoring the molecular dynamics in living cells upon controlled time varying stimuli of  $H_2O_2$  in *in vitro* mammalian cancer cells as model systems. We propose a single stress stimulation pattern for simplicity. Cellular adaptation will be observed in a dose-controlled environment. This process will be characterized once the parameters are identified. In this context, we will try to find if there is a link between glucose metabolism and adaptation. The major negative feedback source controlled by the glucose metabolism will be highlighted by varying the key molecules which control it. Finally, a small introductory study in the death induced by external  $H_2O_2$  will be made. It is a starting point in defining a protocol to study the molecular regulation of cellular death as molecular dynamic process.

## Chapter 2: How to control the H<sub>2</sub>O<sub>2</sub> stimulus?

### 2.1 Introduction

In the inner life of the cell are protective mechanisms dynamically orchestrated by molecules [70]. If the cell cannot recover its initial state, permanent damages can occur. In this way mutations can be created, leading to metabolic diseases as cancer [86]. In this context, one can ask how a system can adapt to a new condition and cells survive or die after a harmful event? [65]. Gradual stress exposure can reduce the cellular sensitivity, which is an important issue in anticancer therapies, where adaptation of cells to ROS mediated treatment can lead to cancer progression [7,87].

An organism is normally exposed to stress factors. Depending by the nature, the amplitude or the duration of the stress applied, the homeostasis of the cell is perturbed. To quantify the output response of the system exposed to new environmental conditions, the input has to be well controlled. This is one of the main outcomes in our experimental work: how to control H<sub>2</sub>O<sub>2</sub> stimulus delivered in order to quantify the cellular response to it? In this context, before choosing the method of H<sub>2</sub>O<sub>2</sub> stimulation, we defined the dose parameters we want to control. Time of exposure to stress has to be longer than the first adaptation signs that could appear, and it is fixed to one hour in our experimental conditions. As pointed out in first chapter, in redox homeostasis adaptation, direct enzymatic modifications can appear in timescales of seconds to minutes [1]. One hour under stimulation will allow observing the adaptation when it will occur. The second aspect we want to control is the concentration of H<sub>2</sub>O<sub>2</sub> applied to the cell, as H<sub>2</sub>O<sub>2</sub> is a very reactive compound. To deliver it in a constant concentration during one hour, its interactions with both the cell and culture medium have to be evaluated before. Considering this, the parameters that matters for making steady state stimulation with H<sub>2</sub>O<sub>2</sub> are discussed. We will present what are the artifacts that can interfere in intracellular H<sub>2</sub>O<sub>2</sub> fine tuning delivery and how to quantify this molecule in a simple or complex extracellular environment. Controlled temporal and spatial stimulation with H<sub>2</sub>O<sub>2</sub> method for *in vitro* cell cultures is proposed. Using it, intracellular hydrogen peroxide dynamics can thus be modulated in cellular cytoplasm.

Once the dose is controlled, our intention is to observe the cellular response to stress. In our study we focus on the regulatory and harmful role of intracellular oxidative processes, in particular H<sub>2</sub>O<sub>2</sub>. Trying to identify the threshold dose at which H<sub>2</sub>O<sub>2</sub> stop having signaling features and when it starts creating cellular damages enough to induce cell death a literature study is made. Varying the dose of H<sub>2</sub>O<sub>2</sub> stimulation, the percentage of dead and surviving cells is experimentally determined and compared with some published results. Modulating glucose metabolism will point out if the cellular vulnerability to H<sub>2</sub>O<sub>2</sub> stimulus is regulated by this process. To find out, similar dose response experiments are made where cellular fate is quantified. Finally, to validate the stimulation method suggested using fluidic system, cell death in both static and microfluidics delivery are compared.

## 2.2 Methods of creating H<sub>2</sub>O<sub>2</sub> stress stimuli

Cell responses to external stimuli are dose dependent. For this purpose controlling the concentration of the stimuli and the time of its appliance is a key parameter [36]. Here are proposed different methods of H<sub>2</sub>O<sub>2</sub> stimulation, extracellular or intracellular creating sources (**Figure 2.1**). Critical overview on the benefits, advantages, disadvantages and limits of H<sub>2</sub>O<sub>2</sub> cellular exposure to create controlled stimulation is presented (**Table 2.1**). Depending on the delivery system steady state stress patterns can be thus created.

Different ways to expose cells to hydrogen peroxide coming from exogenous source have been developed. The simplest and the most common used is the direct addition of H<sub>2</sub>O<sub>2</sub> solution to the experimental sample. The method consists in creating dilutions starting from a stabilized H<sub>2</sub>O<sub>2</sub> solution. The stabilizer of most tested solution on living cells is stannate and phosphorus-containing compounds, added in concentrations of 0.5 ppm respectively 1 ppm [88,89]. Commercially available stabilized solutions have 30% H<sub>2</sub>O<sub>2</sub> concentration (equivalent to 9.7 M). To expose cells to micromolar concentrations, serial dilutions have to be made thus the working solution to be in mM ranges. A certain volume of working solution will be added in the cell culture medium which will be then after added to cells. Precise concentrations of H<sub>2</sub>O<sub>2</sub> can be thus difficult to obtain due to uncertainty generated by dilution cascades.

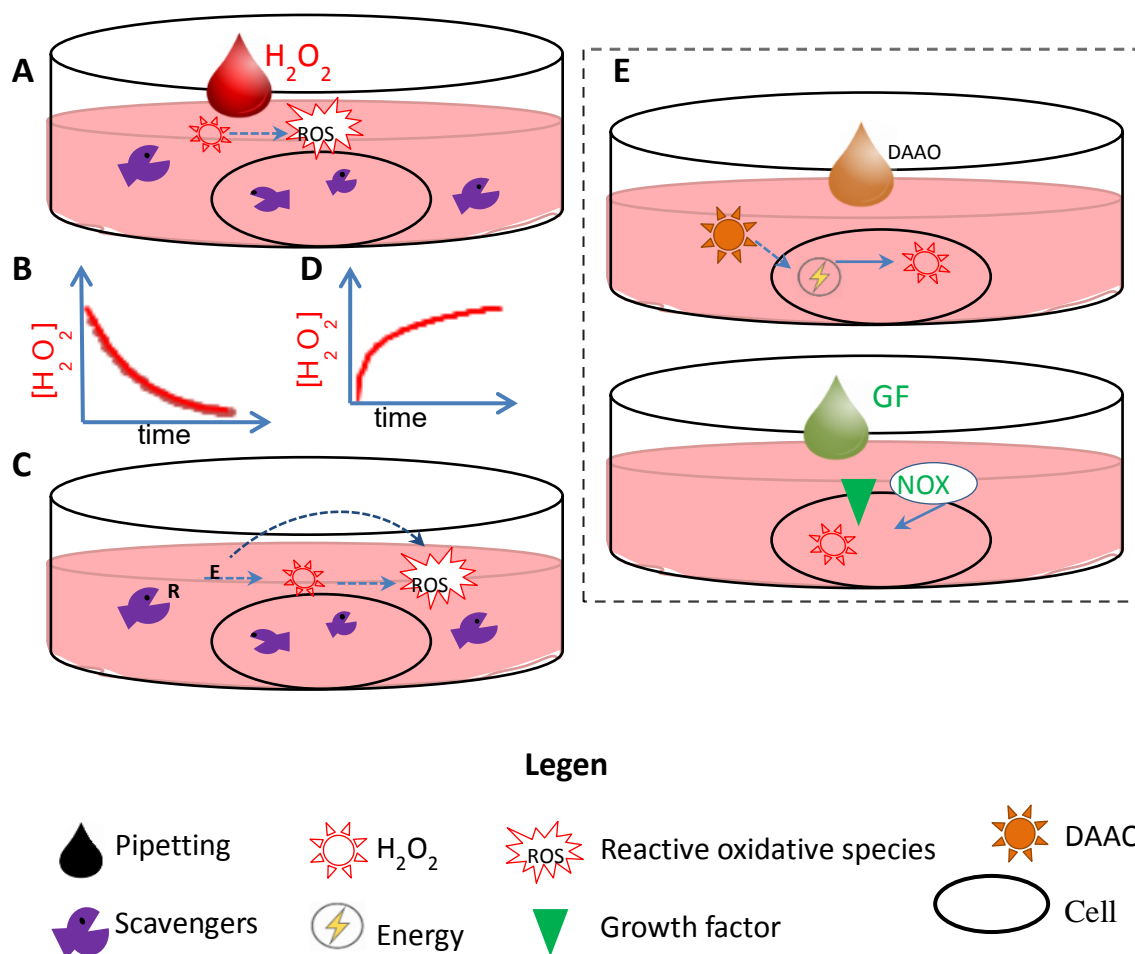


**Figure 2.1:** Methods of  $H_2O_2$  delivery system and the corresponding concentration profiles provided to seeded cells. (A) Bolus or bulk method by mixing  $H_2O_2$  in cell culture media. (B) The presence of scavengers in medium and the cells are reducing the  $[H_2O_2]$  in time. (C) Extracellular reactions often mediated by enzymes E can be initiated in cell culture media as  $H_2O_2$  generating sources. (D) Extracellular  $H_2O_2$  continuous generating source presents a logarithmic profile; the enzymatic activity increases the  $H_2O_2$  production to a certain maximum. Once the substrate of reaction is consumed, the reaction ends. It leads to the decrease of the external stimuli with similar profile as in bolus. (E) Intracellular  $H_2O_2$  continuous generating sources: exploiting the amino acid oxidase (DAAO) sensitivity to d-alanine allows creation of locally intracellular  $H_2O_2$ . Once the DAAO transfection is done, the internal  $[H_2O_2]$  can be varied by modulating the d-alanine concentration added in medium (top); Similarly, NOX pathway can be used to generate internal  $H_2O_2$  sources (bottom).

**Table 2.1:** Different methods of H<sub>2</sub>O<sub>2</sub> temporal oxidative stress stimuli delivery.

	<b>Bolus</b>	<b>Extracellular H<sub>2</sub>O<sub>2</sub> delivery</b>	<b>Intracellular H<sub>2</sub>O<sub>2</sub> delivery</b>
<b>Advantages</b>	Easy to use	Continuous H <sub>2</sub> O <sub>2</sub> generation	Suitable for specific molecular dynamics pathways regulation processes/monitoring  Spatial localized H <sub>2</sub> O <sub>2</sub> production
<b>Limitations</b>		Enzymatic dependent => reaching the steady state [H <sub>2</sub> O <sub>2</sub> ] is dependent by the reaction speed;  Addition of another elements in the cell culture medium; the sensitivity of cells to new compounds is another troubleshooting step and might be difficult to analyze;  Side ROS creation;	Metabolic perturbation  Side ROS creation;
	H <sub>2</sub> O <sub>2</sub> instability in medium;  Static system favors the H <sub>2</sub> O <sub>2</sub> consumption by cells;  One single step stimuli pattern;  To stop the H <sub>2</sub> O <sub>2</sub> stress, using H <sub>2</sub> O <sub>2</sub> quenchers (as catalase) or renew the medium do not allow the immediate stress stop		

The method of pipetting H<sub>2</sub>O<sub>2</sub> solution to the cells is called **bolus** or bulk addition (**Figure 2.1 A**). Mammalian cells, being complex systems, are maintained in a special culture medium containing many organic nutrients. Direct addition of hydrogen peroxide in the cell culture medium does not allow maintaining a constant stimulation source to the cells (**Figure 2.1 B**). The reason is that H<sub>2</sub>O<sub>2</sub> can react rapidly with oxidant molecules contained in culture media, as pyruvate, phenols, amino acids or transition metals [90,91]. Side ROS can be produced either by instantaneous decomposition of H<sub>2</sub>O<sub>2</sub> in free radicals either as reaction products with chemicals in the medium.

A more suitable method of a continuous H<sub>2</sub>O<sub>2</sub> generating system source (**Figure 2.1 C, D**) is its **extracellular production using enzymatic systems** (glucose oxidase, amino acid

**Table 2.2:** Enzymatic mediated reactions used to create extracellular continuous H<sub>2</sub>O<sub>2</sub> generating systems.

Reactants	Products	Enzyme
L-amino acid + O <sub>2</sub> + H <sub>2</sub> O	α-Keto acid + NH <sub>4</sub> + H <sub>2</sub> O <sub>2</sub>	L-amino acid Oxidase
D-galactose + O <sub>2</sub>	DGH + H <sub>2</sub> O <sub>2</sub>	Galactose Oxidase
Glycolipid polysacch. + O <sub>2</sub>		Xanthine Oxidase
Glycoprotein + O <sub>2</sub>		Glucose Oxidase
Xanthine + H <sub>2</sub> O + O <sub>2</sub>	Uric acid + H <sub>2</sub> O <sub>2</sub>	
β-D-Glucose + O <sub>2</sub>	DGL + H <sub>2</sub> O <sub>2</sub>	
Ascorb. + Menadione + O <sub>2</sub>	O <sub>2</sub> → H <sub>2</sub> O <sub>2</sub>	

oxidase) having culture medium elements as substrate (glucose, amino acids). Thus, the presence of the organic elements can be exploited and used for creating a continuous H<sub>2</sub>O<sub>2</sub> source. If those elements cannot be consumed from the medium due to the particularity of the study, a reaction can be initiated by addition of other chemicals which can act as H<sub>2</sub>O<sub>2</sub> generating system. For example, ascorbate and menadione can be added in the medium and, in the presence of atmospheric oxygen, H<sub>2</sub>O<sub>2</sub> can be created as a reaction product. The first ROS created is superoxide that can either become stable specie, thus creating H<sub>2</sub>O<sub>2</sub>, either react with elements existing in the cell culture medium (**Table 2.2**).

A similar issue appears in the enzymatic H<sub>2</sub>O<sub>2</sub> production. ROS can be produced similarly as in bolus method or during the enzymatic reaction as primary or secondary products. During the reaction, another ROS can be created, either directly, either by spontaneous H<sub>2</sub>O<sub>2</sub> decomposition. Moreover, cells can be sensitive to consumption of substrates by the enzymatic systems (glucose, aminoacids) and the results of the study can be influenced by metabolic perturbation of cell. Choosing the medium in which the external stimuli is created is one of the first steps in our study.

From the methods described previously, we can conclude that, to create steady state stimulation, one have to consider the followings: the H<sub>2</sub>O<sub>2</sub> degradation by the chemicals existing in media and if the composition of cell culture media allows creating H<sub>2</sub>O<sub>2</sub> continuous generation.

Both of presented methods are static delivery systems. It was observed that the intracellular antioxidants make the cells themselves H<sub>2</sub>O<sub>2</sub> consumers [91]. When bolus method and glucose oxidase system are compared is observed that the regulatory effects of H<sub>2</sub>O<sub>2</sub>

monitored spatially inside the cell, are differently expressed [92]. To design steady state stress sources, one have to consider all the quenching processes that could decrease the H<sub>2</sub>O<sub>2</sub> concentration during the incubation of cells.

As the extracellular stimulation of cells to a controlled and stabile H<sub>2</sub>O<sub>2</sub> concentration is difficult to be made, **intracellular H<sub>2</sub>O<sub>2</sub> sources** are proposed. In this context tetra butyl hydrogen peroxide is often considered to replace the use of H<sub>2</sub>O<sub>2</sub> solution, due to its stability. Both are relevant ROS forms, but they are not equivalent. There are studies showing that the two can have different effects in the cell [93]. Indeed, being different compounds (one organic, the other inorganic) they will enter differently inside the cell, will have different reaction mechanisms and they will affect differently the cells.

In general, intracellular H<sub>2</sub>O<sub>2</sub> generation methods are preferred because they represent a very good way of avoiding the H<sub>2</sub>O<sub>2</sub> degradation by the extracellular culture medium (**Figure 2.1 E**). The principle of intracellular H<sub>2</sub>O<sub>2</sub> creation is to add a certain substrate as growth factors (EGFR [94], Nox modulators [95]) or aminoacids (D-alanine [96,97]) that will activate some key pathways able to create H<sub>2</sub>O<sub>2</sub>. Unfortunately, these methods of creating H<sub>2</sub>O<sub>2</sub> imply the cell metabolic use also and it is not suitable for studies where the cellular metabolic activity is relevant. On the other hand, the technique of substrate modulation is successfully applied for monitoring local production of H<sub>2</sub>O<sub>2</sub> [98], but the H<sub>2</sub>O<sub>2</sub> concentration is difficult to control.

The first controlled and calibrated method of H<sub>2</sub>O<sub>2</sub> delivery for *in vitro* experimental work combined the bulk and extracellular production of H<sub>2</sub>O<sub>2</sub> to keep the external [H<sub>2</sub>O<sub>2</sub>] constant in complex medium for a certain time (ranging from few minutes to few hours). In this method, H<sub>2</sub>O<sub>2</sub> rate production is dependent by the volume of cell culture medium and the consumption rate is depending by the cell density. Considering that, the steady state H<sub>2</sub>O<sub>2</sub> source is created by using both enzymatic production and H<sub>2</sub>O<sub>2</sub> solution [91].

## 2.3 Creating H<sub>2</sub>O<sub>2</sub> steady state stress pattern using bolus method

Bolus stimulation is the easiest way to stimulate cells and it simply consists in mixing the hydrogen peroxide solution with the cell culture medium, than adding it to the cells. Limitations of using this method are concerning maintaining constant in time the H<sub>2</sub>O<sub>2</sub> concentration. The main intention in this section is to find a sensitive way to quantify the H<sub>2</sub>O<sub>2</sub> temporal stability in extracellular medium. Kinetics consumption of H<sub>2</sub>O<sub>2</sub> in the timescales of our experimental conditions are measured in cell culture medium and in presence of breast cancer cells (MCF7wt).

### 2.3.1 H<sub>2</sub>O<sub>2</sub> degradation by cell culture media

H<sub>2</sub>O<sub>2</sub> is unstable molecule, having a shorter lifetime in biological environment. Comparing to another unicellular organisms growth conditions, the *in vitro* mammalian cells are maintained in a liquid buffer containing many organic compounds and metals that can quench the H<sub>2</sub>O<sub>2</sub>. For this purpose creating a continuous external H<sub>2</sub>O<sub>2</sub> stimulus requires supplementary measurements.

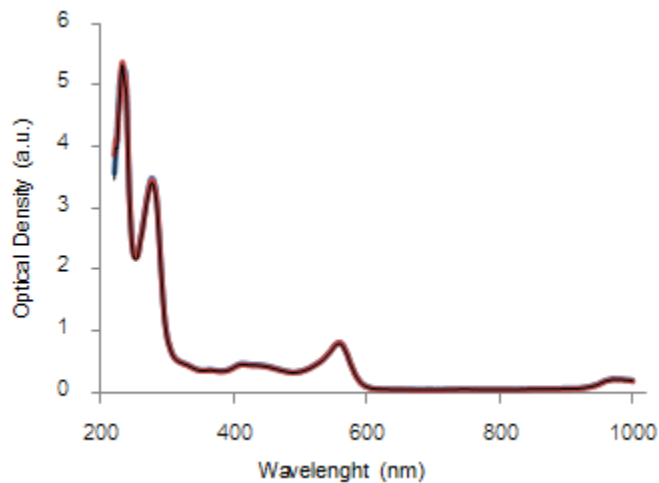
#### 2.3.1.1 Detection method of H<sub>2</sub>O<sub>2</sub> in cell culture media

Choosing the method of H<sub>2</sub>O<sub>2</sub> detection has a particular role in our study. Mammalian cells are growing in a complex media, containing metallic ions and organic compounds as amino-acids, proteins, phenols, etc. Specific and high sensitive H<sub>2</sub>O<sub>2</sub> probes are difficult to use in these conditions. The addition of chemicals in culture medium to create externally cell stimulation can lead to the creation of other reaction products which can show more complex cell responses, as a result of unquantifiable oxidative species generation. Before making external cell stimulation, the stability of H<sub>2</sub>O<sub>2</sub> in the culture media will be studied.

To minimize the error propagation, we are wondering if it would be a way to direct detects the H<sub>2</sub>O<sub>2</sub> in cell culture media. It is a very complex solution, containing many organic compounds, some of them showing UV-vis absorption spectra (**Figure 2.2**). It would be impossible to distinguish the H<sub>2</sub>O<sub>2</sub> absorbance at 240 nm in such a high background. Moreover,

**Table 2.2:** Methods of extracellular H<sub>2</sub>O<sub>2</sub> detection

Method	Principle	Sensitivity	Detection particularities
Titration	$m_2M_1V_1 = m_1M_2V_2$	mM	
Spectrophotometry	$A = \epsilon lc$	$10^2 \mu\text{M} - 10^2 \text{mM}$	direct H <sub>2</sub> O <sub>2</sub> detection; photobleaching; high background
Colorimetry	$f(A) = c$	$10^2 \mu\text{M} - 10^2 \text{mM}$	easy to use and to calibrate; fast response time (few minutes) side ROS production
Fluorescence	Light + dye $\rightarrow$ dye*	$\mu\text{M}$	easy to use and to calibrate; fast response time side ROS production; enzymatic dependent Background signal Photobleaching
Luminescence	Luminescent material + catalyst $\rightarrow$ luminescent material + light	nM - $\mu\text{M}$	No background signal The sensitivity of signal is not limited by interference No stokes shift limitations
Electrochemistry	$E_{\text{red}} = E_{\text{red}}^* - RT/zF \cdot \log(a_{\text{red}}/a_{\text{ox}})$	nM - $\mu\text{M}$	Indirect method

**Figure 2.2:** UV-Vis spectrum of complete cellular culture media (DMEM)

we are interested to stimulate cells with concentrations in micromolar range. The direct detection by reading the absorbance in UV range, does not allow such sensitivity (**Table 2.3**). Moreover, the interaction of H<sub>2</sub>O<sub>2</sub> with UV light can drive to the generation of highly reactive oxidative species as hydroxyl radical ( $\cdot\text{OH}$ ) [99].

I will present the relevant methods of investigation to detect H<sub>2</sub>O<sub>2</sub>, highlighting for each their benefits and limitations for our research question (**Table 2.3**).

Titration method (with iodine, permanganate or ceric sulfate) requires acidic condition of the reaction and would not be efficient in neutral pH conditions as required for *in vitro* cell culture conditions. The metallic ions existing in media can act as catalysts (Fe, Ni, Cr, Cu) in titration reactions. The detection range of this method is on mM order and do not cover the range of  $\mu\text{M}$  detection we are targeting in our experiments [100].

Spectrophotometric methods for measuring the H<sub>2</sub>O<sub>2</sub> concentration in cell culture medium are still indirect H<sub>2</sub>O<sub>2</sub> detection ways, more precise than titration, still on mM range sensitivity, able to exploit the peroxide's reducing properties. In presence of cobalt, iodine, titanium or xylenol orange colored compounds can be created and detected in visible range [100,101].

Most suitable system of H<sub>2</sub>O<sub>2</sub> detection in cell culture media, are the common photoluminescent (fluorescent) sensors enzymatically dependent. Horseradish Peroxidase (HRP) is an enzyme that is activated by an electron donor as H<sub>2</sub>O<sub>2</sub>. In the presence of a substrate as Amplex red [102], Phenol red [103] or ABTS [104] a fluorescent product is created. The complexes are active at 37° C, pH 7.5 and sensitive to a small range of H<sub>2</sub>O<sub>2</sub> concentrations of  $\mu\text{M}$  order.

As H<sub>2</sub>O<sub>2</sub> is a stable molecule only in certain stabilized conditions[88,89], we are looking for a specific and direct detection method. From now, only the fluorescence, known also as photoluminescence method, seems to be suitable for the micromolar range of detection. Unfortunately, the sensitivity of fluorescence is limited by the presence of background signal, interference or stokes shift issues [105].

The electrochemistry methods are exploiting the fact that H<sub>2</sub>O<sub>2</sub> can be decomposed by catalase enzyme in H<sub>2</sub>O and O<sub>2</sub>. Using an oxygen sensor, we are able to estimate the H<sub>2</sub>O<sub>2</sub> degradation by monitoring the O<sub>2</sub> kinetics [91]. The device would have been suitable for measuring the H<sub>2</sub>O<sub>2</sub> stability in different media conditions, but it is still an indirect way of detection, dependent of the enzymatic activity.

As an alternative, chemiluminiscent probes have been developed. Comparing to fluorescent probes, the luminescence presents lower noise background and is few orders of magnitude more sensitive. As the reaction does not require light absorption, there is no risk of photobleaching. Probes based on europium are sensitive to micromolar H<sub>2</sub>O<sub>2</sub> concentrations, suitable to make direct H<sub>2</sub>O<sub>2</sub> detection and easy to use. Unfortunately, they are not active in buffers containing phosphates. Probes based on boronate are more suitable to be used in complex buffers as cell culture media [106].

### 2.3.1.2 Study of H<sub>2</sub>O<sub>2</sub> stability in various cell culture media

Until now, it would be suitable for the *in vitro* study to mix stabilized H<sub>2</sub>O<sub>2</sub> solution in cell culture media. The dilution of hydrogen peroxide is thus created to be delivered to the adherent cells. Being interested to choose the proper medium able to keep a stable stress source, and also being limited by the conditions in which the *in vitro* cell lines can be maintained, we study the degradation kinetics of H<sub>2</sub>O<sub>2</sub> in the possible media to be used for cell stimulation. According to literature, the principal H<sub>2</sub>O<sub>2</sub> quenchers existing in mammalian cell culture medium are pyruvate, FBS and phenols [90,107]. We will test the stability of hydrogen peroxide in different media, removing step by step the main compounds we suspect could be oxidized.

As previously described, there are many ways to detect extracellular H<sub>2</sub>O<sub>2</sub>. Looking for a stable probe in complex solutions as DMEM cell culture media, sensitive to a wide range of H<sub>2</sub>O<sub>2</sub>, between nM to μM we chose a boronate based sensor, HyPerBlu from Lumigen. It

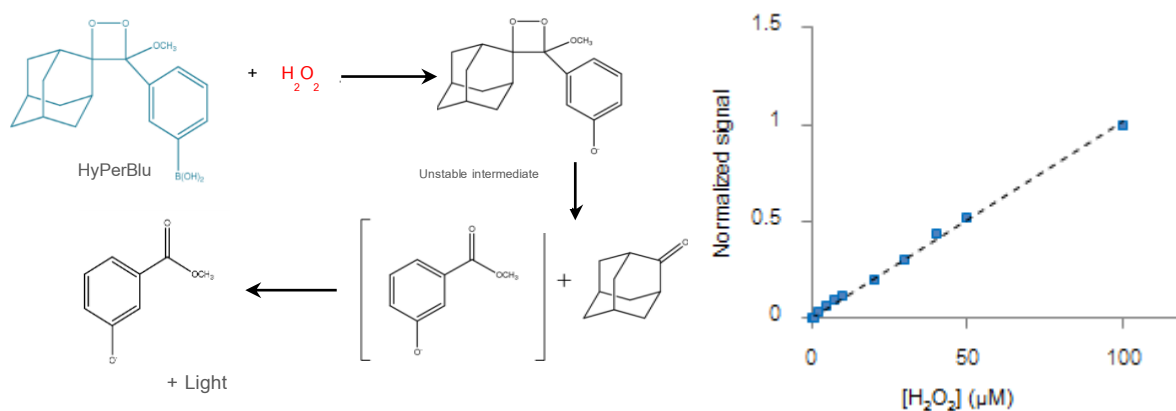


**Figure 2.3:** HyPerBlu reactions with H<sub>2</sub>O<sub>2</sub> leads to luminescent compound (from [108]). Linear detection range from 10<sup>-6</sup> to 10<sup>-4</sup> M of H<sub>2</sub>O<sub>2</sub> using HyPerBlu reagent showing that the H<sub>2</sub>O<sub>2</sub> concentration is proportional with the luminescent signal

exploits the capacity of dioxetane-boronic acid of direct reaction with hydrogen peroxide which produces chemiluminescent signal. Thus an unstable reaction product is created which is disintegrated into another two products, adamantan-2-one and 3-hydroxy-methyl benzoate, the last one emitting an intense and stable light signal [108]. The emitted signal is detected by a photomultiplier of a photodiode and its intensity is displayed as function of time. Varying the H<sub>2</sub>O<sub>2</sub> concentrations the linearity of the signal in the range of interest for our study, from 1 to 100 μM, is observed (Figure 2.3).

HyPerBlu is a compound which does not require enzyme reaction mediator. Hydrogen peroxide reacts directly with it, providing a stable luminescent product, unperturbed by the complexity of the reaction media, being tolerant to many additives [105]. Once HyPerBlu is in contact with H<sub>2</sub>O<sub>2</sub>, the reaction starts slowly, reaching its maximum intensity after 10-15 min. The signal is kept stable for 2-5 minutes, then it decreases. When all H<sub>2</sub>O<sub>2</sub> molecules reacted with HyPerBlu reagent the signal reaches maximum intensity. The signal decreases once the reaction stops due to the lack of hydrogen peroxide thus the unstable reaction product is not generated anymore. This tendency of the HyPerBlu signal to reach the maximum, then decreasing in time corresponds to HyPerBlu kinetics.

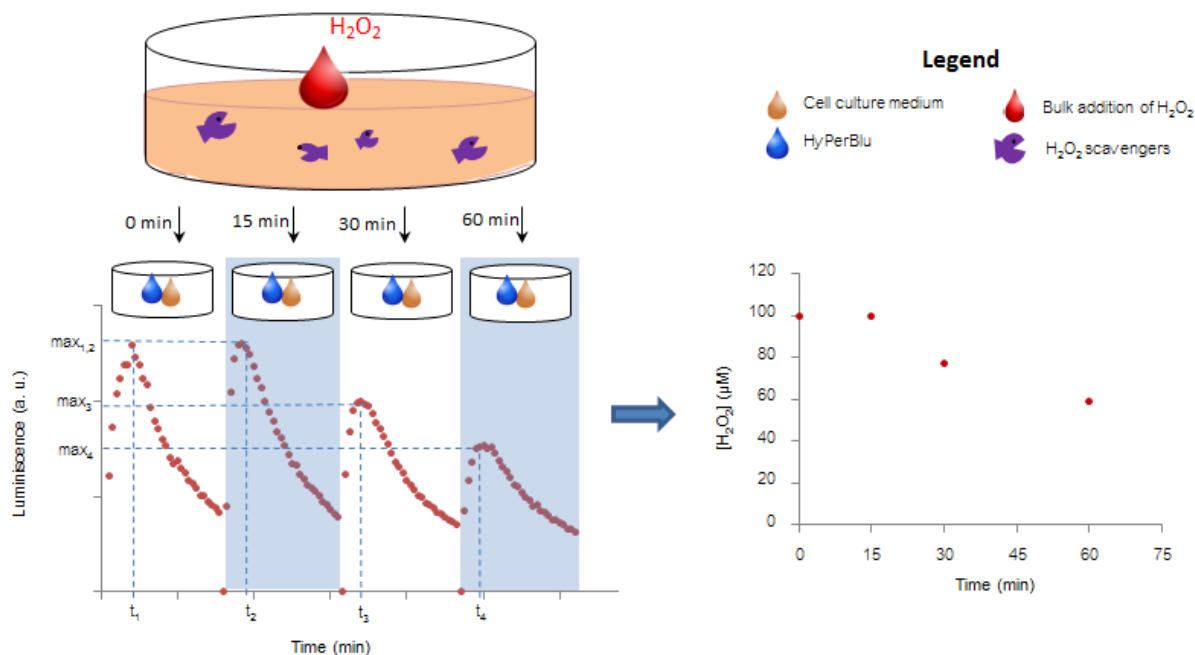


**Figure 2.4:** Mechanism of extracellular  $\text{H}_2\text{O}_2$  quantification using HyPerBlu reagent.

The mechanism of quantifying the extracellular  $\text{H}_2\text{O}_2$  consumption is represented in **Figure 2.4**. Equal volumes of HyPerBlu and cell culture media containing  $\text{H}_2\text{O}_2$  are pumped in the same microtiter well and mixed to obtain homogenous solution. Once in contact, the reagent will react with hydrogen peroxide. Following every minute the kinetics of HyPerBlu, we notice that the maximum signal, which is directly proportional with the amount of  $\text{H}_2\text{O}_2$ , is reached after 15 min. The kinetics of  $\text{H}_2\text{O}_2$  decomposition in cell culture medium is observed. We can quantify thus the amount of peroxide decomposed in cell culture media by following the kinetics of reagent represented by the maxima of each individual peaks, where one peak is one endpoint HyPerBlu kinetics for one given time after addition of  $\text{H}_2\text{O}_2$  in the cell culture media.

As the  $\text{H}_2\text{O}_2$  concentration is proportional with the maximum of emitted luminescent signal the kinetics of  $\text{H}_2\text{O}_2$  stability in different conditions is detected via endpoint reactions: samplings are done from time to time and analyzed with the luminescent probe.

The H<sub>2</sub>O<sub>2</sub> consumption is monitored in various media: DMEM +/- pyruvate +/- glucose; PBS with Ca and Mg +/- glucose. To do so, H<sub>2</sub>O<sub>2</sub> solutions of 100μM are prepared in the corresponding media. For both the HyPerBlu and cell culture media the temperature is equilibrated at 37°C before adding H<sub>2</sub>O<sub>2</sub>. During the test, the medium containing H<sub>2</sub>O<sub>2</sub> is kept in 2 mL eppendorf tubes, closed, incubated at 37°C near, by the experimental setup. The readings are made in triplicates, in white 96 wells plate from Thermofisher. A plate reader (FluostarOmega BMG) is used to scan the luminescent signal which is proportional with the H<sub>2</sub>O<sub>2</sub> concentration. The reaction is initiated and monitored in time. At each time point, 50μl of cell culture media containing H<sub>2</sub>O<sub>2</sub> is added in 1 well of 96 well plate with a pipet. 50μL of HyPerBlu is added with the pump integrated in the platerreader. Right after putting the two solutions in contact, they are mixed for 30 seconds before reading the emitting signal. Instead of incubating the mix for 15 minutes, it is recorded each minute the kinetics of emitted signal than selected the maximal intensity of it as corresponding to a given H<sub>2</sub>O<sub>2</sub> concentration. Being an endpoint measurement, the medium containing H<sub>2</sub>O<sub>2</sub> is added by pipette for each measured time point.

The degradation of H<sub>2</sub>O<sub>2</sub> in DMEM can be ignored for experiments conducted short time (order of minutes), but is significant for one lasting hours (**Figure 2.5**). The stability of H<sub>2</sub>O<sub>2</sub> similarly monitored in PBS in presence or absence of glucose is significantly longer in time.

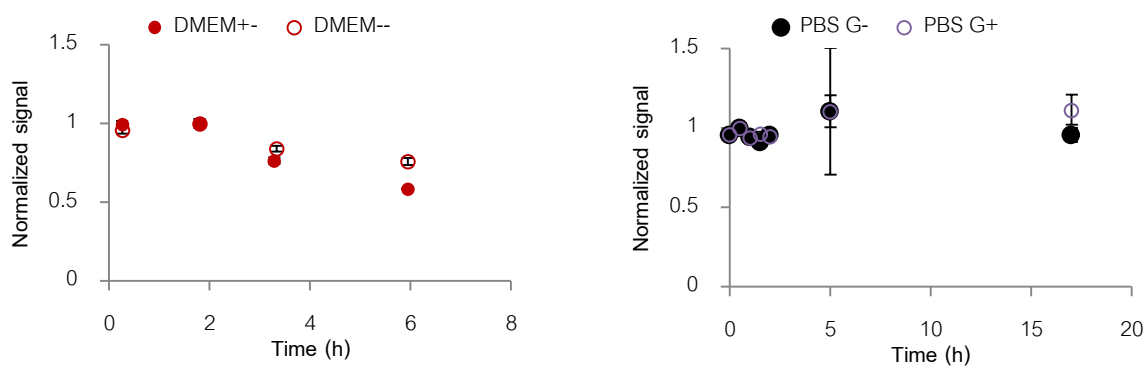


**Figure 2.5:** H<sub>2</sub>O<sub>2</sub> stability in various complex cell culture media: Dulbecco's Modified Eagle Medium without Pyruvate, without Glucose (DMEM--), Dulbecco's Modified Eagle Medium without Pyruvate, with Glucose (DMEM+/-), and very minimal media: Phosphate Buffered Saline 1x with Ca and Mg without glucose (PBS G-), Phosphate Buffered Saline 1x with Ca and Mg with glucose concentration of 4.5 g/L (PBS G+)

However, this buffer containing Ca and Mg can be used as a medium supply for adherent cells in short time experiments (maximum 5 hours). PBS with Ca and Mg supplemented with glucose allows keeping cells longer, providing carbon flux through metabolism. Showing low autofluorescence, PBS is suitable to be used in fluorescence microscopy.

### 2.3.2 Kinetics of H<sub>2</sub>O<sub>2</sub> and cell consumption

The previous tests have been performed in absence of cells, using HyPerBlu reagent from Lumigen. After estimating the stability of H<sub>2</sub>O<sub>2</sub> in different media, we decide to conduct our experiments by preparing H<sub>2</sub>O<sub>2</sub> solution in PBS with Ca and Mg +/- glucose (4.5g/l glucose). The H<sub>2</sub>O<sub>2</sub> stability is monitored in presence of cells, by replacing the cell culture medium with the one that contains a certain initial concentration of H<sub>2</sub>O<sub>2</sub> (by bolus addition). To do so, MCF7wt cells are seeded in duplicates at different confluences: 20, 40 and 80% in 6 well plates. To add the H<sub>2</sub>O<sub>2</sub> solution, the culture media is removed, the cells are 2 times rinsed with PBS without Ca and Mg, then the 100 μM H<sub>2</sub>O<sub>2</sub> dilution prepared in PBS with Ca and Mg is added to MCF7wt cells. In each well are added 3 mL of PBS containing H<sub>2</sub>O<sub>2</sub> that we will call reaction volume. Every indicated times, samplings are analyzed with HyPerBlu in triplicates. The results are displayed as concentration in function of time of cells stimulation with H<sub>2</sub>O<sub>2</sub> (**Figure 2.6**).

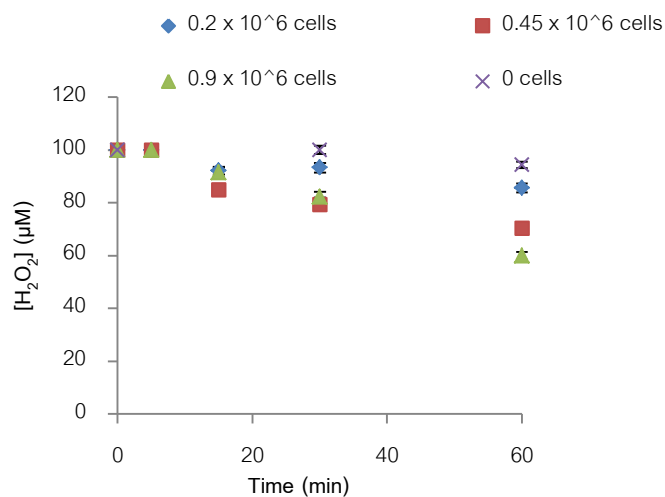


**Figure 2.6** Kinetics of H<sub>2</sub>O<sub>2</sub> consumption by MCF7wt cells during 1h incubation in PBS with Ca and Mg and without glucose. Studies are made in duplicates for each cell confluence and each reading is made in triplicates.

Knowing that the area of one well is 9.5 cm<sup>2</sup>, the cellular division time is approximately 27h, the number of cells the moment of seeding is 0.5x10<sup>5</sup>, 1x10<sup>5</sup> respectively 2x10<sup>5</sup> cells/well and that the stimulus is applied 2 days after seeding, one can estimate the density of cells at the moment of H<sub>2</sub>O<sub>2</sub> pulse as 0.2x10<sup>6</sup>, 0.4x10<sup>6</sup> respectively 0.9x10<sup>6</sup> cells/cm<sup>2</sup>.

The stimulus is prepared in a tube containing 3 mL of PBS in which H<sub>2</sub>O<sub>2</sub> solution is pipetted. The mix is added to the seeded cells, rinsed before with PBS buffer to eliminate the complex growth media. The concentration of H<sub>2</sub>O<sub>2</sub> is decreasing with 5% during 1h of incubation in PBS at 37°C. However, when H<sub>2</sub>O<sub>2</sub> is added as bolus on MCF7wt cells, its decomposition is more significant. After exposing the cells for 1h to 100 μM H<sub>2</sub>O<sub>2</sub>, is observed a drift of 20, 35 and 45% from the initial concentration. This consumption is depending on the number of cells exposed. Comparing our results with the ones found in literature [91], we observe 2 times slower H<sub>2</sub>O<sub>2</sub> consumption by MCF7 in one hour. In [91] the influence of medium over the H<sub>2</sub>O<sub>2</sub> stability is not clear. Another aspect that could explain the difference of cell consumption between our data and the ones from the publication is that the stimulation is performed in absence of external glucose. Also, the MCF7 cell permeability can differ from laboratory to another. We estimated that one cell in our experimental conditions consumes 40 nM of H<sub>2</sub>O<sub>2</sub> in one hour (Figure 2.7) and 1000 gradient is established between extra-intracellular plasma membrane In a recent study, upon bolus stimulation of K562 cells, a 390 gradient is

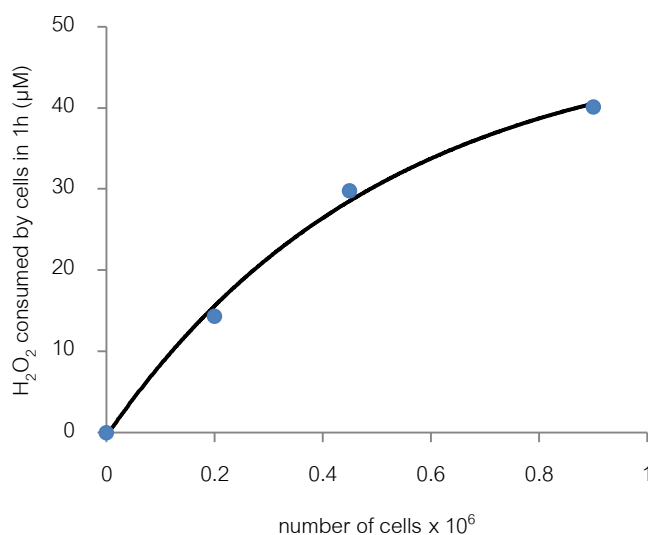


**Figure 2.7** Dependence of H<sub>2</sub>O<sub>2</sub> consumption by the number of cells exposed to stress in static system. After 1h of exposing MCF7 wt cells to an initial concentration of 100μM, the concentration diminishes while the number of exposed cells is higher.

created between the cell membrane [75].

The H<sub>2</sub>O<sub>2</sub> degradation by cells is treated as first order kinetics. The stimulus is prepared in non-reacting medium. The initial [H<sub>2</sub>O<sub>2</sub>] is proportional with the luminescent product created in the HyPerBlu reaction. After a certain time *t*, the [H<sub>2</sub>O<sub>2</sub>] decrease. This new concentration will be noted as [H<sub>2</sub>O<sub>2</sub>]<sub>0</sub>. The H<sub>2</sub>O<sub>2</sub> consumption by cells is described by:

$$\frac{d[H_2O_2]}{dt} = k_{cell} \cdot [H_2O_2]_0 \quad 2.1$$

After integrating, it leads to:

$$k_{cell} = \frac{1}{t} \ln \left( \frac{[H_2O_2]}{[H_2O_2]_0} \right) \quad 2.2$$

The kinetics of cell consumption is influenced not only by the cell number over surface [109] but also by the volume of stimulus [110]. The debit of H<sub>2</sub>O<sub>2</sub> consumption by MCF7 wt cells is estimated according to the equation:

$$k_{debit} = \frac{k \cdot V}{nr. of cells} \quad 2.3$$

where *k* is the rate constant of [H<sub>2</sub>O<sub>2</sub>] consumption over time, *V* is the volume of H<sub>2</sub>O<sub>2</sub> stimulus used for cell incubation and the divisor is the number of cells exposed to stress. In our experimental conditions, the volume of PBS containing stress source is constant, only the number of cells is varying. Treating the consumption of H<sub>2</sub>O<sub>2</sub> by cells as first order kinetics, one can obtain the following kinetic constants 5 · 10<sup>-5</sup> s<sup>-1</sup>, 1 · 10<sup>-4</sup> s<sup>-1</sup> and 15 · 10<sup>-5</sup> s<sup>-1</sup> corresponding from the lowest to the highest cell density. Calculating the debit of H<sub>2</sub>O<sub>2</sub> consumption by MCF7 cells we obtain the following values of *k*<sub>debit</sub> of 0.03 min<sup>-1</sup> · 10<sup>-6</sup> · mL, 0.04 min<sup>-1</sup> · 10<sup>-6</sup> · mL respectively 0.045 min<sup>-1</sup> · 10<sup>-6</sup> · mL for the 3 cell confluences, from lower to higher. It is almost 10 times lower than the ones found in literature for MCF7 wt cells [72]. In this context we are asking what is the role of glucose concerning this aspect? The significant difference between the two modalities of exposing the MCF7 wt cells is the medium composition. While in the cited experiment the authors used RPMI, a minimal medium, we expose the cells to H<sub>2</sub>O<sub>2</sub> without providing any nutrients to the cells during 1h of stimulation. Glucose metabolism influencing the permeability of the membrane might be one of the first signs of a direct link with redox homeostasis regulation. Furthermore, cellular response to oxidative stress is presented by

measuring the cellular survival or death to various stress doses applied on cells experiencing particular metabolic environment.

## 2.4 Cell death upon H<sub>2</sub>O<sub>2</sub> stress

Cell survival after treatment with various environmental stresses is the main issue in anticancer therapies. The resistance of cells against stresses is enhanced in time and has been observed often after multiple transient stress fractions [111]. The cytotoxic effect induced upon stress is depending by the dose received by cells. In this context we ask what is the threshold dose of H<sub>2</sub>O<sub>2</sub> to induce cell death?

The diversity of results concerning cell death threshold of cells exposed to bolus [112–116], continuous H<sub>2</sub>O<sub>2</sub> generation based on glucoseoxidase [117], mixed external H<sub>2</sub>O<sub>2</sub> delivery methods [4] or EGF [94] ranging from doses of 0.1 μM x h to 19 mM x h motivated us to make a comparative literature study. Taking in account that each stimulation method presents its particularities, we focus on a particular delivery method: bolus addition.

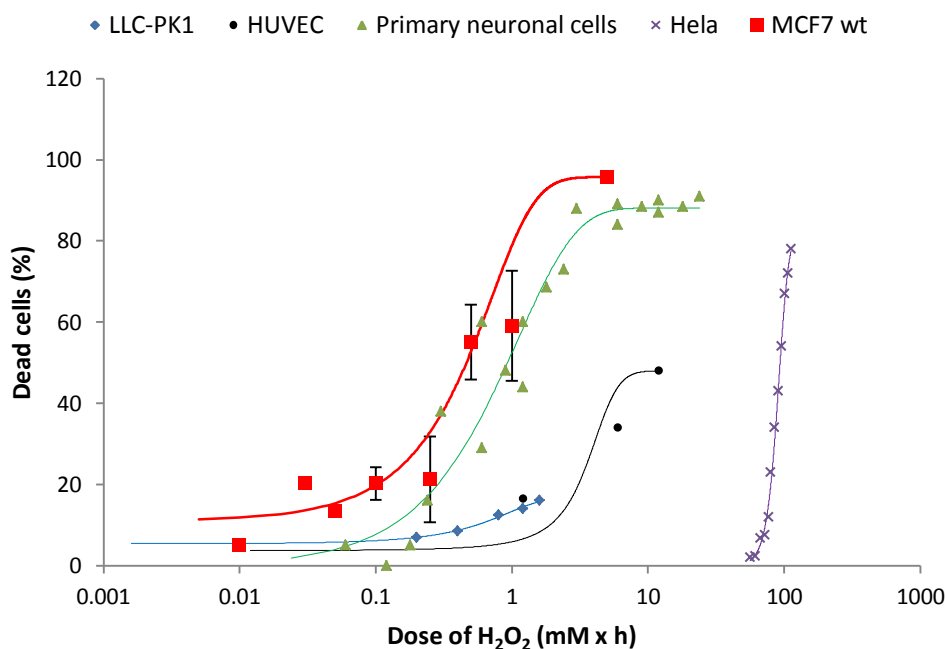


**Figure 2.8:** Dose response with cell type as reported in literature: LLC-PK1 [118], HUVEC [119], primary neuronal cells [120] and HeLa [121]. The sensitivity of MCF7 wt cells is quantified in our laboratory.

The response upon H<sub>2</sub>O<sub>2</sub> exposure depends by different factors as cell type [70,122], the delivery method, amplitude and patterns of the stimulus. Exogenous H<sub>2</sub>O<sub>2</sub> generation can have different effects comparing with endogenous sources production. Moreover, even using the same technique, reproducing data obtained in different laboratories is difficult [91], because often are missing details as cell number, cell culture volume, dish surface [120,123–126]. The diversity of results observed for the same type of study performed in different labs might be an effect of lacking a rigorous protocol for cellular stimulation with H<sub>2</sub>O<sub>2</sub>.

To determine experimentally the fraction of dead cells upon oxidative stress, MCF7wt are stimulated in static system. Cells are seeded in T25 flasks reaching 40% confluence in the day of stress application. For 1h they are exposed to various H<sub>2</sub>O<sub>2</sub> concentrations from 1 μM to 5mM.

The dilutions of H<sub>2</sub>O<sub>2</sub> (Sigma H1009) are made in DPBS (Lonza BE17-513F) and a volume of 5mL is added to the cells. After 1h incubation at 37°C in atmospheric and humidity controlled conditions, the stress is removed and complete media is added (DMEM from Lonza BE12-614F, supplemented with 10% FBS Gibco 10270-106, Penicilin streptomycin mix Lonza DE17-602E and L-glutamine Lonza BE17-605E) to allow the recovery.

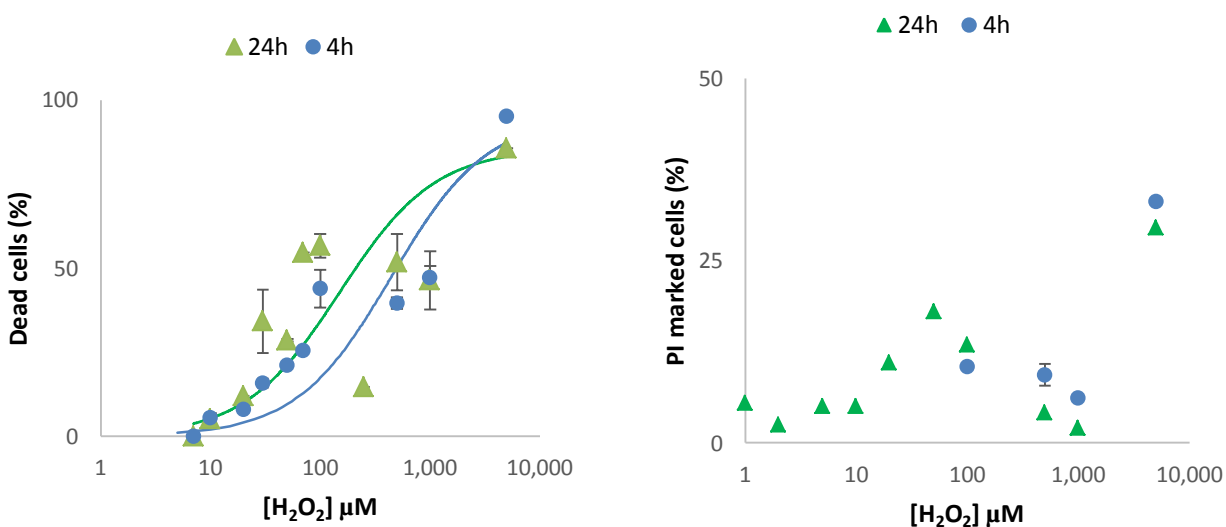


**Figure 2.9:** MCF7wt dose response short (4h) and long (24h) time after stimulation with H<sub>2</sub>O<sub>2</sub>. The stress is applied for 1h using various [H<sub>2</sub>O<sub>2</sub>]. During stress, the cells are kept in minimal medium without glucose, then recovered in their normal growth conditions. Percentage of dead cells is quantified reporting to cell survival observed in bright field images (left) or by using PI marker (right).

Cell death is quantified using two methods: counting the number of living adherent cells before and after stimulation or by using Propidium Iodide (PI Sigma P4170) 1x concentration. Images of cells are recorded in 20 different regions of the flask, both brightfield and PI fluorescence at 4 and 24h after stress exposure. Thousands of cells are monitored and their response to stress is quantified (**Figure 2.9**). Measurements are made in duplicate and the variability of data reproducibility is indicated with error bars. Relating the cellular response with the dose of H<sub>2</sub>O<sub>2</sub> stimulation are depicted the survival-death thresholds. All cells survive at doses lower than 10 μMxh. Higher doses are gradually increasing the fraction of dead cells and signs of reaching a plateau are targeting doses up to 100 μMxh. All cells are dead or detaching right after stimulation with highest H<sub>2</sub>O<sub>2</sub> concentration of 5 mM. Interestingly, this behaviour is not noticed while using PI. The percentage of cells increasing the nucleus membrane permeability thus allowing PI to become fluorescent by binding the DNA is significantly lower. One hypothesis is that different death types can be induced using H<sub>2</sub>O<sub>2</sub> stimulation. Depending by the method of cell death quantification, this phenomenon can be noticed at different intensities.

The alternation of cellular vulnerability upon oxidative stress is showing that the mammalian cells are responding according to cell type. To be more precise, similar dose responses of MCF7 wt cells are extracted from literature to compare with the data we obtained. Following the dose response in literature, different sensitivity of MCF7wt cells to external H<sub>2</sub>O<sub>2</sub> stimulation is observed (**Figure 2.10**). Moreover, comparing with our experimental data, this variability of response is maintained. Comparing the results obtained on breast cancer MCF7 cells, using the same H<sub>2</sub>O<sub>2</sub> exposure method, we still observe the modulation of cell death threshold. This motivated us to find and quantify the error sources that can occur.

Comparing the studies where the stress is applied using a bolus method, one can observe that it is not possible to predict the dose of H<sub>2</sub>O<sub>2</sub> with modulatory or killing effect on living cells. Favorable survival effects to chronic H<sub>2</sub>O<sub>2</sub> stress applied by bolus have been reported, by increasing the cell growth, while the same H<sub>2</sub>O<sub>2</sub> concentration applied for lower time had inhibitory effect [114]. Significant damaging effects as DNA lesions and death have been observed to lower doses [112,113,115,116]. As the H<sub>2</sub>O<sub>2</sub> stimulation is performed in a static system and a complex cell culture media containing H<sub>2</sub>O<sub>2</sub> quenchers, we have reasons to wonder whether a single step stimulation has been performed, with constant concentration in time. In the

presence of H<sub>2</sub>O<sub>2</sub> consumers, we suspect that the stimulus is performed as multiple pulses, with maximal amplitude at its addition (every time when the medium is renewed) and minimum amplitude in less than one hour, depending on the cell density [109], the volume and the type of medium where the hydrogen peroxide is added [92]. In our study the stress is mixed in very minimal medium avoiding this way the H<sub>2</sub>O<sub>2</sub> decomposition by cell culture conditions. In the papers we use to compare our data, during stimulation complete medium is used.

When a static method of H<sub>2</sub>O<sub>2</sub> delivery to cells is used, the degradation of external H<sub>2</sub>O<sub>2</sub> has to be considered by the two main consumers: cell culture media and the adherent cells. Few literature studies are showing the impossibility of making a bulk stimulus in a static system by simply adding H<sub>2</sub>O<sub>2</sub> solution to cells [4,92]. An artifact in the concentration stability over time might be one of reason of different death thresholds doses. Another factor is the detection method of cell death. This process can occur instantaneously, right after or during the stress, or even after 48h [127]. To be able to compare the results existing in literature, the precise time of death quantification is also relevant information. Cell death is actually a complex process that can appear even during the stress or it can manifest in longer time after within 24h. It can occur accidentally or as a programmed process, both situations having an irreversible terminal effect of death [77,78]. We try to identify the quantity of external ROS and the minimal exposure time necessary to kill a cell. The perspective of this study is to confront the cell dose response to molecular dynamics. However, preliminary data concerning the non-adaptive response of the cell which leads to cell death will be further presented.

Considering the [H<sub>2</sub>O<sub>2</sub>] consumed after 1h by cells, the dose of exposure will be lower while the cell density increases. We can conclude that the cell is a dynamic system, containing antioxidants with significant quenching activities. This aspect is reported and our data show that seeded cells are the major H<sub>2</sub>O<sub>2</sub> quenchers when exposed in static system. In our experimental conditions, the MCF7 cells are incubated with 100 μM H<sub>2</sub>O<sub>2</sub> for 1 h. If the stimulus would have been remaining constant, at steady state, the dose received by cells would have been:

$$\text{Dose} = [\text{H}_2\text{O}_2] \times \Delta t \quad 2.4$$

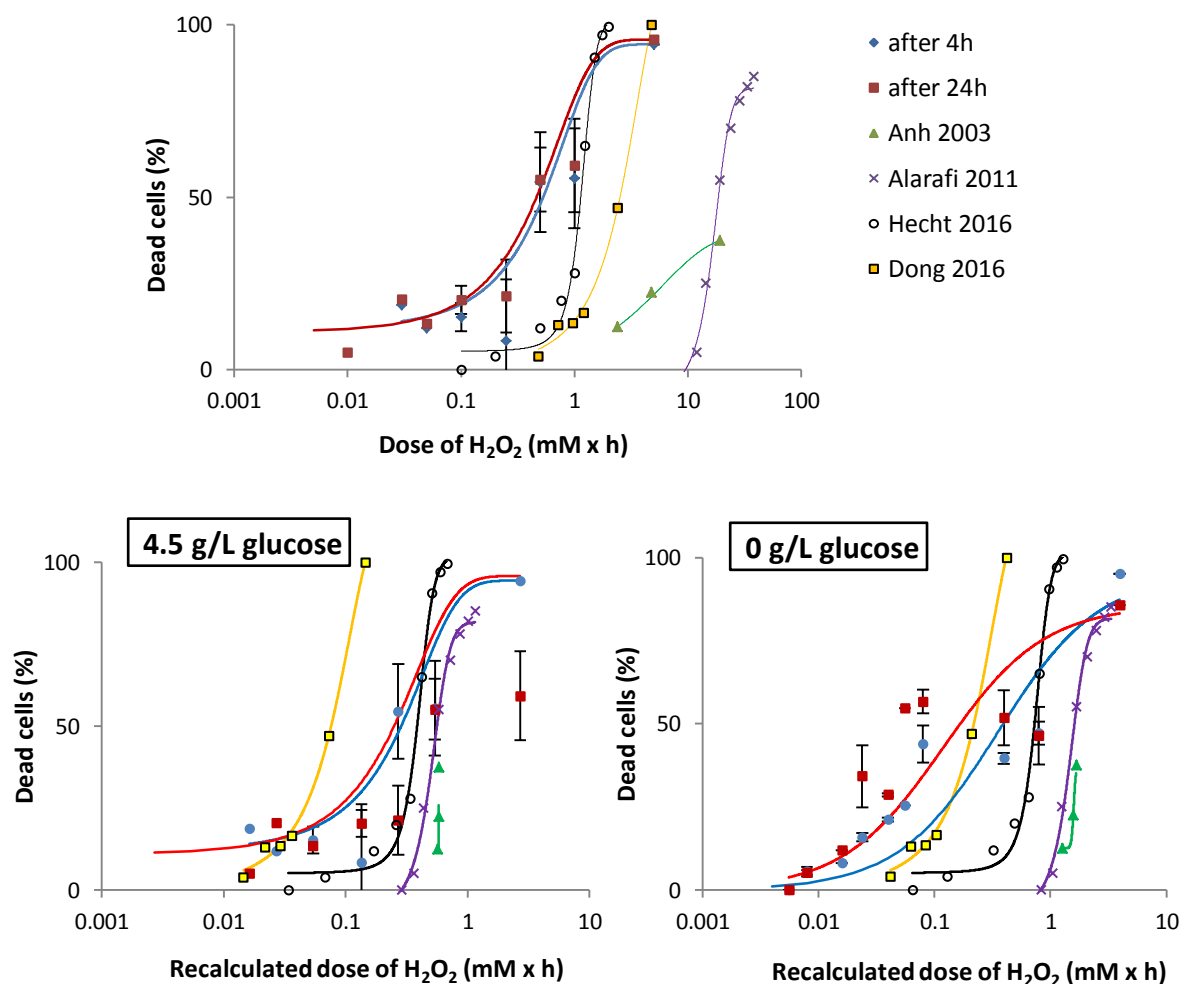


**Figure 2.10:** MCF7 wt dose response to various doses of H<sub>2</sub>O<sub>2</sub>. Correcting the dose in the results extracted from literature (top) we observe that the time of stress exposure in static conditions is a key parameter. Here are recalculated the doses of H<sub>2</sub>O<sub>2</sub> stress from publications [115,116,128,129] in both lack (G-) and presence (G+) of glucose. Significant shift is observed comparing with the original data. The kinetic constants used to correct the results are extracted from literature ( $k_{G^+}=1.38 \text{ h}^{-1}$  from [72]) or obtained in our experimental conditions ( $k_{G^-}=0.48 \text{ h}^{-1}$ )

where  $\Delta t$  is the time interval of stress duration.

In **Figure 2.10** is simulated the H<sub>2</sub>O<sub>2</sub> degradation over time in presence or absence of glucose. The dose is calculated by multiplying the initial H<sub>2</sub>O<sub>2</sub> concentration with the duration of time. The degradation of H<sub>2</sub>O<sub>2</sub> in presence of cells is calculated by integrating over time the initial H<sub>2</sub>O<sub>2</sub> concentration multiplied with  $e^{-kt}$ . Significant shifting of the dose response after recalculation are observed in the data extracted from literature [115,116,128,129]. One can conclude that longer time exposure leads to different doses, comparing the recalculated stress dose [H<sub>2</sub>O<sub>2</sub>] x 24h [128] with shorter times [H<sub>2</sub>O<sub>2</sub>] x 2h [129]. As the results are not overlapping even after dose recalculation, we are wondering what is the role of adaptation to stress in the case of long time exposure systems?

Previously we discuss different artifacts that can interfere when defining the threshold H<sub>2</sub>O<sub>2</sub> killing dose. In this context, a correction and a stimulus protocol are proposed. Forward will be discussed 3 main aspects concerning:

- dose response of MCF7 cells in different metabolic conditions; the time of exposure is modulated from 0.5h to 4h, while the H<sub>2</sub>O<sub>2</sub> concentration is fixed to 250 $\mu$ M;

- dose response of MCF7 cells in different metabolic conditions; the time of exposure is fixed to 1h, while the H<sub>2</sub>O<sub>2</sub> concentration varies from tens of  $\mu$ M to mM range;

- comparison between cell death response monitored in static respectively continuous flow conditions.

## 2.4 Role of glucose metabolism in cell death process: stimulus dose approach

Cell death induced by external H<sub>2</sub>O<sub>2</sub> stimulation is a complex process, more difficult to achieve than predicted. Here our intentions are to modulate the two main parameters that we suspect to change the cellular vulnerability to stress: time of stress exposure and cellular metabolism.

### 2.4.1 Dose response in different metabolic conditions varying the exposure time

In the context of dose defining we perform bolus stimulation with H<sub>2</sub>O<sub>2</sub> where the time is varied between 0.5 to 4h (**Figure 2.11**). MCF7wt are seeded in T25 flasks at 40% confluence. The concentration of stimulus is kept constant at the level of cells, the PBS containing the stimulus being renewed every 30 minutes in the flask.

Control experiments are made by exposing cells for the corresponding durations to PBS G+ or PBS G-. Up to 2h in PBS, cells do not divide as expected their number remaining constant after 24h, while in normal conditions cells amplify their number with 50%. However, when applying 250 μM H<sub>2</sub>O<sub>2</sub> stress in presence of glucose, massive cell death is observed, comparing with lack of glucose conditions. Increasing the time of exposure leads to complete cell death few hours after. PI positive marked cells are reflecting one fraction of dead cells, suggesting that another death types might be involved.

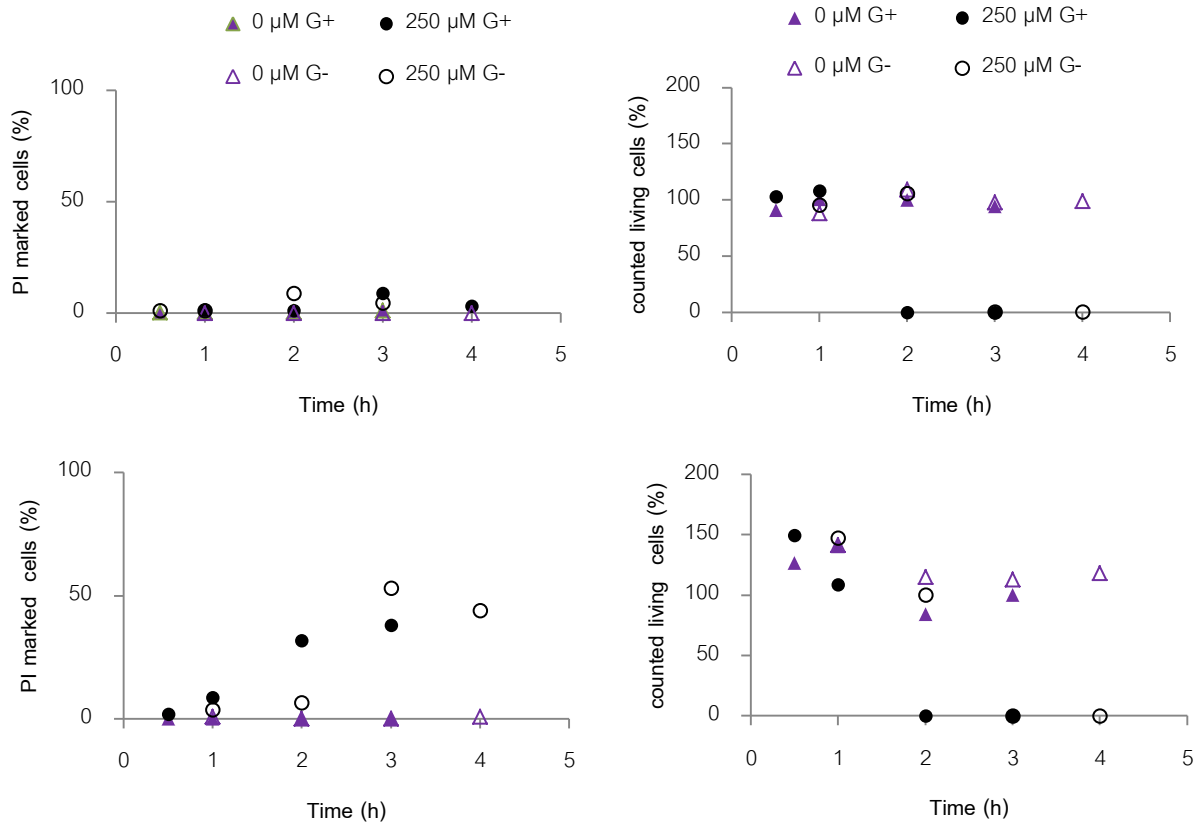


**Figure 2.11:** Dose response of MCF7wt cells to H<sub>2</sub>O<sub>2</sub> stimulus applied in bolus for various durations (30min, 1h, 2h, 3h or 4h). The stimulation is performed in minimal medium (PBS) in two different metabolic conditions: presence (G+) or absence (G-) of glucose. After stress the cells are recovering in their normal growth medium. Cell death is quantified using PI. The survival is observed in brightfield images in unstained cells. Both death and survival are quantified 4h (top graphs) and 24h (lower graphs) after recovery upon stress.

### 2.4.2 Dose response in different metabolic conditions varying the stimulus concentration

After 1h of exposure in PBS with or without glucose, the cells recovery after 24h is the same as in normal conditions, increasing their number with 50%. For this purpose, a new dose response is discussed in this section. The time of stress exposure is fixed to 1h, while the H<sub>2</sub>O<sub>2</sub> concentration is varying from tens of  $\mu\text{M}$  to mM range (**Figure 2.12**). In our experimental condition the cell survival is quantified by counting the living cells and the PI marked cells in various fields of view. They are imaged before, shortly after and 24h after stimulation with H<sub>2</sub>O<sub>2</sub>. While PI reagent is directly binding the cellular DNA, showing the fact that the cellular membranes are damaged by the stress, counting the living cells allows the observation of detached cells and another death features.

During stimulation, the cells are experiencing also particular metabolic states like complete removal of carbon sources from external medium (G-) and pentose phosphate pathway inhibition using 6aminonicotiamide (6AN).

The 6AN treatment is applied 24h before stimulation, thus the main pool of NADPH regeneration is inhibited, leading to a lower antioxidant system scavenging power in the cell cytoplasm. Alternative routes are involved in cell fate. Indeed, removing glucose leads to similar death responses as in normal carbon sources. However, inhibiting the PPP, a different death behavior is depicted, longer time after stress. The results are showing the direct relation between cellular metabolism and its sensitivity to oxidative stress. It has been observed that the glucose metabolism is directly linked to programmed cell death [130,131]. Inhibiting the PPP or completely removing the glucose, is leading to similar fate. In normal metabolic conditions, the cell death seems to be a spontaneous process where the H<sub>2</sub>O<sub>2</sub> stress is disrupting the cellular membrane.

Incubating cells with H<sub>2</sub>O<sub>2</sub> added as bolus does not allow steady state stimulation. A variation of the concentration with maximum 20% is one of the accepted standards in the protocols of today [110]. This variation can be controlled in our experimental conditions by varying the number of cells. However, it would be very difficult to maintain the stimulus at steady state in static system in presence of cells.

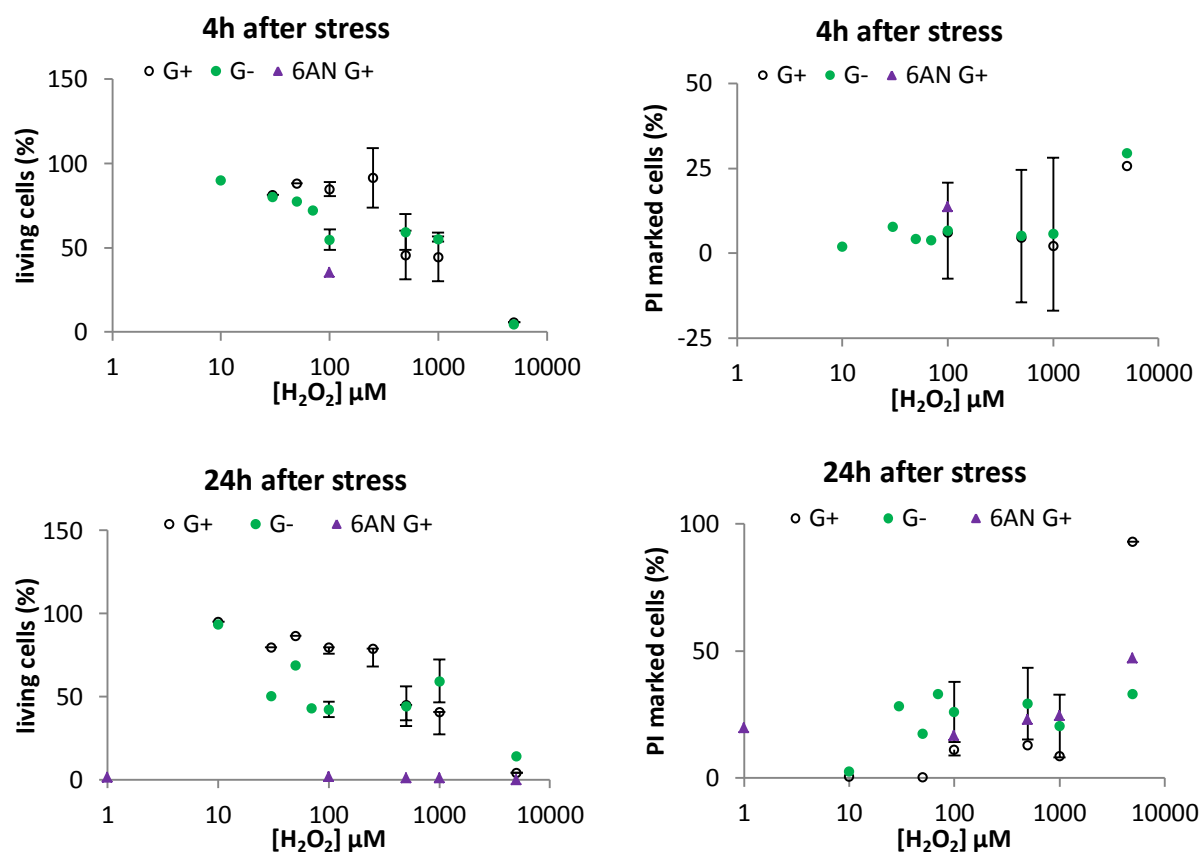


**Figure 2.12:** Dose response of MCF7wt cells to various concentrations of  $H_2O_2$  applied for 1h, after 4 and 24h of recovery in complete medium, the fraction of dead and living cells are quantified and represented as function of  $[H_2O_2]$ . In glucose starvation the cell has to use the existing resources to fight against stress. In normal glucose conditions the cell fate is regulated according to stress severity. Inhibiting the PPP the NADPH cytosolic production pool is reduced, another defensive pathways being involved in cell defense.

Our interest is to find a strategy to deliver steady state stimulus to cells. We observe that the  $H_2O_2$  consumption is strongly depending on the cell density when it is delivered to *in vitro* cultures using a static method as bolus. Renewing the extracellular  $H_2O_2$  concentration faster than it is consumed is the approach we want to apply to rectify the  $H_2O_2$  consumption observed in static systems. Thus we decide to expose the cells to  $H_2O_2$  constantly flowing the stimulus to have controlled, continuous and controlled  $H_2O_2$  source. This strategy is also allowing the creation of different temporal stress patterns (stress/recovery or modulation of different stimulus concentration). The temporal patterns control is of important interest when modulating the molecular dynamics in living cells.

## 2.5 Design fluidic system

It is difficult to maintain the H<sub>2</sub>O<sub>2</sub> concentration at **steady state in a static system**. Using combined methods does not allow creation of temporal stress patterns. Building a microfluidic system to stimulate cells enables the continuous H<sub>2</sub>O<sub>2</sub> flow over the seeded cells and the creation of controlled temporal extracellular stress patterns. The system has been tested only on yeasts [80] and does not seem to be easily applied to mammalian cells due to their culture particularities. In parallel, we develop in our lab a similar system, designed for mammalian cells stimulation. By creating a laminar flow, the cells are exposed to a constant concentration of H<sub>2</sub>O<sub>2</sub>. It allows the creation of temporal patterns and the monitoring of intracellular molecular dynamics *via* microscopy upon addition and removal of the stimulus.

We design a fluidic system built from commercially available elements, to expose the mammalian cells to constant H<sub>2</sub>O<sub>2</sub> external stimulus (**Figure 2.13**). It consists from a rectangular macrochamber of 55 x 5 x 1,7 mm<sup>3</sup> connected with tubes to the exposure solution (input outlet). The output is connected to syringe controlled by peristaltic pump which maintain the flow at a constant rate. In our designed system, the waste is collected by a syringe of 140 mL volume. The input solution is kept at 37°C in dry incubator. It is connected to a gas mixing which maintains 5% CO<sub>2</sub> in the atmosphere of the incubator. A switching button allows changing the flow from medium (simple tube in **Figure 2.13**) to medium containing H<sub>2</sub>O<sub>2</sub> (tube with red symbol) and vice versa. As previously described, a very minimal medium is used: PBS with or without glucose, due to its optical properties in fluorescence microscopy and the low reactivity with H<sub>2</sub>O<sub>2</sub>.

The MCF7 cells are seeded in custom macrofluidic chambers created to mimic the growth conditions of the cells in flasks culture. The chambers are built from commercially available materials: red silicone sheet of 1.6 mm thickness (JTR-S-2.0, 1.6mm Thick, Red Silicone Sheet Grace Bio-Labs) and Glass coverslip (D 263 M Schott glass, No. 1.5H, 170 +/- 5  $\mu$ m). They are sterilized with ethanol and rinsed with miliQ water before using.

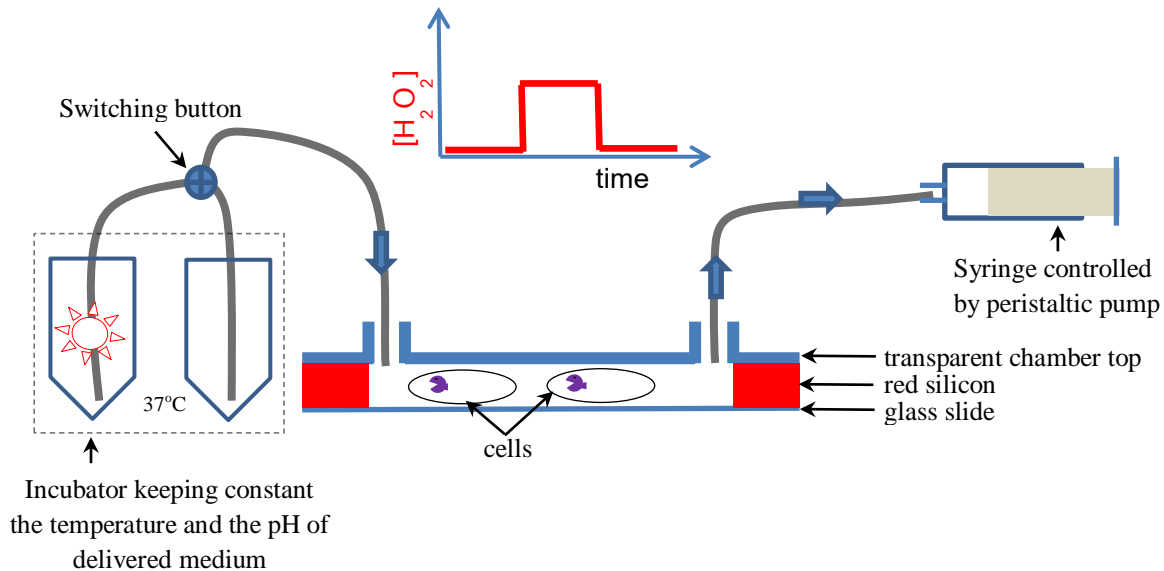


**Figure 2.13** Fluidic system to create controlled temporal H<sub>2</sub>O<sub>2</sub> stimulus on mammalian adherent cells.

The silicone is cut to create a channel similar with the one created by the Ibidi sticky-Slide I Luer. The growth area thus created, 2.5 cm<sup>2</sup>, is 4 times smaller than a P35 mm dish area (10 cm<sup>2</sup>). The chamber is created by assembling the silicon on the coverslip. The mounted chamber is rinsed with PBS, then warm complete culture medium is added. The height of the chamber (1.6 mm) allows reproducing similar conditions with the cultured cells in T75 flask. The cells are seeded in monolayer by pipetting them in the chamber. To avoid osmotic stress, the sample is inserted in a 100 x 20 mm sterile dish where a compartment of 2 mL of PBS is placed. The sample is incubated in cellular physiological conditions (37°C, 5% CO<sub>2</sub>). Two days after seeding, the chamber is closed by placing the Ibidi sticky slide I Luer (0.1 mm channel height) on the top. It is fulfilled with medium before connecting to the fluidic system, to avoid air bubbles in the flow.

All the components used to build the chamber can be used again, except the glass coverslip. In order to reuse the Sticky-Slide I Luer, the glue is removed with acetone and sterilized with ethanol any time needed.

The flow rate has to be chosen taking in account two main parameters: cell consumption kinetics and shear stress. When MCF7 wt cells are exposed in absence of glucose one can estimate that the half-life of H<sub>2</sub>O<sub>2</sub> is in the range of 1-4h, depending by cell density seeding. However, cells are consuming faster external H<sub>2</sub>O<sub>2</sub> when in normal glucose conditions. The H<sub>2</sub>O<sub>2</sub> half-life is estimated in literature to 20-30 min [91]. To maintain constant stimulus, the volume of the chamber has to be renewed faster than the cells ability to consume H<sub>2</sub>O<sub>2</sub>. The chamber connected to the fluidic system has a volume of 0.5 mL which means setting a flow rate between 0.5 mL/min-1 mL/min that allows the medium to renew faster than it can be consumed by cells.

The flow profile is monitored in the system using a fluorescent dye with known diffusion coefficient<sup>1</sup>. To estimate the H<sub>2</sub>O<sub>2</sub> stimulus rise and fall time in the custom chamber, the following equation is used:

$$\frac{\tau_{Rho}}{\tau_{H2O2}} = \frac{\sqrt{D_{Rho}}}{\sqrt{D_{H2O2}}}$$

where  $\tau_{Rho}$  is the rise time measured with Rhodamine 110,  $D_{Rho}$  is the diffusion coefficient of Rhodamine 110,  $D_{H2O2}$  is the diffusion time of H<sub>2</sub>O<sub>2</sub> and  $\tau_{H2O2}$  is the rise time of H<sub>2</sub>O<sub>2</sub>.

To obtain the diffusion length time, the following equation is used:

$$D = L_d^2 \times T$$

where D is the diffusion coefficient and T is the time of diffusion defined as ratio between the volume of the tubing (0.3 mL) and the flow rate. (0.5-1 mL/min).

The rise time of H<sub>2</sub>O<sub>2</sub> thus calculated can be used to obtain the diffusion length time:

$$L_d = \tau \times v$$

where v is the speed of the flow (0.2-0.4 cm/min). The diffusion length time is small (0.9 cm) allowing a constant stimulus delivery in real time.

<sup>1</sup> The diffusion coefficients measured in water for H<sub>2</sub>O<sub>2</sub> is  $1.3 \times 10^{-5} \text{ cm}^2/\text{s}$  [183] and for Rhodamine 110 is  $4.4 \times 10^{-6} \text{ cm}^2/\text{s}$  [184]

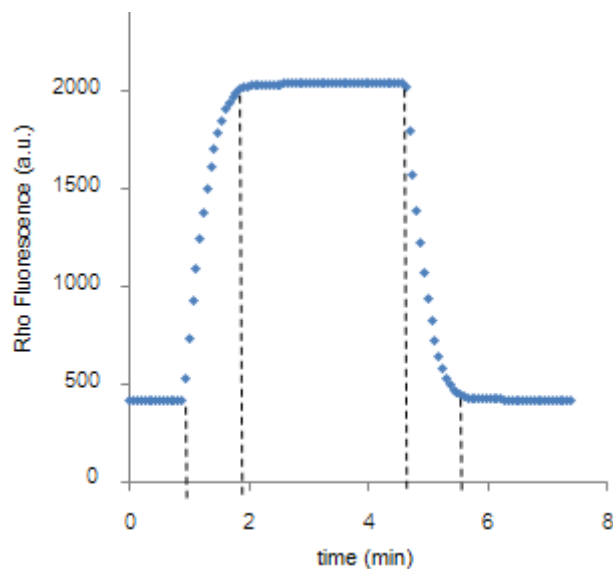


**Figure 2.14:** Flow profile measured in the center of the chamber using Rhodamine 110.

The cell line we chose is not growing normally in shear stress conditions. Being a breast cancer cell type, MCF7 are not normally exposed under flow conditions. This is the reason for which the flow speed have to be adjusted in such a way to create a shear stress in the range of 0.1 dyn/cm<sup>2</sup> or even lower [132]. A flow rate of 1 mL/min leads to shear stress of  $3 \cdot 10^{-2}$  dyn/cm<sup>2</sup>

The designed set-up allows creating controlled temporal stimulus of H<sub>2</sub>O<sub>2</sub> on mammalian cells to study molecular dynamics. The fine tuning of intracellular H<sub>2</sub>O<sub>2</sub> concentration enables experimental observation of molecular adaptation upon external stress.

To validate the steady state of H<sub>2</sub>O<sub>2</sub> stimulus delivery in fluidic system, the cell death responses in both fluidic and static conditions are compared. MCF7 wt cells (ATTC) are normally cultured in DMEM (Lonza, BE12-614F) supplemented with 10% FBS (Gibco, 10270), 5% L-glutamine 200 mM (Lonza, BE17-605E) and 1% Penicilin-streptomycin mixture (Lonza, DE17-602E). For static stimulation, cells are seeded in T25 flasks at 40% confluence, while cells stimulated under flow are seeded 48h in the silicon Petri dish that will be used to build the chamber.

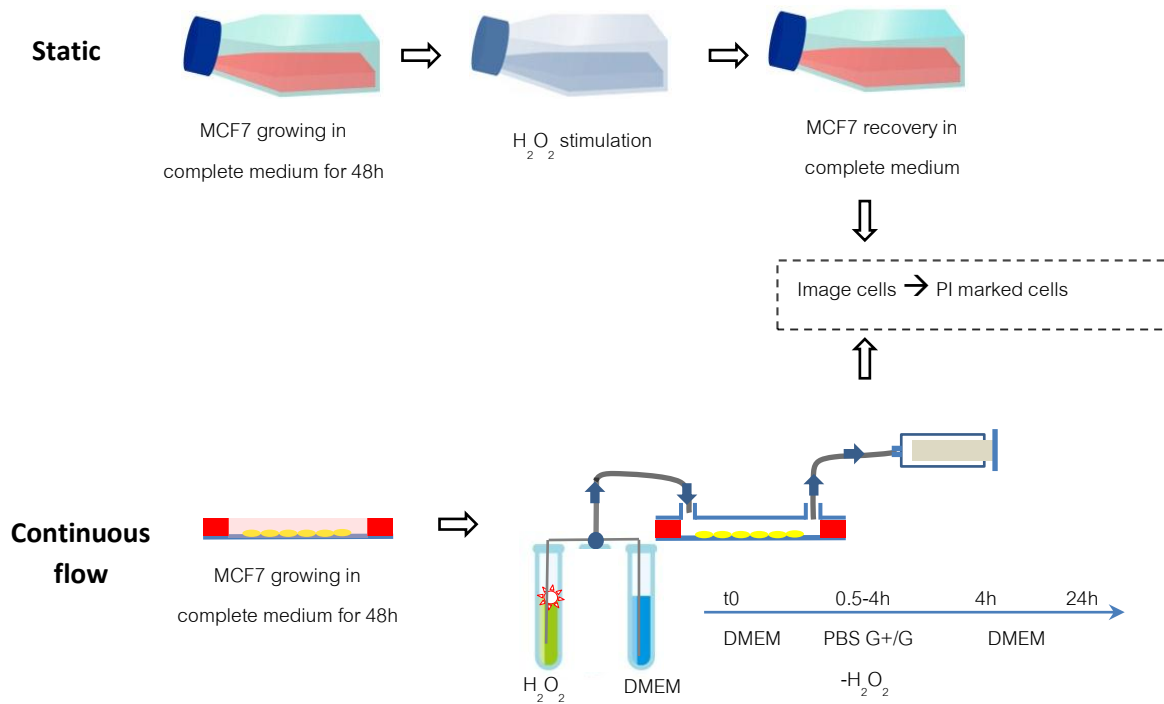


**Figure 2.15:** Cell death in response to hydrogen peroxide: comparing the cellular dose responses observed in static (top) and in continuous external  $\text{H}_2\text{O}_2$  delivery systems (bottom). For stimulation in static conditions, cells are seeded in the T25 flask 48h before stimulation. The stress is made by changing the complete medium with the PBS containing  $\text{H}_2\text{O}_2$ . After incubation, the stress is stopped by removing it and rinsing the cells with PBS. For recovery the cells are incubated in complete medium (DMEM). They are imaged right after the stress and 24 h later. Cells stimulated in continuous system under flow are seeded 48h in the fluidic channel, in static conditions. Right after stress, cells are recovering in DMEM for 24h.

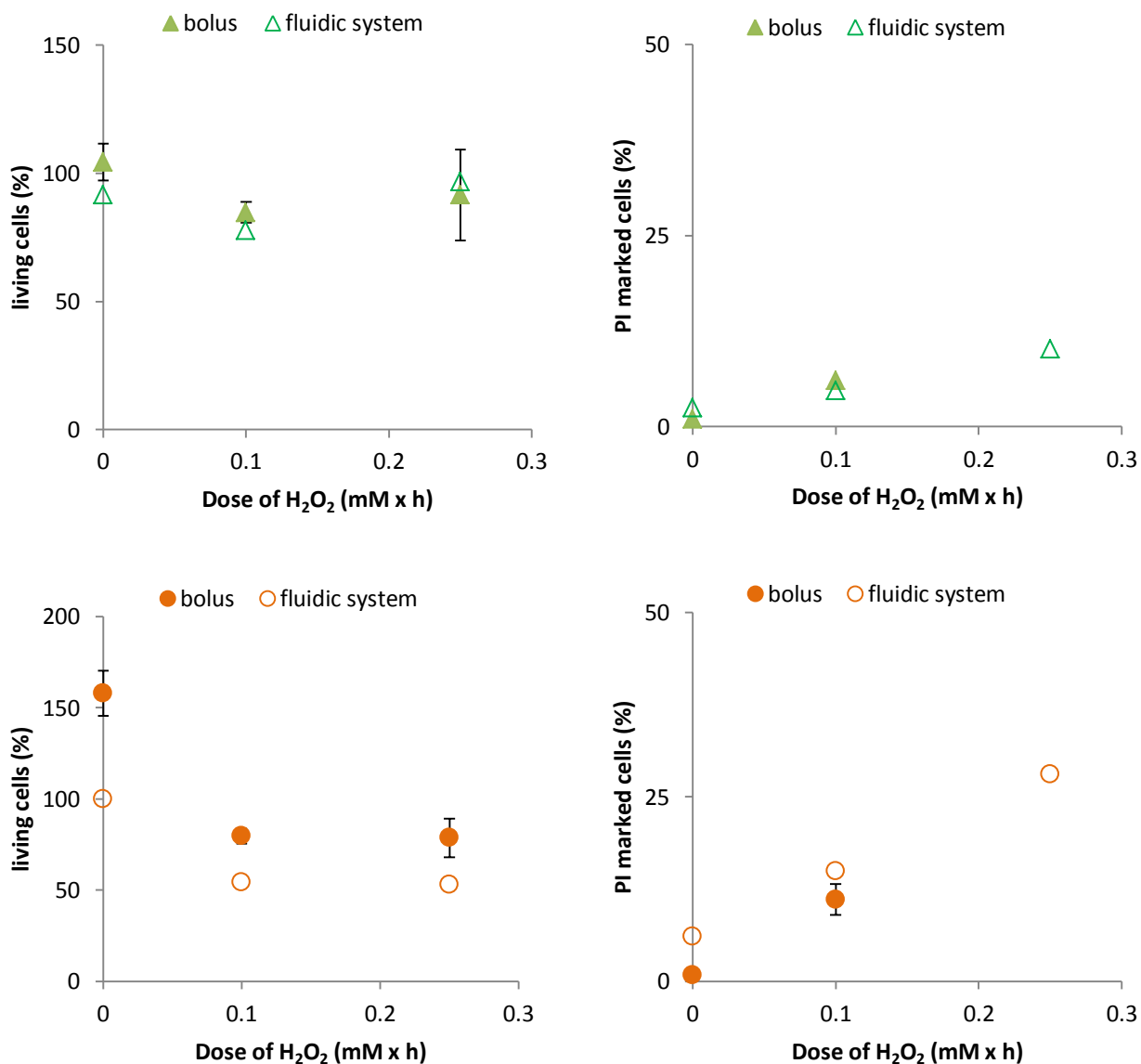


**Figure 2.16:** Comparing MCF7 wt cell death observed in static and continuous flow systems, upon 1h stimulation at various concentrations of H<sub>2</sub>O<sub>2</sub> (0, 100  $\mu$ M 250 $\mu$ M). Cell death (upper and lower right plots) and survival (upper and lower left plots) are quantified 4h (triangles) and 24h after stimulation (circles). The external H<sub>2</sub>O<sub>2</sub> stress is performed in very minimal medium (PBS G+), while the recovery is made in complete DMEM. Experiments in bolus are performed in duplicate, while the ones in fluidic system only once.

Cell death is quantified using Propidium Iodide (PI, Sigma. P470) to mark dead cell. It is added in the complete recovering medium at 1x concentration. For cells stimulated under flow,

the complete recovery medium is incubated, 24h before, at 37° C 5% CO<sub>2</sub> in T175 flask (Sarstedt, 8339120).

Cells stimulated in static and fluidic system conditions are imaged before the stress, right after and 24h after stress. Cells are visualized in 20 random chosen regions with 4x objective (Nikon MRH20041), in T25 flask. 6 regions are recorded in fluidic system. Images are recorded both in bright field and PI fluorescence.

In fluidic system is not observed the cell division after 24h, while in static the number of cells is 50% increasing. Upon stimulation, the amount of PI marked cells is still lower than the dead cells observed in brightfield. However, 50% of cells are observed to lose their viability in fluidic system, while in static most of cells stop dividing and lower cell death being noticed (**Figure 2.16**).

Observing significantly higher cell death in fluidic system comparing with static is confirming that the dose received by cells during one 1h is better controlled in this condition. This result is motivating us to perform the stimulation under flow to study molecular dynamics.

## Chapter 3: Cellular adaptation to oxidative stress

### 3.1 Introduction

#### 3.1.1 Background

Tumors can be removed by surgery or by therapy induced by radiations [111], chemicals [133,134] or light [22]. Except surgery, the others strategies are exploiting the ROS mediated mechanisms to kill cancer cells or to reduce their growth. Comparing with normal cells, it has been suggested that cancer cells have higher basal ROS level. This assumption is used as standard therapeutic selectivity strategy. Small increasing of endogenous ROS level would promote the cellular proliferation while an excess is leading to oxidation of macromolecules. Increasing the internal ROS concentration allows overpassing the lethal threshold in cancer cells but not in their normal counterparts. Perturbing the redox homeostasis thus leading to irreversible damages in cancer cells without damaging the normal tissue is the goal in anticancer therapy [6]. However it has been observed that the basal ROS level in cancer and non-cancer is not highly different, in consequence the selectivity between cancer and non-cancer cells is not so easy to target. Furthermore the cancer cells vulnerability under oxidative stress is underestimated and the fundamental therapeutic principle of selectivity is under a major concern [135].

Malignant cells are known for their particular metabolism due to their extreme living conditions. It can be a second aspect to consider in for selectively target cancer cells. The assumption of higher production rate of ROS in cancer cells is strongly related with their faster proliferation comparing with normal cells [136]. During this process higher metabolic activity is required to create building blocks and energy for the cellular division. High energy synthesis taking place mitochondria, higher side ROS will be produced in the respiratory chain process. This results in consequence to higher ROS scavenging pool necessity whose production rate is also strongly related to cell glucose metabolism *via* pentose phosphate pathway [137].

Perturbing the internal ROS-antioxidants balance in anticancer therapy is a hallmark in anticancer therapies. Inhibiting metabolic pathways and increasing ROS level *via* chemo and radiotherapy is a promising therapeutic approach [138]. On the other hand, the precise mechanism of regulation in terms of spatial and temporal organization is still not fully understood. Furthermore it is unclear how the cellular sensitivity can be related to the dose of

stress. The cell sensitivity to stress dose should correlate with adaptive response or cell death when it reaches a toxicity threshold. In pharmacology the dose-response relation is a sigmoidal representation of cell response as function of dose. It allows identifying the magnitude of response to stimulus, where maximal response is cell death and minimal is describing the cellular tolerance to it [135]. But  $\text{H}_2\text{O}_2$  has dualistic conflicting roles. It is a signaling molecule promoting different functions as cell proliferation but it can be also a toxic agent able to diffuse through the cell compartments creating free radicals. Exploiting its cytotoxicity properties involves controlling the delivery dose. Precise and specific track of spatial localization and temporal activity allows identifying its fine tuning in redox regulation.

### 3.1.2 Cellular adaptation to oxidative stress

Due to the dynamically changes of the environment, adaptation of any life form is a required condition to survive. To adapt, the systems (cells, organisms) are regulating different functions, pathways or gene expression, according to the changes. Specific receptors are integrated in their structure, constantly tracking the environmental variations [63]. For example, when glucose is sensed by a cell, it will activate proteins involved in the trans-membrane transport to internalize glucose, then to metabolize it. When damages encounter, repairing pathways will be regulated and defensive mechanisms will be activated [64].

The major issue in anticancer therapies is the cell resistance to treatment. To understand this behavior, it is required to investigate how cells respond to the oxidative stress. To do so, the ROS-antioxidants balance will be modulated by applying extracellular  $\text{H}_2\text{O}_2$  (**Figure 3.1**). Likewise  $\text{Ca}^{2+}$ , within a cell the basal  $\text{H}_2\text{O}_2$  amount is maintained under tight control, in the nanomolar range. Various intracellular  $\text{H}_2\text{O}_2$  sources have been identified, generated by some stressors or by metabolic cues. Its quenching is constantly made by effective reducing systems thus the  $\text{H}_2\text{O}_2$  flux being regulated by proteins with reversible oxidation targets involved in many physiological processes [139].

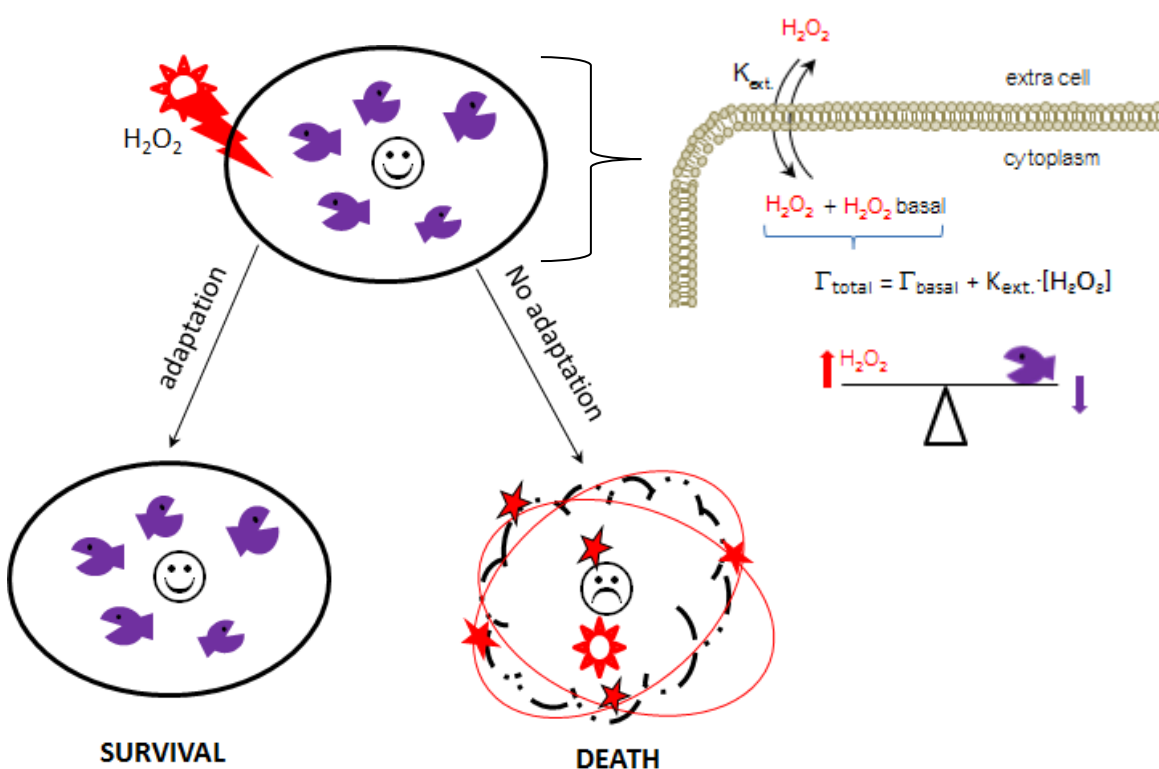


**Figure 3.1:** Oxidative stress response and cellular fate: upon  $\text{H}_2\text{O}_2$  stimulation a cell either adapts to an oxidative stress and thus survive or dies. Death occurs when nucleus cannot be protected by the antioxidants pool (in purple). This behavior is strongly controlled by the cellular ability to restore the ROS-antioxidants balance. The cell is producing internal  $\text{H}_2\text{O}_2$  during metabolism at basal rate  $\Gamma_{\text{basal}}$ . External  $\text{H}_2\text{O}_2$  is imported *via* passive or active diffusion across the cellular membrane thus varying the total effective production rate  $\Gamma_{\text{total}} = \Gamma_{\text{basal}} + K_{\text{ext}} \cdot [\text{H}_2\text{O}_2]$ , where  $K_{\text{ext}}$  is a constant.

Every time an external perturbation factor as  $\text{H}_2\text{O}_2$  is applied, the intracellular  $\text{H}_2\text{O}_2$  production rate increases perturbing the cellular homeostasis. To establish it again, the cells will use the existing detoxification antioxidants as thioredoxins, glutathione and NAD(P)H regulated enzymes [140]. The intracellular enzymatic systems involved in  $\text{H}_2\text{O}_2$  decomposition are fast preserving small  $\text{H}_2\text{O}_2$  levels in each cellular compartment, with second order rate constants between  $10^{-5} - 10^{-8} \text{ M}^{-1}\text{s}^{-1}$  [139]. The cellular homeostasis is set up when the ratio between oxidants and antioxidants is 1. It is obvious that, when the intracellular  $\text{H}_2\text{O}_2$  level increases, the cell will rise the antioxidants level too and a new basal level will be reached. The defensive

response is sustained by the intracellular negative feedback and is responsible by adaptation of cell in oxidative stress conditions [141].

However, a system exposed to a stimulus, able to sense and respond to it, is considered adapted if it can return to initial state or near to it, after certain time duration. Limiting the duration response, the redox homeostasis of the system is involved in maintaining the basal activity. The process of reaching the basal level after stimulation is defined as perfect adaptation. When the system returns close to basal level without reaching it, is considered near perfect adaptation [65].

Redox homeostasis is constantly maintained in cells by a negative feedback loop. It manifests when a stress source occurs and the cell will initiate a protection mechanism to fight against damages by reducing/inhibiting it, bringing the cell back to equilibrium. There are also situations when opposite effect can be preferred, when the system has to move farther away from the normal range. This is the positive feedback that intensifies the modification in the physiology of the system to a definite end point [66]. In this context, the adaptation is the ability of a system to sense and to regulate the stimulus in order to reach back its redox homeostasis. Homeostasis imbalance persistence occurs due to irreversible damages *via* positive feedback mechanisms or overwhelmed negative feedbacks. If the internal balance cannot be controlled and properly regulated, it can lead to diseases [2].

Reaching the steady state after stimulation should not depend on the input [65,67]. In perfect adaptation process, even if the signaling pathway is transiently responding to stimulation the response is independent of an input stimulus. Different behaviors are expected after stress removal from a non-adapting system. Supposing that the stimulus is removed when partially adaptation signs have been observed, it is obvious that the  $H_2O_2$  removal will show higher antioxidants level reached during stimulation. The non-adapting systems will maintain the ROS levels high even after stimulus removal. The timescales of those behaviors are of interest for better understanding fundamental driven molecular processes.

## 3.2 Molecular dynamics of oxidative stress

In therapy, the modulation of parameters describing the dose is still an issue. The cytotoxicity of stress has been observed to be linked with the precision of molecular adaptation to stimuli [142]. For a better understanding of dose concept, internal concentration with modulatory role and the timescales of molecular adaptation are relevant parameters to consider. Following the target molecule in space contribute to the interpretation of the role it plays in the pathway regulation, considering the fact that each cell compartment performs different functions.

The aim of this work is to quantify the kinetics of molecules highlighting cells vulnerability in oxidative stress conditions. The redox cellular homeostasis adaptation is reflected in the response of stress sensors (HyPer probe and enzymes containing reversible oxidation targets as Grx1) or hydrogen donors mediating the enzymatic regeneration (NADPH cofactor) to  $H_2O_2$  [139]. The molecular dynamics of reactive oxygen species and their biochemical scavengers in living cells will be studied with fluorescence microscopy.

Averaged population data exhibit phenotypic heterogeneity that can bias the interpretation [143,144]. In this context statistical data obtained from single cell can offer a better description of the cell behavior. Critical overview concerning the intracellular molecular detectors which will be used in our study will be further presented.

### 3.2.1 Monitoring the dynamics of $H_2O_2$

$H_2O_2$  is the major ROS in redox regulation. In the last years the intracellular detection of  $H_2O_2$  has been significantly improved. Chemical fluorescent probes as  $H_2DCFDA$  has been widely used to detect the intracellular ROS species in living cells. Being a small molecule, it diffuses inside and outside the cell, from one compartment to another, leading to misinterpreting results. They are useful as endpoint reporters for global changes of ROS produced in a long period of time. Also, their irreversible oxidation does not allow their use as detectors of dynamic events in real time imaging. Their non-specificity to  $H_2O_2$  is also a major disadvantage for studies targeting this particular molecule [145].

60 years ago a new generation of intracellular detectors has been developed with the discovery of green fluorescent proteins [146]. The ability of creating a fluorescent probe controlled by and integrated in the DNA of the cell provides a useful tool in imaging the dynamics of intracellular molecules. This approach motivated researchers to improve the quality of detection considering not only the specificity of sensors. For this reason, genetically encoded proteins has been developed allowing quantitative measurements and drifts corrections. The major disadvantage of using genetically encoded proteins as intracellular detectors is the fact that the cellular system is transformed into a new one and it is difficult to determine the number of plasmids that will integrate the cellular DNA. However, fusing the interest tags in a bacterial genome limits the interaction of detection probe with similar proteins produced by mammalian cells. [147].

HyPer is a genetically encoded protein selectively sensitive to  $H_2O_2$  [148]. It consists of a yellow protein with Tyr residues fluorescent in both protonated (420 nm) and charged (500 nm) forms (**Figure 3.2 A**). The sensitive domain is incorporated in Oxy-RD bacterial derived compound which forms disulfide bridges in presence of  $H_2O_2$ . In this process the changes in shape of Oxy-RD are detected by chromophore, leading to the decrease of 420 nm absorption peak and the increase of 500 nm. The reversible conversion of HyPer from oxidized state to reduced form is maintained by Grx or Trx (**Figure 3.2 B**). HyPer was designed as a specific  $H_2O_2$  detector, placing the active residues in a special conformation acting as hydrophobic pocket. It facilitates the selection of amphiphilic molecules to interact with cysteines, restricting charged oxidants as superoxide to arrive to the active site [147]. HyPer can be expressed in a specific cell compartment by integrating the corresponding localization tag in the plasmid construction. This allows spatial monitoring of  $H_2O_2$  molecule dynamics in cytoplasm, the cellular compartment of interest for our study. The probe has been tested in many systems already, from transfections in yeasts, bacteria, plants, mammalian cells to *in vivo* samples [95,149–152].

Being a ratiometric probe, both reduced and oxidized forms of HyPer can emit at 520 nm, after excitation at 420 respectively 488 nm (**Figure 3.2 C**). The intracellular  $H_2O_2$  can be

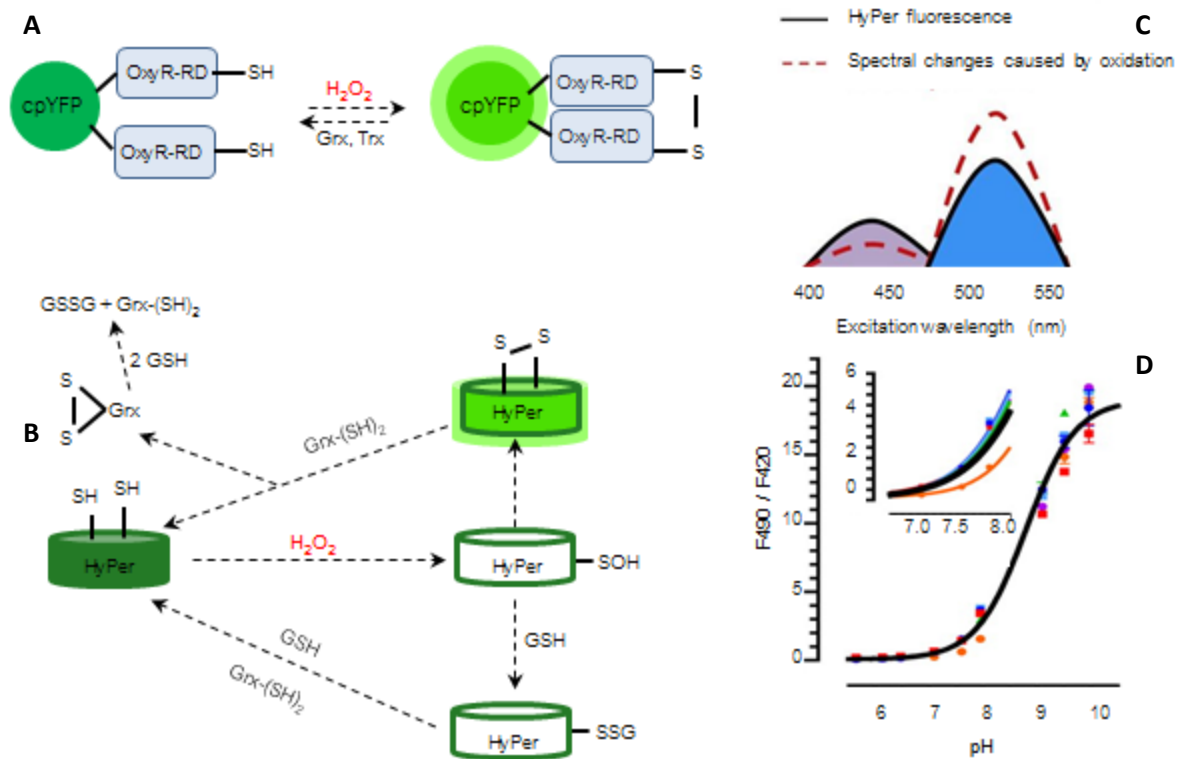


**Figure 3.2:** (A) HyPer construction in reduced and oxidized form (from [153]). (B) Their states are regulated by  $\text{H}_2\text{O}_2$  respectively Grx, Trx. In the variations of HyPer fluorescence ratio have to be considered the contribution of each fraction of HyPer in a certain oxidation form at that time (from [154]). (C). Changes in excitation spectrum of HyPer upon oxidation by  $\text{H}_2\text{O}_2$  (from [75]). (D) Calibration of SypHer (in situ), reflecting the pH sensitivity of HyPer. In zoom: the variation of fluorescence ratio of sensor at physiologic pH (from [155]).

quantified by the ratio of the two fluorescence signals. It is proportional with the H<sub>2</sub>O<sub>2</sub> concentration whose calibration inside the cell is difficult to estimate. That's why, when adding H<sub>2</sub>O<sub>2</sub> stimulus over the cell, HyPer signal is often interpreted in terms of folds changes. Half oxidation time of HyPer is 30 s and its half reduction time is 2 min [74]. The kinetics of HyPer oxidation does not directly reflect the dynamics of H<sub>2</sub>O<sub>2</sub> penetration to cells while estimations of H<sub>2</sub>O<sub>2</sub> concentration profile reaching steady state in a cell within 1ms after H<sub>2</sub>O<sub>2</sub> addition [48,75]. HyPer is a successfully probe to estimate the intermembrane H<sub>2</sub>O<sub>2</sub> gradient and intracellular H<sub>2</sub>O<sub>2</sub> concentration [75] with a fast reaction rate of  $2.5 \times 10^5 \text{ M}^{-1} \text{ sec}^{-1}$  [151]. Until recently it was not possible to quantify the intracellular concentration of H<sub>2</sub>O<sub>2</sub> in living cells. Experimental measurements found cytosolic H<sub>2</sub>O<sub>2</sub> at nM range and the gradient between external and internal H<sub>2</sub>O<sub>2</sub> concentration was estimated around 400 folds [75].

The detection limits of HyPer protein are measured both inside and outside the cell. *In vitro* tests using purified HyPer protein identified that 25 nM of H<sub>2</sub>O<sub>2</sub> are necessary to induce changes in fluorescence (1.5 folds changes in ratio), while 250 nM concentration of H<sub>2</sub>O<sub>2</sub> leads to full oxidation of the protein [126]. Signal suprasaturation is observed for extracellular concentrations between 10-25  $\mu\text{M}$  in mammalian cells (K562, Hela) and *E. coli* [75,148]. The two measurements in nM range are physiologically relevant to intracellular concentrations of H<sub>2</sub>O<sub>2</sub>.

The common issues appearing while working with fluorescent proteins are photobleaching and dark state induction. To avoid blocking the protein into dark state, the oxidized form is first excited, than the reduced one [145].

The properties described above overcome the drawbacks of chemical detection and recommend HyPer as an appropriate tool to monitor intracellular dynamics of H<sub>2</sub>O<sub>2</sub> in real time. HyPer is a specific H<sub>2</sub>O<sub>2</sub> detector, but it is also sensitive to pH. SypHer is a pH specific probe having the same pH sensitivity as HyPer (**Figure 3.2 D**). It can be used as a control of pH changes in cell cytoplasm or mitochondria. It has been reported that high external concentrations of H<sub>2</sub>O<sub>2</sub> applied for short time (few minutes range) does not modify the intracellular pH [75]. However, metabolic modulation leads to intracellular pH changes [156–158].

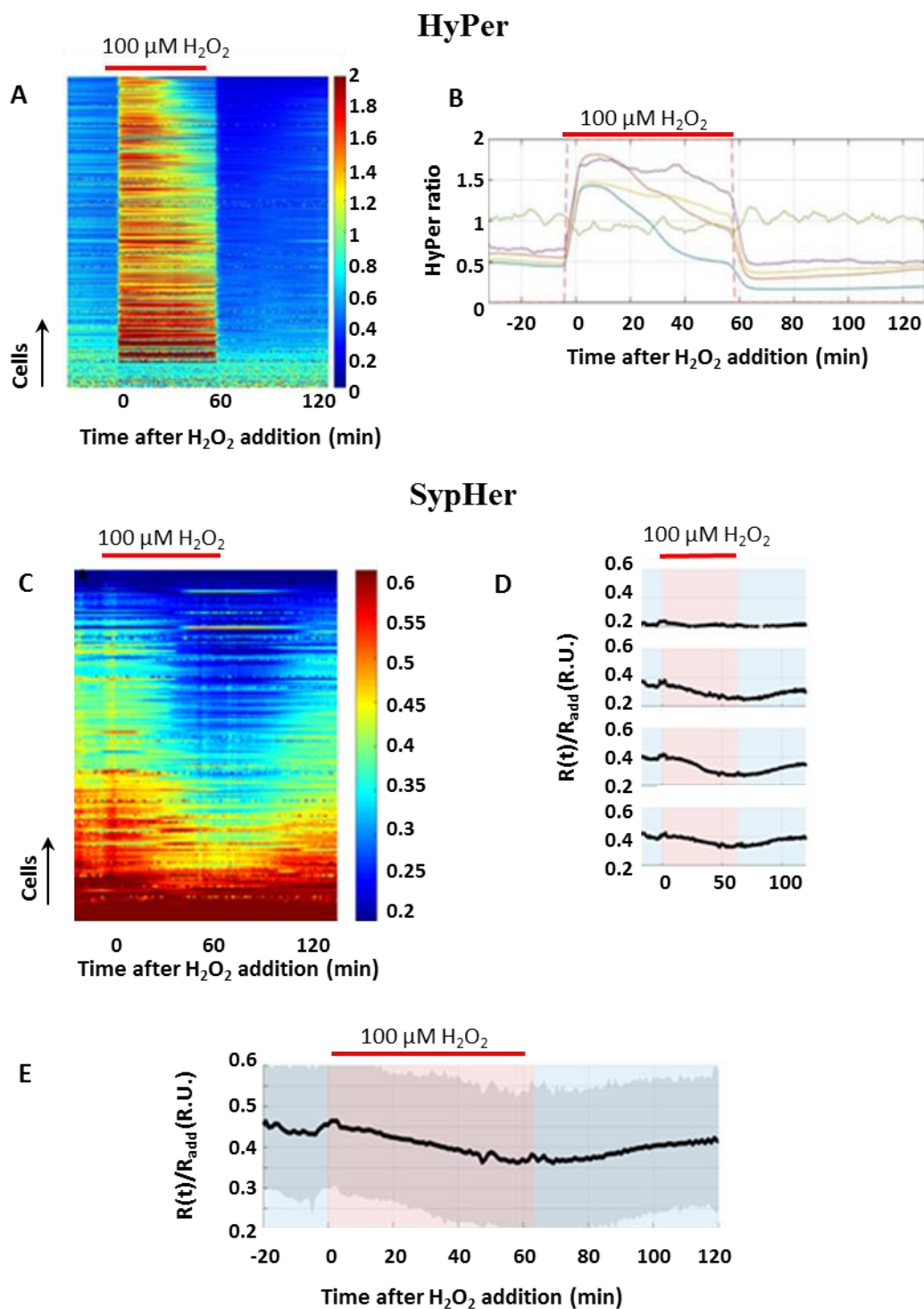


**Figure 3.3:** pH variation during  $\text{H}_2\text{O}_2$  stimulation: intracellular HyPer (A-B) and SypHer (C-E) fluorescence are monitored 30 minutes pre-stimulation, 1h during and after stimulation. MCF7 cells are exposed during 1h to 100  $\mu\text{M}$  of external  $\text{H}_2\text{O}_2$  solution prepared in DPBS supplemented with glucose (4.5 g/L). Heat maps are corresponding to ratio of the signal observed in single cells (A, C). Suggestive features of single cell responses are extracted (B, D). The absolute SypHer ratio is represented in E, where the black line is the mean of the pH variation in MCF7 cytosol before, after (blue background) and during  $\text{H}_2\text{O}_2$  stimulation (pink).

For signal accuracy, control test of intracellular pH should be performed, using a more pH stable  $\text{H}_2\text{O}_2$  sensitive probe. For this purpose, in our experimental conditions, MCF7 cells stable transfected with HyPer are exposed to 100  $\mu\text{M}$   $\text{H}_2\text{O}_2$  stimulation for one hour. The cytosolic  $\text{H}_2\text{O}_2$  dynamics is imaged 30 minutes pre-stimulation, during 1h under stress exposure and one hour after. In parallel, similar stimulation is performed on MCF7 SypHer transient transfected cells. The changes of HyPer and SypHer ratio are monitored every minute (**Figure 3.3**). Hundreds of cells are imaged and statistically displayed on the heat map. Each horizontal line in **Figure 3.3 A, D** represents the changes in the fluorescence ratio corresponding to one cell. The false colors are indicating the ratiometric fold changes, where blue is the minimum and red is the maximum fluorescent ratio. Based on the signal ratio variation during stress, different clusters can be identified on the heat maps. Suggestive single cell dynamics of each cluster are extracted for both HyPer (**Figure 3.3 B**) and SypHer (**Figure 3.3 D**). Variations in fluorescence ratio  $R$  compared to its basal level relative to maximum change  $R_{\text{add}}$  upon  $\text{H}_2\text{O}_2$  stimulation are presented.

The single cell signal can be interpreted as follows: in the first 30 minutes, no ratiometric change is observed, thus the target molecule is on steady state in the cell cytoplasm. Right after external  $\text{H}_2\text{O}_2$  stimulation, the HyPer fluorescence ratio increases. During stimulation, after 30 min, most of cells are showing a drift in HyPer signal which can be due to  $\text{H}_2\text{O}_2$  scavenging system or pH variation. The increase in  $\text{H}_2\text{O}_2$  concentration can lead to pH acidification thus the SypHer fluorescence ratio decrease (**Figure 3.3 C-E**).

In the context of different adaptation features depicted with HyPer probe (**Figure 3.3 A-B**), we are questioning what is the purity of the signal? According to literature, HyPer is sensitive to pH changes. Is it possible that during  $\text{H}_2\text{O}_2$  stimulation the cytosolic pH is varying. In this context, the perfect adaptation to  $\text{H}_2\text{O}_2$  observed in the signal detected with HyPer (complete relaxation during external stimulation) to be actually bias by pH detection in parallel with the one recorded for  $\text{H}_2\text{O}_2$ . To quantify the amount of HyPer signal involved in detecting intracellular pH changes, a new cellular construction is made using SypHer. SypHer is probing the pH variation, taking in account the cell-to cell variability identified by analyzing 160 cells in one experiment (**Figure 3.3 C, E**).

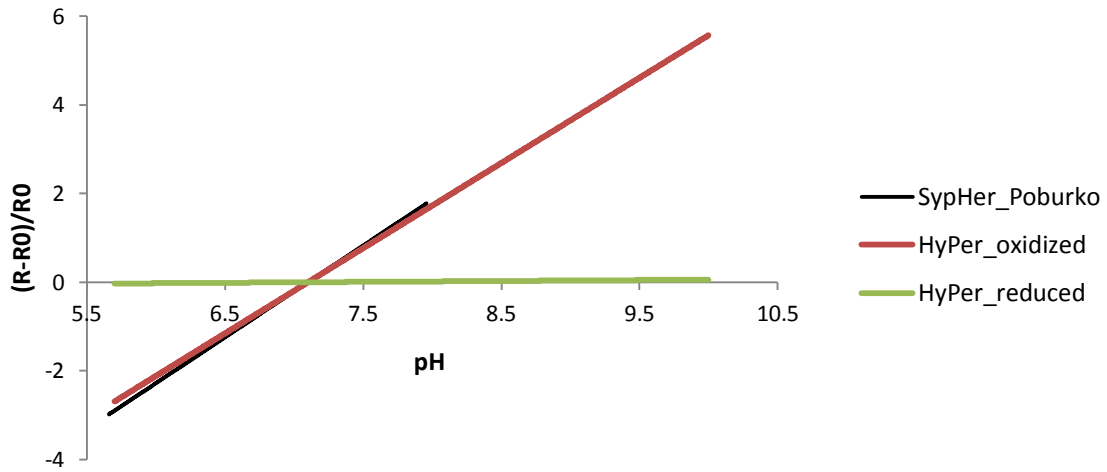


**Figure 3.4:** Calibration plot of SypHer and HyPer normalized signal as function of pH using data from [126,155].

The basal pH in MCF7 cytosol is 7.15 [159]. The mean of absolute ratio of SypHer in cytosol in our experimental data is varying with 20%, from 0.45 to 0.36, during 1h of stimulation with 100  $\mu\text{M}$  of  $\text{H}_2\text{O}_2$ . To convert the SypHer signal obtained experimentally into pH, calibration plots published in literature will be used [155]. A similar calibration curve has been done to relate the ratio of HyPer changes to pH [126]. The pK of SypHer is 8.6, the same as the one found for HyPer [160]. The sigmoidal relation in the calibration curve is often fitted with the following equation [161]:

$$R = R_{min} + \frac{R_{max} - R_{min}}{1 + 10^{(pKa-pH) \cdot Hill\ slope}} \quad 3.1$$

where: R is the ratio of HyPer or SypHer fluorescent signal,  $R_{max}$  is the upper asymptote of the sigmoid,  $R_{min}$  is the lower asymptote of the sigmoid, Hill slope is the slope of the plot .

The SypHer and HyPer normalization in the calibration plot (**Figure 3.4**) have been made according to the equation:

$$\frac{R - R_0}{R_0} = \alpha \cdot \frac{pH - pH_0}{R_0} \quad 3.2$$

where  $\alpha$  is the first order derivative for  $pH = pH_0$ :

$$\alpha = \frac{dR}{dpH} = \frac{(R_{max} - R_{min}) \cdot \log_{10} \cdot 10^{\log_{10}(pKa-pH_0)}}{(pKa - pH_0) \cdot (10^{\log_{10}(pKa-pH_0)} + 1)^2} \quad 3.3$$

According to the calibration plot, a variation of pH between 7.15 - 6.9 is observed in the cytosol, during 1h of 100  $\mu$ M H<sub>2</sub>O<sub>2</sub> stimulation. The signal is decreasing within 20%. Our results are coherent with the one found in literature, where a decrease of pH with 0.2 units leads to 23% decrease of HyPer signal [162].

### 3.2.2 Methodology of monitoring the intracellular glutathione redox potential

Redox processes have been difficult to follow in living cells till recently. In addition to HyPer, monitoring the intracellular potential of glutathione system allows an indirect measurement of intracellular H<sub>2</sub>O<sub>2</sub> dynamics [163]. For this we chose an intracellular ratiometric detector based on roGFP2 [34]. The excitation spectrum of roGFP2 is sensitive to redox changes (**Figure 3.5 B**). The average redox potential of roGFP was identified as -280 mV close to the redox potential of glutathione E<sub>GSH</sub> -240 mV. In living cells redox potential is varying according to the oxidation degree of sulfide bridges. Coupling roGFP2 to Grx1 allows electron transfer between the two partner compounds, improving temporal response and the sensitivity of the probe (**Figure 3.5 A**). The equilibrium between glutathione redox potential E<sub>GSH</sub> and intracellular redox sensor redox potential E<sub>roGFP2</sub> is established according to Nerst equation [34]:

$$E_{GSH} = E_{GSH}^0 - \frac{RT}{zF} \ln \frac{[GSH]^2}{[GSSG]} = E_{roGFP2}^0 - \frac{RT}{zF} \ln \frac{[roGFP2_{red}]}{[roGFP2_{ox}]} = E_{roGFP2} \quad 3.4$$

The 100% Grx1-roGFP2 probe oxidation and its 100% reduction correspond to maximal and minimum fluorescence ratios. They can be used to determine the actual glutathione redox potentials [34]:

$$E_{GSH} = E_{roGFP2} = E_{roGFP2}^0 - \frac{RT}{zF} \ln \left( \frac{1 - OxD_{roGFP2}}{OxD_{roGFP2}} \right) \quad 3.5$$

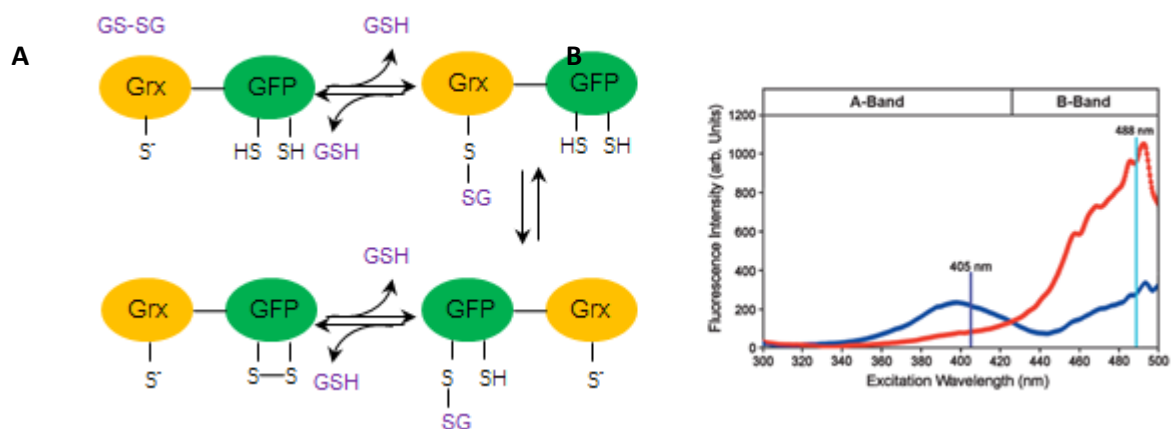


**Figure 3.5:**(A). Molecular mechanism of Grx1-roGFP2 sensor following its reversible conversion. Its regeneration is mediated by GSH; (B): roGFP2 excitation bands depicted in total oxidized (blue) and total reduced (red) forms (from [164]).

Grx1-roGFP2 responds to stimuli on a timescale interval of 90-120 seconds (our data). The detector is sensitive to physiologic relevant changes of GSSG and GSH of nM respectively mM concentration orders [34]. Stimulation of minimum 5  $\mu$ M of extracellular  $H_2O_2$  is necessary for the cells expressing the sensor to detect the response. Up to 100  $\mu$ M of stimulus saturates the signal. Comparing with HyPer, Grx1-roGFP2 detects maximum ratio change of 4.4 upon external  $H_2O_2$  stimulation, while HyPer is fully oxidized at 2.4 ratiometric changes. Moreover, the sensor is not sensitive to pH under physiological ranges simplifies the signal interpretation [34].

### 3.2.3 Monitoring the dynamics of NAD(P)H

The quantification of NAD(P)H is of great importance, given the crucial role it has in restoring the redox state on the cell. The issue that was puzzling its intracellular detection during the years is that both NADH and NADPH present the same excitation-emission spectrum [165]. To overcome this difficulty, chemical probes and GFP have been developed but they are difficult to interpret in terms of physiologic relevance. Dedicated device as fluorescence lifetime imaging microscopy (FLIM) was designed to directly detect NADH and NADPH in living cells [166].

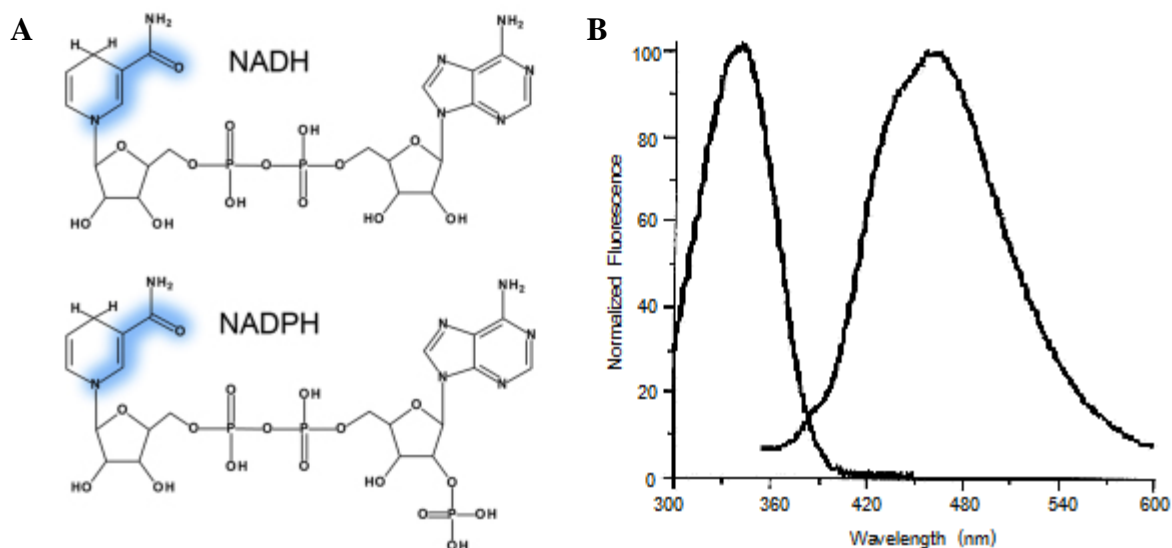


**Figure 3.6:**(A)The chemical structure of NADH and NADPH. In blue is highlighted the fluorescent part after light absorption (from [33]). (B) As the fluorescent group is identical in both molecules, their spectral characteristics are overlapping (from [165]).

Given the advantages of a direct detection, one can ask how to distinguish the autofluorescence of NADH and NADPH, using a more accessible tool as fluorescence microscopy. The main issue is that both NADH and NADPH are absorbing and emitting on the same bands and the two spectra are overlapping (**Figure 3.6**). Our detection is based on the assumption that the pools of NADH and NADPH are maintained with different redox potentials in cell compartments: the ratio of NADP<sup>+</sup>:NADPH in cytosol is low,  $3 \times 10^7 / 3 \times 10^{-5} = 10^{-2}$  [47], comparing with NAD<sup>+</sup>:NADH (700 in cytosol; 7-8 in mitochondria [50–53]). The previous ratios quantification were determined *via* endpoint measurements, on lysed cells, 50 years ago. Their values are still used in modeling, because of the lack of recent determination in real time data.

Real time experimental data are still on troubleshooting, due to the existing detector limitations. The known NAD<sup>+</sup>:NADH ratios are quantified between 100-850 using Sonar probe in various mammalian cells [54] while free NADPH:NADP<sup>+</sup> were recently determined in cytosol, nucleus and mitochondria as 55-80, 40-67 respectively 175-325 using time-correlated single photon counting TCSPC FLIM and FRET NAD(P)-Snifits sensor in U2OS cells [55].

Those results are supporting our assumption that higher NADPH level is maintained in cytosol while NADH is mainly produced in mitochondria [49].

In this work both NADH and NADPH are directly detected and are usually noted as NAD(P)H, referring to both. However, in this work the NAD(P)H dynamics is monitored in cellular cytoplasm and it will be estimated as NADPH detection for simplification.

### 3.3 Intracellular redox balance

#### 3.3.1 Perturbing the intracellular H<sub>2</sub>O<sub>2</sub> balance

Our first approach to modulate the intracellular redox balance is to increase the intracellular production rate of H<sub>2</sub>O<sub>2</sub>. For this purpose a simple step stimulation pattern is made, by applying 1h extracellular H<sub>2</sub>O<sub>2</sub>, then removing it. Crossing the membrane, the H<sub>2</sub>O<sub>2</sub> enter into the cell *via* diffusion. The change is fast detected by the molecules sensitive to peroxide. A complex protection mechanism is thus activated to prevent the oxidation of important macromolecules and restore the H<sub>2</sub>O<sub>2</sub> back to the basal level or near to it (**Figure 3.7**).

Glucose is the main nutritional source whose metabolism is controlling the antioxidants production rate. To observe the molecular dynamics before, after and during the stress, we identify the threshold survival-death dose of H<sub>2</sub>O<sub>2</sub> upon 100 μM of constant H<sub>2</sub>O<sub>2</sub> stress exposure (Chapter 2). Redox homeostasis is thus perturbed and the cellular metabolism will increase the flux in order to support the H<sub>2</sub>O<sub>2</sub> scavenging system. This regulation is the first sign of negative feedback controlled by PPP. However, cells can respond differently to the same stimulus as noticed in dose response experiments. To identify cell-to-cell variability, single cells are imaged and statistic results are necessary to interpret their response to stimulation.



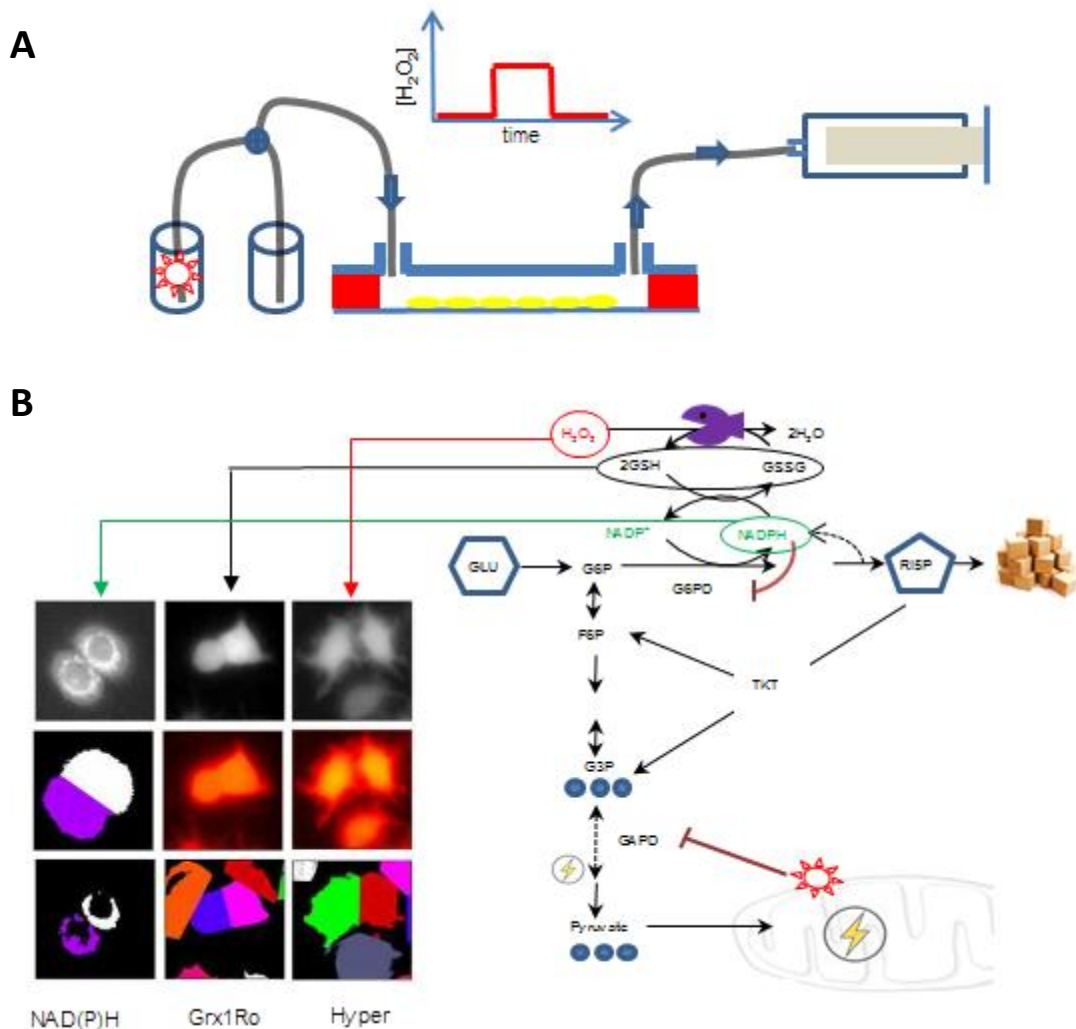


**Figure 3.8:** (A) Scheme of experimental microfluidic chamber in order to create time varying stimulus. (B) Schematic representation of the glucose metabolism highlighting the target molecules imaged by fluorescence microscopy; NAD(P)H is observed by its auto fluorescence, glutathione redox dynamics are monitored with Grx1-roGFP2, while  $\text{H}_2\text{O}_2$  and pH variations are targeted with HyPer. Both Grx1roGFP2 and HyPer are ratio metric genetically encoded sensors indicating fold changes of redox homeostasis.

emissions at 520 nm are recorded after excitation on 420 nm and 488 nm for both HyPer and Grx1-roGFP2. The NAD(P)H auto fluorescence is monitored by recording its fluorescence at 460 nm. Its excitation being in UV range at 360nm, the dose of light is adjusted to avoid photo bleaching and cytotoxicity issues. For a similar purpose the bright field images are recorded only before and after the experiment and are used to create the mask for cellular image analysis and signal extraction. MCF7 cells have been transfected using FuGene (Promega) according to the recommended protocol. The HyPer cyto vector is purchased from evrogen (pHyPer-Cyto FP941). Grx1-roGFP2 is bought from Addgene (#64975) then modified as non-lentiviral. To obtain permanent transfected clones, antibiotic selection with G418 is made. MCF7 HyPer cytoplasmic is in addition selected *via* FACS cytometry. All experiments have been performed on polyclonal MCF7 cell lines.

The variation of parameters characterizing adaptation process (**Figure 3.9**) is directly linked with the stress stimulus. Cells are imaged half an hour before applying one hour  $H_2O_2$  external stress, then their recovery for 1h is recorded. The molecular dynamics is thus monitored. When the step stimulus is applied suddenly and continuously maintained for one hour one can observe the ability of the system to sense the stimulus intensity, then to fight against it by restoring to the basal level or near to it. The recovery is imaged after removing the stimulus and

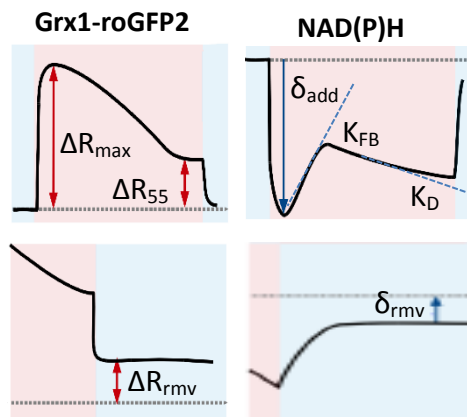


**Figure 3.9:** Parameters characterizing adaptation of cells during and after stimulation: cellular response following 1h of  $H_2O_2$  stress (upper panels). The adaptation responses are depicted and quantified by different parameters. After stress removal the system readapts to the initial state or close to it (lower panels)

is meant to front the system to the new change, the stress removal.

The adaptation index ( $\alpha_{\text{add}}$ ) is related to maximum amplitude of stress response right after its appliance ( $\Delta_{\text{add}}$ ) and the amplitude of signal recovery ( $\Delta_1$ ) during 1h stimulation and it is defined as  $\alpha_{\text{add}} = \Delta R_{55} / \Delta R_{\text{max}}$  for Grx1-roGFP2 ratio (see **Figure 3.9**). If this ratio is equal to 1, no adaptation is observed. The system is adapted when the ratio between the two amplitudes is smaller than 1. Similarly, the adaptation index is estimated after stress removal where  $\Delta_{\text{rmv}}$ ,  $\Delta R_{\text{rmv}}$  and  $\delta_{\text{rmv}}$  are the maximum variation of Grx1-roGFP2 ratio respectively NAD(P)H fluorescence gap following  $\text{H}_2\text{O}_2$  removal.

The NAD(P)H adaptation response is characterised right after stimulation by maximum variation of fluorescence relative to  $F_0$  ( $\alpha_{\text{add}}$ ) following  $\text{H}_2\text{O}_2$  addition. To evaluate the  $\Delta_1$  parameter in NAD(P)H signal, the effective fluorescence drift rate is estimated long after  $\text{H}_2\text{O}_2$  stimulation ( $K_D$ ) by a linear fit. The kinetics of molecular adaptation is estimated upon a linear fit of the drifting signal observed during the stress applied in the system. The effective fluorescence recovery rate  $K_{\text{FB}}$  shortly after  $\text{H}_2\text{O}_2$  stimulation can be extracted from NAD(P)H signals.

### 3.3.3 Adaptive dynamics in cellular cytoplasm: results and discussions

Glutathione potential ( $E_{\text{GSH}}$ ) and NADPH are targeted in cell cytoplasm and visualized before, during and after the stress.  $E_{\text{GSH}}$  changes are observed with Grx1-roGFP2. NADPH variation is estimated by monitoring the NAD(P)H auto-fluorescence in cytoplasm and the cumulated signal of both NADH and NADPH retrieved is estimated as NADPH. This approximation is made considering the biological assumption that NADH is mainly produced in mitochondria, while NADPH is majority produced in cytoplasm *via* PPP. MCF7 cells are stimulated with 100  $\mu\text{M}$  of  $\text{H}_2\text{O}_2$  under constant flow during one hour monitoring their molecular dynamics in cellular cytoplasm. The statistics are made with data extracted from hundreds of single cells recorded in one experiment.

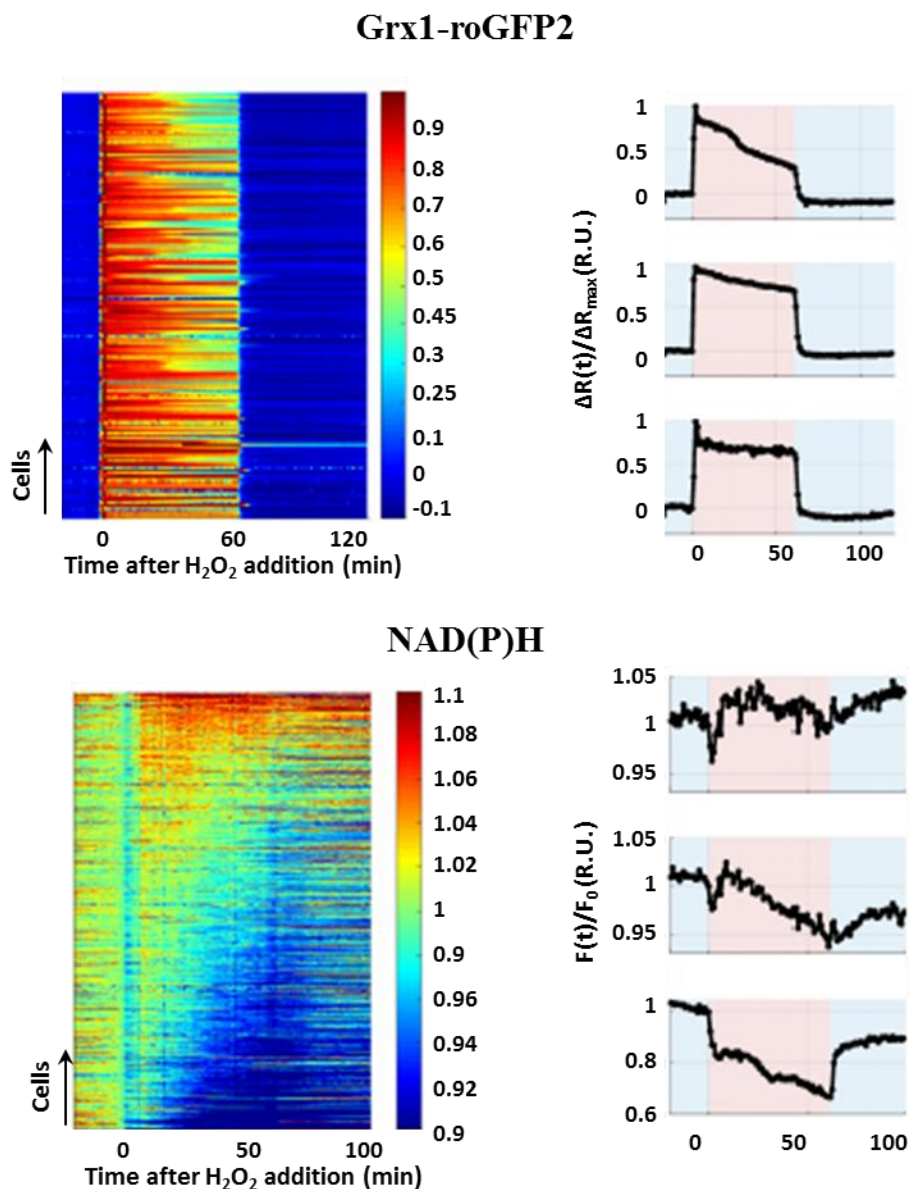


**Figure 3.10:** Molecular dynamics in MCF7 cells upon 100  $\mu\text{M}$   $\text{H}_2\text{O}_2$  stimulation: Grx1-roGFP2 and NAD(P)H cytoplasmic are monitored to observe adaptation features upon addition and removal of continuous 100  $\mu\text{M}$  of  $\text{H}_2\text{O}_2$ . Suggestive single cell features are extracted.

Analyzing single cells allows us to observe the variability of the response. Considering the fact that the stress is applied on a multi-clonal population of cells, each being in different cell cycles phases, the variability of response to stress can lead from this biological assumption [154]. Using unsynchronized cells allows observation of different adaptation features. Suggestive trends of single cells signal are extracted on the right side of heat map (**Figure 3.10**)

Cytoplasmic glutathione potential sensor, Grx1-roGFP2 is known as pH insensitive under physiologic conditions, thus near perfect adaptation features due to redox homeostasis restoring are observed during stimulation (**Figure 3.10**). The most common behavior noticed with it is slow signal decrease, suggesting a slow kinetic degradation of  $H_2O_2$  by the intracellular quenchers. However, some cells do not perform a scavenging tendency at all. Right after stimulus removal, all transfected cells recover suddenly to the basal level or near to it.

NAD(P)H cytoplasmic signal is showing also few distinctive responses (**Figure 3.10**). All cells are fast responding to external stimulus with different intensities. Almost 80% of cells are recovering to their basal level in the first minutes and are able to maintain it 10 minutes (25% of total) or 30 minutes (approx. 20% of total), then their signal decreases significantly. Interestingly, around 35% of cells are able to maintain their basal level on the duration of stress. Interestingly, right after applying the  $H_2O_2$  stimulation a small gap restoring fast is noticed.

After stress removal the 25% of cells lowering the NAD(P)H signal after 10 minutes under stimulation do not reach back their basal level after 1 h of recovery. 10% of total cells are increasing the NAD(P)H level after stress removal, behavior manifested during stimulation also. The rest of cells (around 45%) retrieve to their initial NAD(P)H pool 20 minutes after removing the stimulus. 10% of total cells sensed the stimulus removal by lowering the NAD(P)H level in the first minutes, then it increases back or higher than the pre-stimulus level.

The dynamic processes inside the cell lead to a continuous regulation of pH, being a key dynamic parameter. Likewise  $H_2O_2$ , the intracellular pH is influenced by extracellular pH. However, additional internal pH tuners are involved in cytoplasmic pH thus regulating processes as cell division [167]. Metabolic processes are constant acids supply in cell. To maintain the metabolic rate, thus a constant intracellular pH, the acidic end products resulted during glucose metabolism has to be quenched by an adequate scavenging system. Enzymes, buffers and transporters are involved in maintaining the homeostasis of pH. As the activity of functional enzymes is strongly modulated by pH changes, each cell compartment maintains a specific pH value. The spatial distribution of pH in the cell is regulating the cellular function too [158]. The first description of  $H^+$  ions role in regulating the intracellular metabolism has been made by Warburg, while observing the particular aerobic glycolysis enhanced in cancer cells. In this

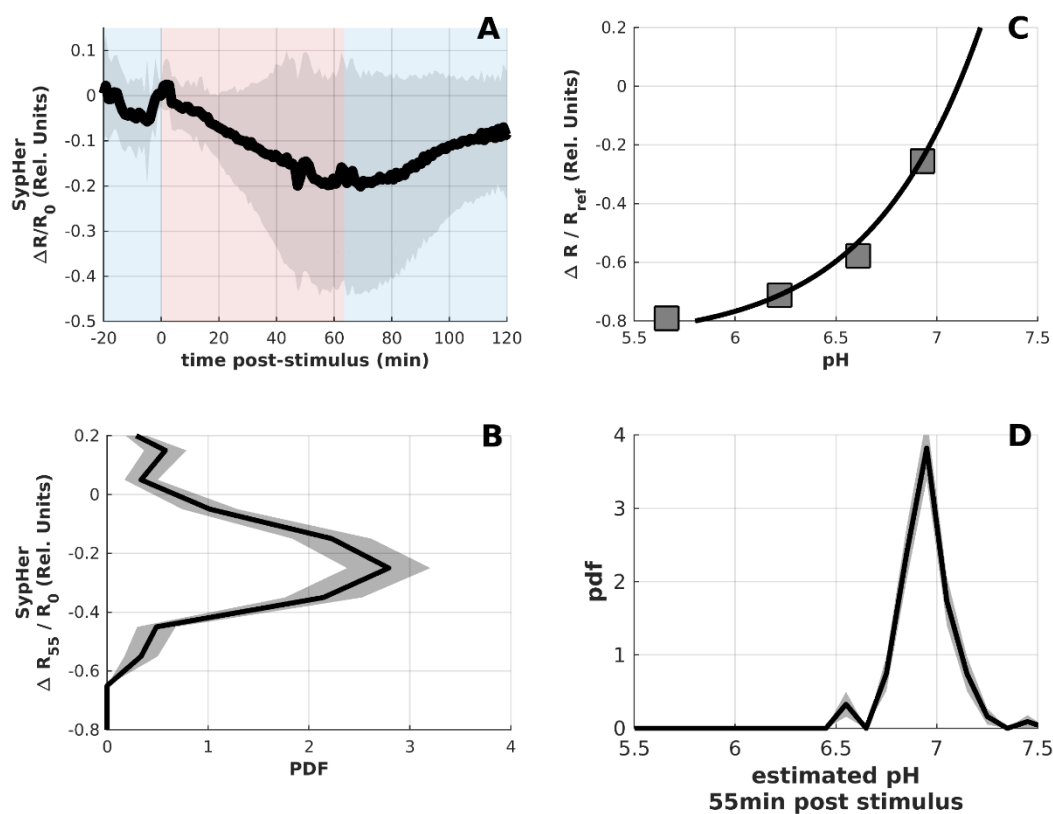


**Figure 3.11:** pH estimation *via* SypHer in acidic cytosol. (A) SypHer kinetics: black line represents the mean signal, while the grey area is the variability of the signal corresponding to single cells. The blue background is represented the pre-stimulus and post stimulus SypHer variation, while in pink is highlighted the pH variation during 100  $\mu\text{M}$   $\text{H}_2\text{O}_2$  stimulation. On y axis is plotted  $\Delta R/R_0$  where  $R_0$  is SypHer ratio pre-stimulus and  $\Delta R = R(t) - R_0$ ; (B) Histogram of  $\Delta R_{55}/R_0$  where  $\Delta R_{55} = R_{55\text{min}} - R_0$ ; (C) Calibration of SypHer ratio versus pH. Data are fitted with  $R = R_1 + R_2 / (1 + e^{nu(pK_a - pH)})$ , where  $R_1 = 0.1$ ;  $R_2 = 9.4968$ ;  $pK_a = 8.4$ ;  $nu = 2$ .  $pH_{\text{ref}} = 7.1$  corresponding to cytosolic pH, thus  $\text{Ref} = 0.758$ ; (D) Conversion of data in B with calibration on fig. C.

process the cells are producing ATP in the cytoplasm, leading to increased acidic pH due to lactic and carbonic acids higher production rate.

Most fluorophors are pH sensitive. As metabolic modulation will be performed in our experimental conditions, the pH fluctuation estimation is of interest. The most acidic cytosolic condition is expected during  $\text{H}_2\text{O}_2$  stimulation under maximum glycolytic flux. To obtain this condition (**Figure 3.11**), the Pentose Phosphate Pathway is inhibited using 6-aminonicotiamide (6AN). MCF7 SypHer cells are incubated 1h before imaging with 6AN at 500  $\mu\text{M}$  concentration, blocking the main antioxidant pool in the cytoplasm. SypHer fluorescence is recorded 30 min

pre-stimulus, 1h during 100  $\mu\text{M}$   $\text{H}_2\text{O}_2$  stimulation and 1h during recovery. The cells are maintained during imaging in PBS with glucose (4.5 g/L glucose concentration).

The SypHer kinetics (**Figure 3.11 A**) is here represented as  $\Delta R/R_0$  to avoid the technical implications induced by experimental device particularities used for recording the signals, as illumination conditions.  $\Delta R$  is the SypHer fluorescence ratio monitored during experiment.  $R_0$  is the SypHer fluorescence ratio imaged pre-stimulation assumed to correspond to pH 7.1. The variation of this ratio is displayed as Probability Density Function (PDF). It allows identifying the interval of SypHer ratio variation (**Figure 3.11 B**). This modulation in the most acidic experimental conditions allows estimating the Grx1-roGFP2 sensitivity to pH. In this context, Grx1-roGFP2 is exposed to various pH. For this purpose, MCF7 Grx1-roGFP2 cells seeded in silicon rectangular dishes are stimulated with  $\text{H}_2\text{O}_2$  for 10 min (100 $\mu\text{M}$   $\text{H}_2\text{O}_2$  prepared in DPBS with glucose 4.5 g/L concentration) than fixed with paraformaldehyde (4% PFA). Connecting the sample to the flow system, the cells are exposed to various pH ranges (pH<sub>2</sub>) of 6.9, 6.7 or 6.5, where the pre-stimulus reference pH is 7.1. The cytosolic pH is regulated by controlling the extracellular pH of PBS pumped in the chamber during imaging. Both SypHer and Grx1-roGFP2 are imaged in the same illumination conditions, using the same device. The  $\Delta R/R_{\text{ref}}$  is also calculated for Grx1-roGFP2 signals and used as pH calibration plot (**Figure 3.11 C**). The SypHer ratio variations during the most acidic experimental conditions we target are now converted into pH units (**Figure 3.11 D**).

Grx1-roGFP2 ratio increases when pH decreases while we notice the decrease of ratio under stimulation (**Figure 3.12**). No significant variation of ratio when changing from pH=7.1 to pH=6.9 is observed.  $\Delta R$  is +3% for pH=6.5 while  $\Delta R$  is -15% upon stimulation. Furthermore, looking closely at each channel both fluorescent channels of Grx1-roGFP2 decrease when pH decreases while both increase under stimulation.

We are interested to know if the pH variation under physiological range is interfering in the detection of redox potential in cellular cytosol using Grx1-roGFP2 probe. The pH variation during glycolysis and  $\text{H}_2\text{O}_2$  stimulation is monitored with SypHer in living MCF7 cells. If we assume cytosolic pH=7.1, we find on average cells at pH=6.9, 55min post-stimulus. Taking into account the cell to cell variability, it can be concluded that the cytosolic pH is not lower than 6.5 in the most acidic metabolic and ROS perturbation condition.

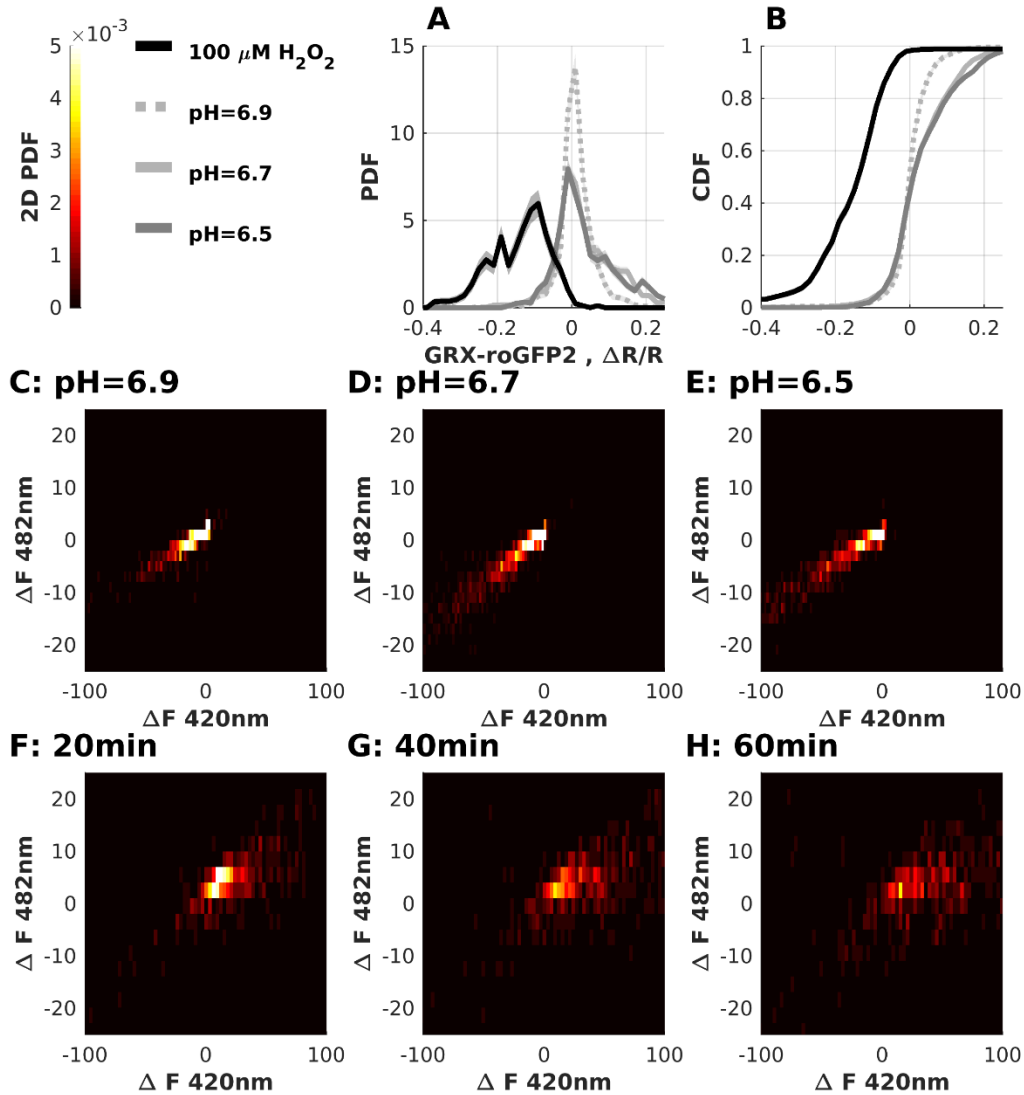


**Figure 3.12 :** Comparison of Grx1-roGFP2 ratio variation upon 100 $\mu\text{M}$   $\text{H}_2\text{O}_2$  stimulation and pH variation. (A, B) comparison of Grx1-roGFP2  $\Delta R/R$ : for 100 $\mu\text{M}$   $\text{H}_2\text{O}_2$  stimulation  $R=R_{\text{max}}$  while after stimulation  $\Delta R = R_{55\text{min}}-R_{\text{max}}$ ; for pH variation  $R=R_{\text{pH}=7.1}$  and  $\Delta R=R_{\text{pH}2}-R_{\text{pH}=7.1}$ , where  $\text{pH}_2$  is 6.9, 6.7 or 6.5; (C,D,E) Comparison of fluorescence variation in each channel at various pH, where the reference is  $\text{pH}=7.1$ , is plotted the 2D PDF; (F,G,H) Comparison of fluorescence variation in at various time following 100 $\mu\text{M}$  stimulation, where the reference is prestimulus, is plotted the 2D PDF

From our knowledge, adaptation timescales of 30 min have been reported on GSH:GSSG ratio after short time stimulation with a high  $\text{H}_2\text{O}_2$  concentration stimulus intensity [125]. We cannot compare the rest of our results while in literature are not reported adaptation timescales during the type of stimulation performed.

Taking into account the two different methods of molecular detection: direct for NADPH and indirect for  $E_{\text{GSH}}$  one can say that the biases of the probes have to be considered. In the extreme acidic case targeted in our experimental condition, pH may hide some feedback in Grx1-roGFP2 signal, but its effect is much smaller than  $\text{H}_2\text{O}_2$  ( $\Delta R=+3\%$  compared to  $-15\%$ ).

### 3.4 External $\text{H}_2\text{O}_2$ concentration effect on adaptation dynamics

After depicting different adaptation behaviors during stimulation, the intensity of the stimulus will be modulated to observe cytosolic regeneration pool in oxidative stress conditions. On the assumption that the dualistic role of  $\text{H}_2\text{O}_2$  is dose controlled, modulating the dose, will be targeted the adaptation/non-adaptation threshold dose in mammalian systems. To depict the two behaviors, mild concentrations of 30 and 50  $\mu\text{M}$   $\text{H}_2\text{O}_2$ , high and very high doses of 100 respectively 250  $\mu\text{M}$  during 1h will be used to stimulate the cells.

During molecular imaging, the MCF7 cells are kept in the chamber under flow. The basal level is monitored for half hour, than the stimulus of various  $\text{H}_2\text{O}_2$  concentrations is applied for one hour. After stress removal, their recovery is followed for one hour. All experiments are performed in DPBS with Ca and Mg supplemented with glucose at 4.5g/L concentration. We represent averaged data over the population analyzed before, during and after stimulation (**Figure 3.13**).

Parameters characterizing adaptation dynamics are extracted from experimental data and are represented together with the corresponding Probability Density Function (PDF) (**Figure 3.14**). The PDF representation is showing a bell shape, where the values under the curve indicate statistically the probability of the event to occur in a certain interval. Here, looking at the first graph (**Figure 3.14 A**) it is likely that the amplitude of the signal retrieved by monitoring the Grx1-roGFP2 fluorescence ratio in time upon 10  $\mu\text{M}$   $\text{H}_2\text{O}_2$  stimulation to be in the interval of

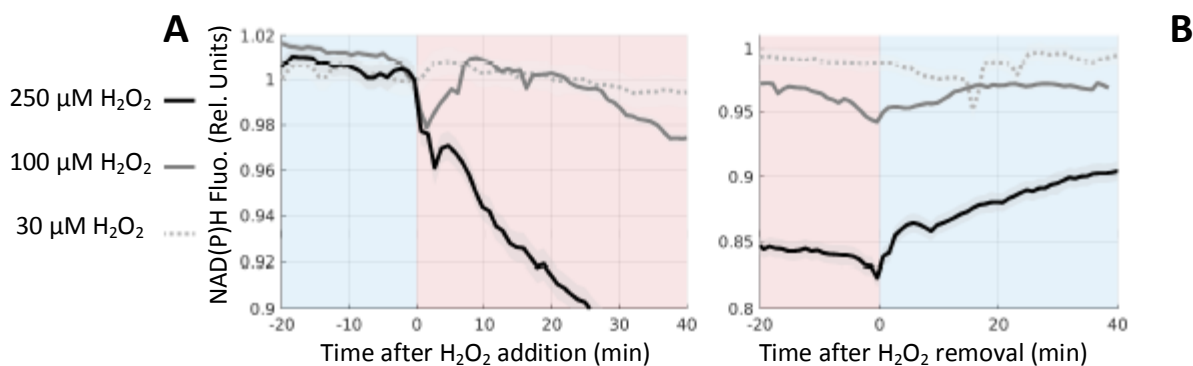


**Figure 3.13:** Effect of  $[H_2O_2]$  dose on molecular adaptation dynamics in cytosol observed with NAD(P)H fluorescence. Pre-stimulus (blue background A), stimulus (pink background A-B) and post-stimulus (blue background B) fluorescent signals are here averaged over cell population. Normalized NAD(P)H fluorescence kinetics upon various  $[H_2O_2]$  stimuli are represented: in black solid line 250  $\mu M$ , in grey solid line 100  $\mu M$ , grey dashed line 30  $\mu M$ .

(0-0.1), while for higher concentrations as 500  $\mu M$  it is noticed in a broader interval (0.05-0.2). The discrete value of this parameter is indicated in the panel above (**Figure 3.14 B**). Similarly, the PDF is represented for the adaptation parameters retrieved in NAD(P)H signal (**Figure 3.14 E**).

Near adaptation features (see **Figure 3.10**) have been noticed during 100  $\mu M$  H<sub>2</sub>O<sub>2</sub> stimulation looking at Grx1-roGFP2 fluorescence ratio. Modulating the intensity of stimulus we notice stronger feedback when redox homeostasis is more disturbed. One can say that higher the amplitude of redox homeostasis perturbation, stronger is the feedback retrieved (**Figure 3.14 C**). Similarly, the amplitude of NAD(P)H fluorescence increases with the stimulus intensity (**Figure 3.14 F**). The fast ( $K_{FB}$ ) and the long time ( $K_D$ ) regulation kinetic parameters are both sensitive to external H<sub>2</sub>O<sub>2</sub> stimulus delivered to cell, increasing when higher concentration (**Figure 3.14 G, H**). However, the NAD(P)H fluorescence is not an echo of Grx1-roGFP2. The removal of stress leads to fast decrease of fluorescence (**Figure 3.14I**) and the recovery is usually lower than the initial basal level.

Concerning cytoplasmic NAD(P)H perturbation, they are proportional in intensity with the intensity of applied stimulus. Its recovery is unsuccessful during high concentrations of H<sub>2</sub>O<sub>2</sub> stimulation. The mild stress of 30  $\mu M$  applied is not significantly perturbing the intracellular

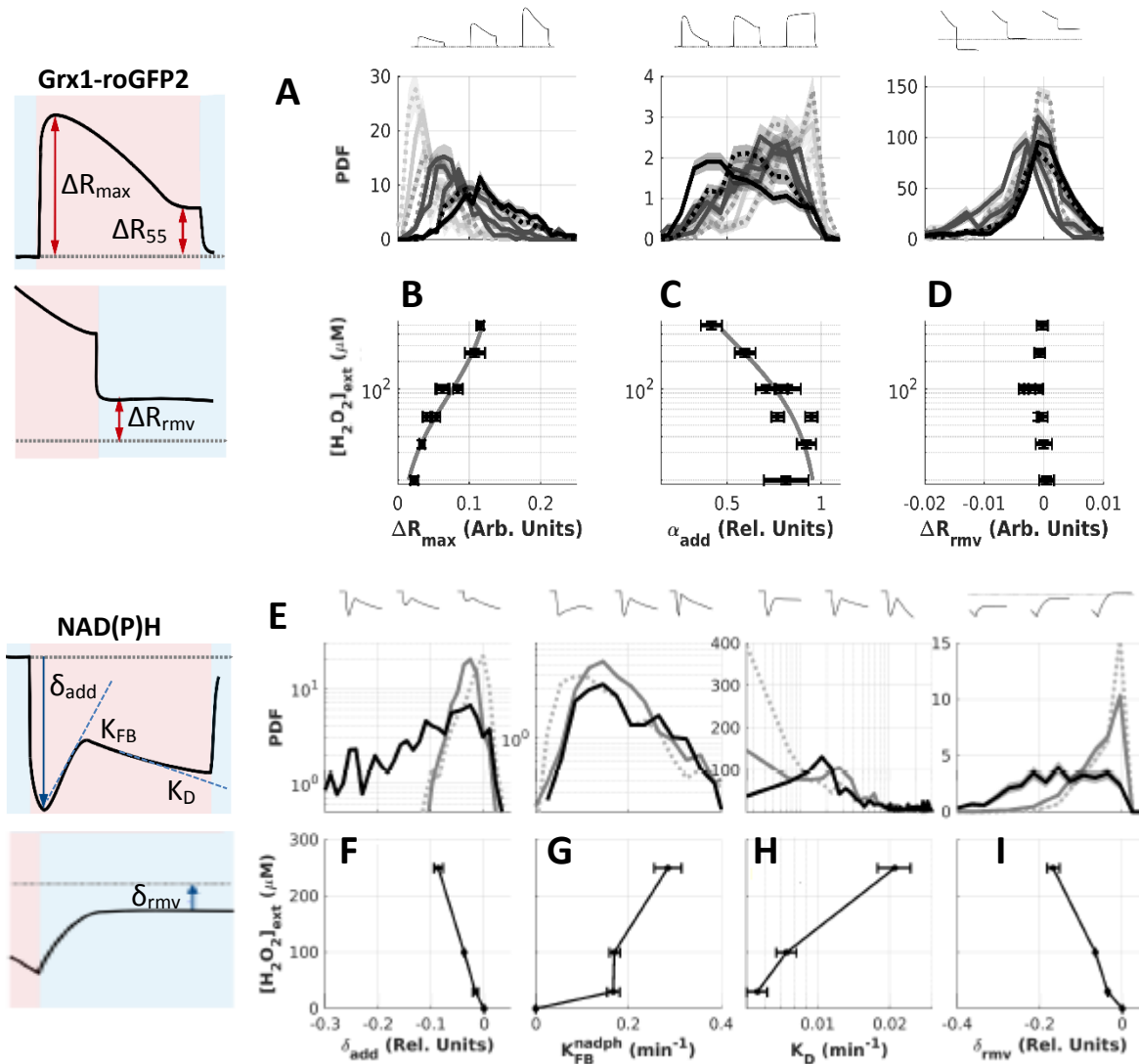


**Figure 3.14:** Effect of  $[\text{H}_2\text{O}_2]$  dose on molecular adaptation dynamics in cytosol observed with Grx1-roGFP2 – redox potential sensor (A-D) and NAD(P)H fluorescence (E-I). Left panel; schematic definition of parameters characterizing Grx1-roGFP2 and NAD(P)H. The corresponding probability density function (PDF) of each parameter described is depicted in upper panels. (A, E); (B) maximum variation of Grx1-roGFP2 ratio  $\Delta R_{\max}$  following  $\text{H}_2\text{O}_2$  addition; (C) adaptation index  $\alpha_{\text{add}} = \Delta R_{55}/\Delta R_{\max}$ ; (D) maximum variation of Grx1-roGFP2 ratio ( $\Delta R_{\text{rmv}}$ ) following  $\text{H}_2\text{O}_2$  removal; (F) maximum variation of fluorescence relative to  $F_0$  ( $\delta_{\text{add}}$ ) during  $\text{H}_2\text{O}_2$  stimulation; (G) effective fluorescence recovery rate shortly after  $\text{H}_2\text{O}_2$  stimulation  $K_{\text{FB}}$ ; (H) effective fluorescence drift rate longer after  $\text{H}_2\text{O}_2$  stimulation  $K_{\text{D}}$ ; (I) NAD(P)H fluorescence gap between pre-stimulus and steady state following  $\text{H}_2\text{O}_2$  removal  $\delta_{\text{rmv}}$ .

NAD(P)H fluorescence. It can be due to the insensitivity of the cell to the stress or to the low signal to noise ratio in our imaging settings.

The variation of maximum Grx1roGFP2 signal is linearly dependent with the amplitude of signal recovery during prolonged stress, indicating that the feedback is stronger when the redox homeostasis is disturbed (**Figure 3.14 A-C**). Similarly, both the maximum variation of Grx1roGFP2 ratio following H<sub>2</sub>O<sub>2</sub> addition and removal are correlated pointing that the intensity of scavenging perturbation is controlling the cellular adaptation to a specific stressful environment.

In order to describe the adaptation mechanism upon H<sub>2</sub>O<sub>2</sub> stimulation and to identify the negative feedback response induced by thioredoxins and glutathione scavengers, MCF7wt are permanently transfected with Grx1-roGFP2 genetically encoded probe, thus transforming the cell to a new system. Despite the advantages provided by transfection of detecting cellular response in real time, we are aware that the sensor can interfere in the biological normal functionality. Slow correlation of the Grx1-roGFP2 probe with the adaptation parameters describing the negative system is thus identified in our experimental conditions.

Varying the external H<sub>2</sub>O<sub>2</sub> stimulus from 10 to 500 μM, the half maximum H<sub>2</sub>O<sub>2</sub> concentration where  $\Delta R_{\max}$  saturates is 70 μM. We cannot conclude if this concentration reflects the maximum import rate of H<sub>2</sub>O<sub>2</sub> or it is the limit of detection of Grx1roGFP2 probe [34].

Cell-to-cell variability is strongly observed after stress removal in both Grx1roGfp2 and NAD(P)H signals. Moreover, after stimulation, Grx1-roGFP2 is returning to the basal level while the NAD(P)H recovery is slower. The different sensitivity of cell to the two high stimuli is described by an effective fluorescence recovery rate shortly after stimulation (**Figure 3.14 D, I**). The fluorescence gap between pre-stimulus and steady state following H<sub>2</sub>O<sub>2</sub> removal is showing also perfect adaptation signs after 30 μM and 100 μM stimuli removal. The similar trend of NAD(P)H fluorescence gap between pre-stimulus and steady state following H<sub>2</sub>O<sub>2</sub> removal is pointing out the metabolic modulation in the cytosol as an effect of stress response.

Different adaptation signs of cytosolic H<sub>2</sub>O<sub>2</sub> and NAD(P)H have been observed to be correlated with the stimuli intensities. Adding external [H<sub>2</sub>O<sub>2</sub>] leads in consequence to the increase of internal [H<sub>2</sub>O<sub>2</sub>] rate also. Comparing the adaptation features observed with H<sub>2</sub>O<sub>2</sub>

sensors and NAD(P)H fluorescence, we can conclude that complex mechanisms are involved. NAD(P)H pool is fast adapting for  $[H_2O_2]$  up to 100  $\mu M$  which makes us wondering if it is a mechanism directly supported by the glucose metabolism. While the maximum variation of Grx1-roGFP2 ratio ( $\Delta R_{mv}$ ) following stress removal is close to 0, the NAD(P)H fluorescence gap in the very beginning of recovery is confirming the link of glucose metabolism in the defense mechanism against oxidative stress. On the following will be deeply studied the implications of glucose metabolism in oxidative stress adaptation process.

### 3.5 Glucose in adaptation dynamics

After varying the dose of  $H_2O_2$  stimulation, different adaptation signs have been depicted to Grx1-roGFP2 and NAD(P)H. We conclude that the adaptation mechanism might be more complex and we are wondering what the total intracellular antioxidants pool is and how to completely disturb it. For this purpose; in this scenario, glucose, the main bio-product able to support the cellular defense by maintaining the NAD(P)H formation is removed (**Figure 3.15**). The adaptation features in presence or absence of glucose upon the same stress is thus compared.

Significant signal drift has been observed in Grx1-roGFP2 fluorescence ratio during stimulation with 100  $\mu M$  external  $H_2O_2$ , in presence of glucose. As already discussed in previews section, it is suggesting that antioxidant production is increasing in cytoplasm and is restoring the redox homeostasis during stress. The data are represented as variation of its fluorescence ratio relative to maximum variation (**Figure 3.16 A**). In parallel,  $H_2O_2$  and pH variations are together detected, using HyPer (**Figure 3.16 C**). We notice that the glutathione potential changes, detected with Grx1-roGFP2 probe, are describing a similar behavior as HyPer. Interestingly, after stimulus removal, during recovery, only HyPer ratio is varying towards negative values reaching back to pre-stimulus level after few minutes. Grx1-roGFP2 signal its restoring fast to the basal level, right after stimulus removal, without showing the fluorescence ratiogap observed with HyPer.

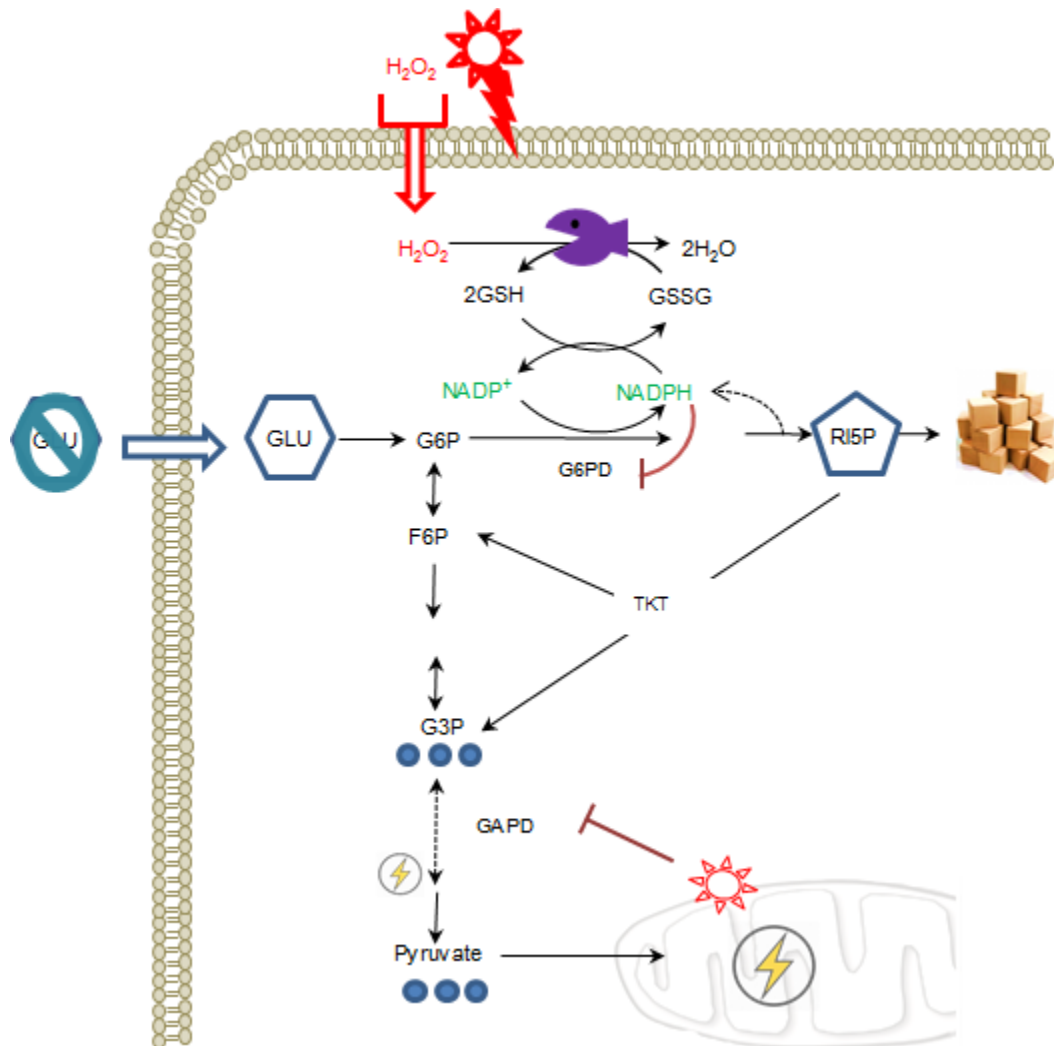


**Figure 3.15:** Schematic representation of metabolic pathways. Adding  $H_2O_2$  external stress performed in lack of external carbon source during stimulation, the cell is limited to use the existing resources to defense against stress.

In similar experimental conditions, NAD(P)H fluorescence is slightly drifting (**Figure 3.16 B**), suggesting that the cell is able to defend against stress when glucose resources are available.

Removing the glucose from external medium, similar experiment is performed. Comparing the adaptation parameters of the 3 fluorescent targets: Grx1-roGFP2, NAD(P)H and HyPer, they are all shifting according to the corresponding PDF (**Figure 3.16**), except NAD(P)H level after stimulus removal and initial HyPer ratio.

In lack of glucose, mean of HyPer and Grx1-roGFP2 fluorescent ratios are clearly not showing adaptation signs, the fluorescence ratio remaining constantly to maximum amplitude during stimulation (**Figure 3.16 A, C**). Interestingly, the NAD(P)H fluorescence is showing signal gap in the firsts minutes of stimulation, at higher amplitude than observed in presence of glucose, where it was slightly depicted. Small shift toward lower values of initial fluorescence imaged during pre-stimulation is also observed in PDF (**Figure 3.16 B**). However, no changes in the basal level are noticed with HyPer and Grx1-roGFP2 sensors.

The decrease of Grx1-roGFP2 signal in the first 20-30 minutes can be associated of a scavenging in buffering the  $H_2O_2$ . An increase of the signal is observed suggesting that the excess of cytosolic  $H_2O_2$  cannot be quenched by the existing antioxidants. The slow drift depicted in NAD(P)H auto-fluorescence few minutes after stimulation indicates that the NAD(P)H level is maintained at a new steady state during stress. NAD(P)H is recovering to the basal level 10 min after removal of external  $H_2O_2$ . The antioxidants pool cannot be restored in absence of glucose.

No fluorescence drift is observed in control experiment, suggesting that 2.5h of glucose starvation is not affecting the steady state of the cell. The basal level of cytosolic NAD(P)H is observed to be slightly higher in presence of glucose when analyzing single cells data. This difference is expected given the assumption that during glucose metabolism side ROS are created in mitochondria leading to cytosolic  $H_2O_2$ . It is not a feature that can be observed in averaged data, except NAD(P)H which is slightly lower in lack of glucose. Reduced NAD(P)H generation has been observed before under glucose limitations [168]. The hypothesis explaining this behavior is that NAD(P)H is used for regeneration of GSH which is required by glutathione

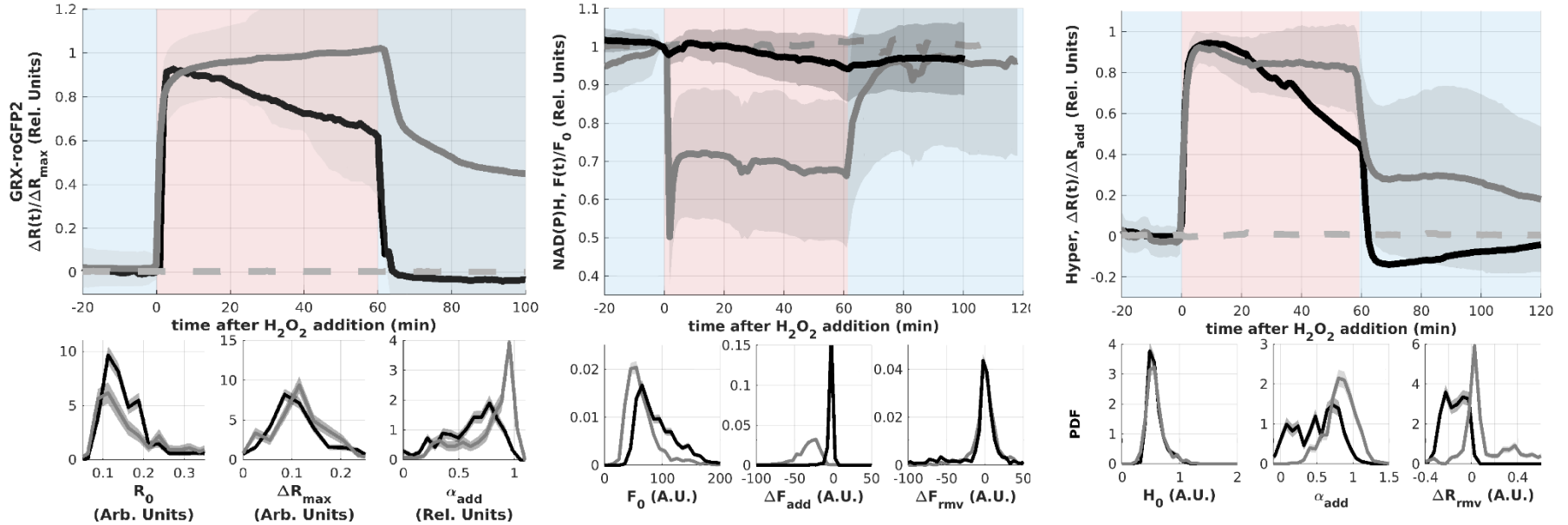


**Figure 3.16:** Averaged data concerning molecular dynamics upon  $\text{H}_2\text{O}_2$  stimulation and its removal for starving and glucose importing systems. HyPer (A), NAD(P)H (B) and Grx1-roGFP2 (C); On bottom of each panel are represented the histograms corresponding to the adaptation parameters: initial HyPer ratio ( $H_0$ ), initial NAD(P)H fluorescence level ( $F_0$ ), initial Grx1-roGFP2 ratio ( $G_0$ ) maximum ratio variation ( $\Delta R_{\max}$ ), minimum NAD(P)H fluorescence level less than 10 min after stimuli addition ( $F_{\max}$ ), HyPer respectively Grx1-roGFP2 ratio variation at 55 min following  $\text{H}_2\text{O}_2$  addition ( $\Delta R_{55}$ ), fluorescence level at 55 min following  $\text{H}_2\text{O}_2$  addition ( $F_{55}$ ), minimum HyPer respectively Grx1-roGFP2 ratio variation after  $\text{H}_2\text{O}_2$  removal ( $\Delta R_{\text{rmv}}$ ) and NAD(P)H fluorescence level 55 min after  $\text{H}_2\text{O}_2$  removal ( $F_{\text{rmv}}$ ).

peroxidase to convert  $H_2O_2$  in non-toxic products. Interestingly, we do not observe higher  $H_2O_2$  signs with Grx1-roGFP2 or HyPer probes under glucose starvation, not even in single cell data.

During stimulation, two different molecular adaptations have been depicted: in the first 10 min are observed signatures of negative feedback as the NAD(P)H level is showing increase in fluorescence, thus lowering the  $H_2O_2$  level. During prolonged stress, the antioxidant system is not able to regenerate anymore in glucose starvation. However, starving the cells from glucose, allows observing the short time adapting profile. This behavior has been slightly depicted in presence of glucose, especially in some single cells, but glucose starvation allows a better observation of the system oscillations. Following the temporal evolution of redox potential, a drift is observed in the first 20-30 minutes under stimulation, showing a second adaptation type, occurring on longer timescales. This profile might suggest a specific network regulation, involving *de novo* synthesis of antioxidants.

Monitoring the HyPer dynamics in cell cytoplasm in both glucose (G+) and carbon source starvation (G-), cumulated  $H_2O_2$  and pH kinetics is observed (**Figure 3.16 B**). Comparing the restoring mechanism noticed with Grx1-roGFP2 probe, we suspect that the pH is a key parameter involved in redox homeostasis restoring process.

Our results suggest that the adaptation phenotype is dependent of the cell metabolism. The cells manage to adapt to oxidative stress conditions in presence of glucose, while without glucose, the intracellular antioxidants system is not able to regenerate. The profile observed comparing the two metabolic conditions is indicating that the glucose metabolism plays a key role in maintaining a negative feedback during the oxidative stress. Further PPP implications in cellular defense will be analyzed to observe its amplitude in negative feedback under stress conditions.

Glucose deprivation can induce oxidative stress by reducing the NAD(P)H production in PPP [168]. Our results are showing that the basal  $H_2O_2$  level is not changing during glucose starvation. However, the NAD(P)H dynamics shows that the intensity of stress is higher sensed when external carbon resources are lacking.

### 3.6 PPP role in adaptation upon oxidative stress

Cancer cells have particular metabolism, due to their higher necessity of faster division. In consequence they present higher demand of using the pentose phosphate pathway [60]. In the previous section has been observed the role of glucose in supporting the cellular defensive mechanism against  $H_2O_2$  stress. Glucose is metabolized via glycolytic and pentose phosphate pathways strong connected through key sugar molecules: G6P, F6P and G3P (**Figure 3.17**).

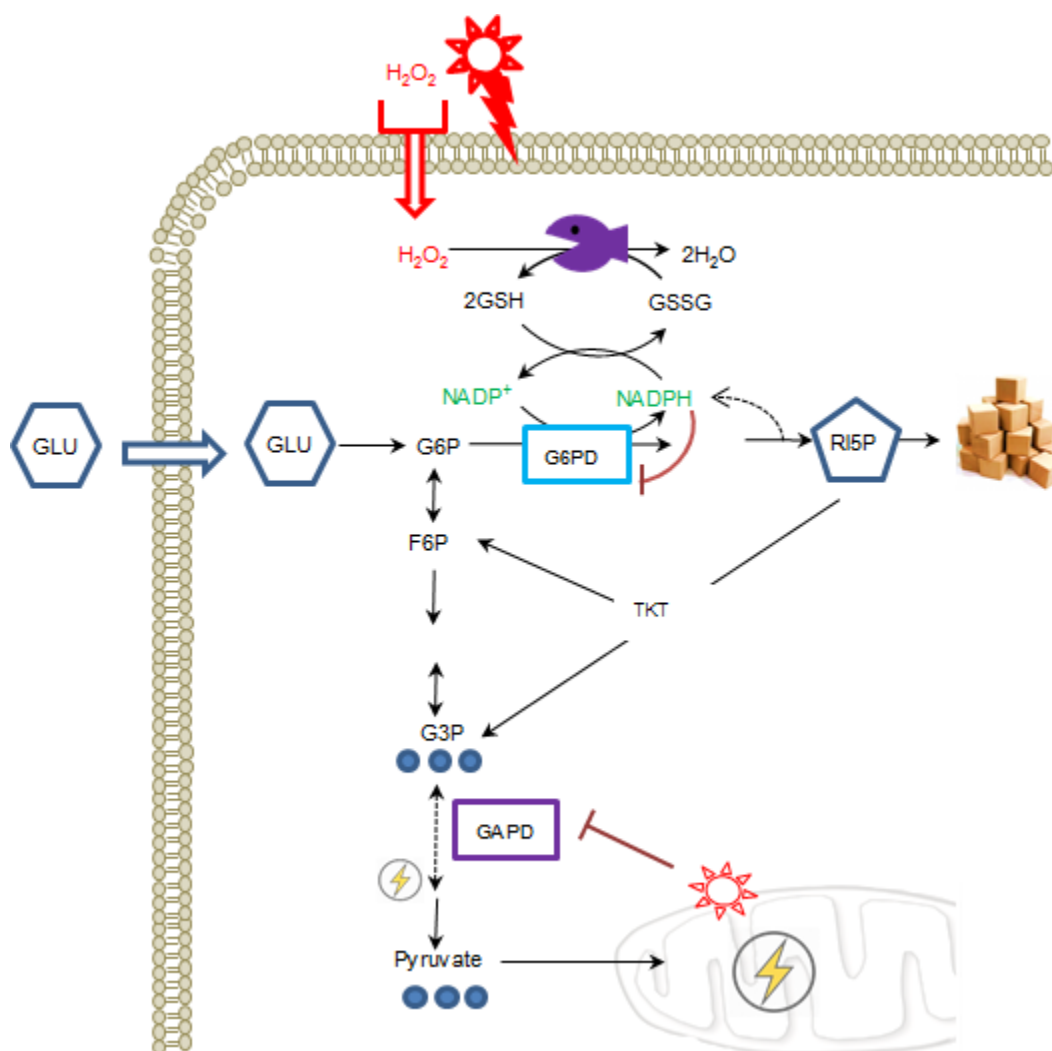


**Figure 3.17:** Schematic representation of the glucose metabolic pathways showing the link between PPP and intracellular ROS quenchers. The flux of PPP key molecules will be varied by inhibiting or overexpressing the corresponding enzymes: G6PD and GAPD.

The use of sugar is enzymatically regulated according to the cellular needs. While cancer cells need to produce more building blocks necessary for cell division, higher flux of pentose production is required. During this process, NADPH cofactor will be produced and will be used in antioxidant reduction thus maintaining the defensive mechanism against oxidative stress. NADPH is created from NADP<sup>+</sup> in a process mediated by dehydrogenase enzymes, G6PD and 6PGD. To support the metabolic flux in oxidative PPP branch direction, rotational carbon mechanism mediated by TKT enzymes have been developed. It is the non-oxidative phase of PPP which support the regeneration of sugar substrate without energetic cost. Despite the oxidative phase of PPP, the non-oxidative reaction chains are reversible. The reaction products created can be used in both PPP and glycolysis, their use being controlled enzymatically by GAPDH enzyme and allosteric hexokinase.

Dehydrogenase enzymes are gatekeepers of PPP flux and they are, in consequence, the main NADPH source controllers. The G6P flux through PPP can be modulated by increasing or silencing the G6PDH activity. Increasing the G6PDH expression cause the G6P rerouting to oxidative pentose phosphate pathway. This is leading to production of antioxidants, thus amplifying the cytosolic reducing power. This strategy is improving the cellular resistance to oxidative stress. Reduced G6PDH activity is reducing the flux of G6P to oxidative phase of PPP, reducing in consequence the NADPH production amount. In this scenario NADPH won't be sufficient to regenerate the GSH. In consequence, the oxidants can react with another biomolecules, the cellular system being more vulnerable to oxidative stress.

To study the involvement of oxidative PPP in adaptation process under oxidative stress conditions, the expression levels of NADPH supporting enzymes is modulated. To reduce the flux of G6P through the PPP, an antimetabolite as NADP<sup>+</sup> competitive binder is used. 6-aminonicotiamide is converted to 6aminoNADP by NADP<sup>+</sup> glycohydrolase. In this conditions the dehydrogenase enzymes, G6PDH and 6PGDH activities are reduced, leading to the decrease of NADPH cofactor production [169].

To increase five folds the concentration of G6PDH, the enzyme is overexpressed via transient transfection. The increase of G6PDH level is confirmed with Western blot test. The metabolic modulation of G6PDH is made by transiently transfecting the MCF7 cells. The transfection reagent is added during cell passage to optimize the plasmid insertion into the cell. It

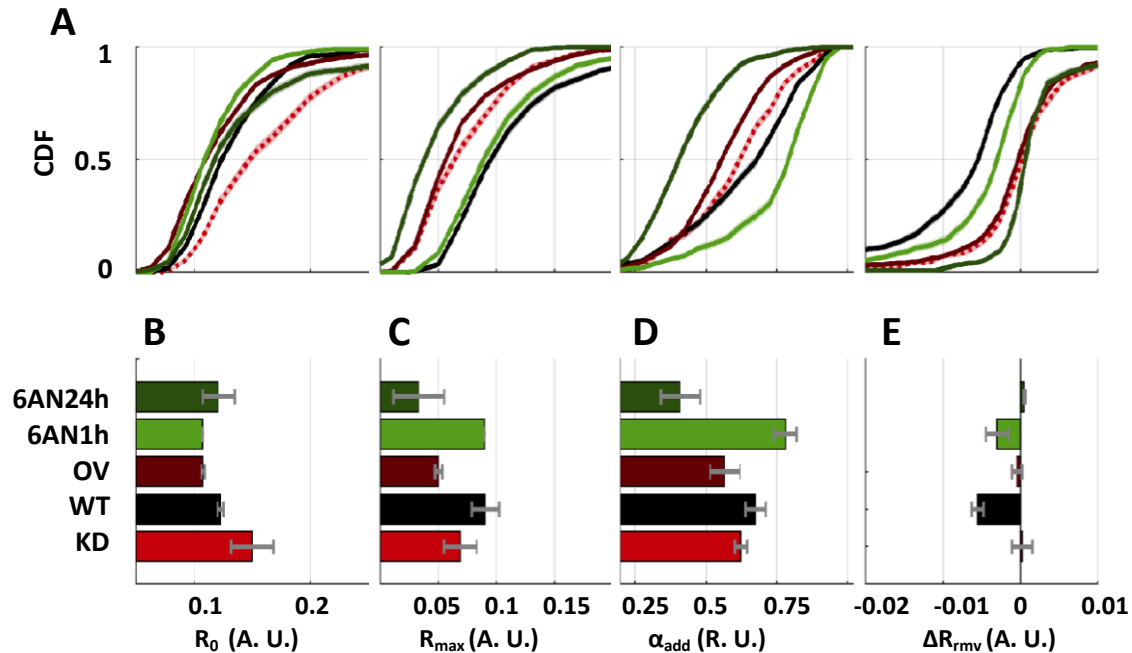


**Figure 3.18:** Effect of PPP gatekeepers modulation by G6PD over expression and knock down; following the adaptation dynamics after exposing cells to 100µM H<sub>2</sub>O<sub>2</sub> for 1h. The MCF7 cells are maintained in normal glucose conditions (4.5 g/L). The error bars are representing the variation of adaptation parameters corresponding to Grx1-roGFP2 before (R<sub>0</sub>), during (R<sub>max</sub>, α<sub>add</sub>;) and after stimulation (ΔR<sub>rmv</sub>). (A) Cumulative Density Function (CDF) where the color code is defined in lower panels (B) initial Grx1-roGFP2 ratio R<sub>0</sub> reflecting the basal redox potential (C) maximum variation of Grx1-roGFP2 ratio ΔR<sub>max</sub> following H<sub>2</sub>O<sub>2</sub> addition; (D) adaptation index α<sub>add</sub> = ΔR<sub>55</sub>/ΔR<sub>max</sub>; (E) maximum variation of Grx1-roGFP2 ratio (ΔR<sub>rmv</sub>) following H<sub>2</sub>O<sub>2</sub> removal.

is prepared mixing the DNA (G6PD/pRK5 #41521 from Addgene) and FuGENE HD (Promega, Charbonnieres, France) at 1:3 ratio, in Optimem. It is then incubated 10 min at room temperature. The mix is added in a 15 mL tube containing 1x10<sup>6</sup> MCF7 cells at passage 12, in suspension, in a volume of 4.6 mL DMEM supplemented with l-glutamine. After gentle mixing, the cells are transferred in T25 flask and incubated overnight. The medium is replaced next day, with DMEM (Lonza BE 12-614F) supplemented with L-glutamine and FBS. 48h after transfection, the cells are seeded in silicon chamber. 70h after transfection, the cells are stimulated with 100 µM of H<sub>2</sub>O<sub>2</sub>.

The activities of G6PDH and 6PGDH are reduced with 6-Amininicotiamide (6AN) purchased from Sigma-Aldrich (A68203-5G). The cells are incubated 1h or 24h before experiment with 6AN of 500  $\mu\text{M}$  concentration, prepared in complete DMEM medium.

To increase or reduce the carbon flux to PPP the GAPDH level is modulated by overexpressing or silencing the enzymatic activity. The enzymatic amount increased 2 folds by overexpressing the GAPDH. For this purpose, the MCF7 cells are transfected with custom GAPDH plasmid before the experiment. The overexpression of GAPDH is made by transfecting the MCF7 cells. pET30-2-GAPDH (83910, Addgene) is modified in our laboratory by changing the bacterial vector with mammalian equivalent. The transfection on MCF7 cells is made using FuGENE according to the manufactures recommendations. 40h after transfection the sample is used in the experiments (Western blot and 1h stimulation with  $\text{H}_2\text{O}_2$  of 100  $\mu\text{M}$  concentration).

On the other way around, the GAPDH activity is silenced. Using siRNA, the cytoplasmic amount of GAPDH decreased 3 fold, according to Western blot test performed. The GAPDH activity is silenced by transfecting the MCF7 cells with siRNA (AM4633, Invitrogen). To do so, siRNA is integrated in lipidic vesicles created with Lipofectamine RNAiMAX (LifeTechnology 13778-075) mixed in Optimem. siRNA GAPDH thus prepared is added at a final concentration of 60nM in the cell culture media. The cells are incubated overnight. The medium is changed the day after. Low cell death is observed after this metabolic transformation of the system. 70h after siRNA insertion the sample is used to quantify the GAPDH amount with Western blot and the stimulation with  $\text{H}_2\text{O}_2$  is performed.

At least 24h before stimulation, MCF7 are transiently transfected to overexpress TKT. Plasmids purchased from Addgene (72419) are inserted in the cell according to the FuGENE HD transfection reagent protocol (Promega). To monitor the sensitivity to oxidative stress in the new metabolic conditions, the cells are exposed for 1 h to 100  $\mu\text{M}$  of external  $\text{H}_2\text{O}_2$ . Their ability to adapt is quantified monitoring changes in NAD(P)H fluorescence.

The changes in glutathione potential while modulating the PPP flux are quantified in cellular cytoplasm using Grx1-roGFP2 probe. The parameters of adaptation as the initial Grx1-roGFP2 ratio  $R_0$ , adaptation index  $\alpha_{\text{add}}$ , and minimum variation of Grx1-roGFP2 ratio following  $\text{H}_2\text{O}_2$  addition  $R_{\text{add}}$  or removal  $R_{\text{rmv}}$  are displayed on cumulative density function (CDF, **Figure 3.18 A**). CDF is an integral representation of the corresponding histogram and represents the

probability to find a cell with a shape parameter. Its numerical value is between 0 and 1. The corresponding mean data of the defined adaptation parameters are represented below CDF (**Figure 3.18 B-E**).

Small variations of basal glutathione redox potential level are observed when overexpressing or reducing the G6PDH activity (**Figure 3.18 B**). No direct correlation with the basal expression level and  $\text{H}_2\text{O}_2$  stress response is observed. However, the PPP flux is clearly regulating the maximum variation of Grx1-roGFP2 ratio ( $R_{\text{max}}$ ) following  $\text{H}_2\text{O}_2$  addition. In consequence, any PPP modulation is decreasing the amplitude of cellular response at 100  $\mu\text{M}$   $\text{H}_2\text{O}_2$  stress, thus favoring significantly the adaptation process (**Figure 3.18 C, D**). Interestingly, short time PPP inhibition of 1h leads to stress resistance comparing to longer modulation time of 24h (**Figure 3.18 D**). Removing the stimulus, similar recovery patterns are noticed (**Figure 3.18 E**).

PPP is the main NADPH producer in the cell. While noticing signs of a negative feedback processing the  $E_{\text{GSH}}$  signal changes, one can expect that the NADPH pool to be also disturbed. For this purpose here the NAD(P)H auto-fluorescence is followed in various metabolic condition, when modulating the PPP flux. As previously done while monitoring Grx1-roGFP2 dynamics, here single cells have been imaged 30 minutes pre-stimulation, 1h under 100  $\mu\text{M}$   $\text{H}_2\text{O}_2$  and 1h after stimulation. The adaptation parameters are extracted and their mean is thus represented (**Figure 3.19**).

No basal NAD(P)H change is noticed when overexpressing the G6PD activity. However, modulating GAPDH or TKT expression in the cell, the basal NAD(P)H level is significantly reduced in both overexpression and silencing. The effective fluorescence drift rate shortly and longer time during stimulation is significantly reduced, confirming PPP as main negative feedback noticed previously. While shortly after stimulation the NAD(P)H fluorescence is also reduced when GAPDH and TKT are overexpressed in cell, longer time during stimulation the kinetics increases comparing to control (wild type cels). This behavior is suggesting that the feedback is not strong in these metabolic conditions, GAPDH and TKT not participating as main regulators in redox homeostasis.

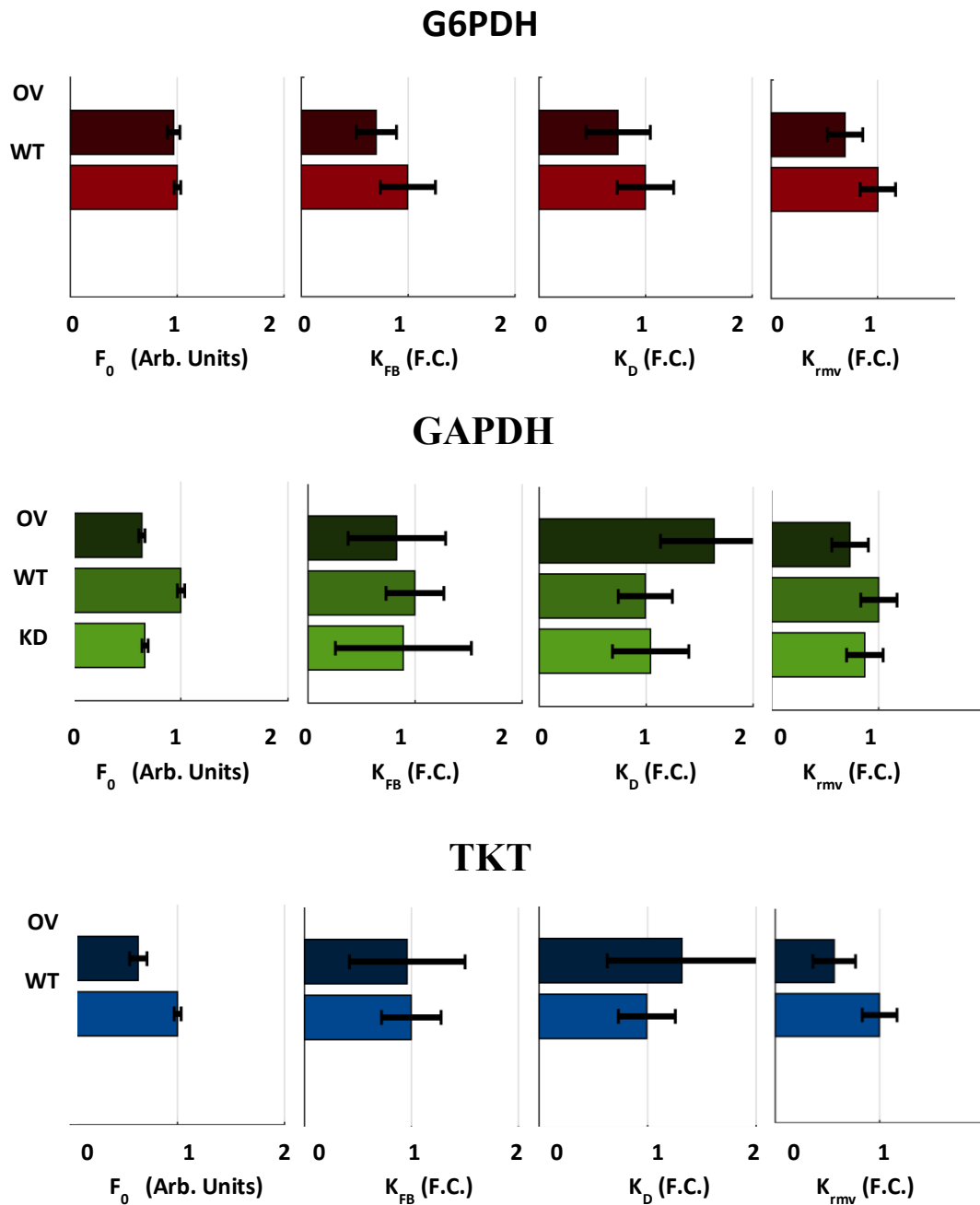


**Figure 3.19:** NADPH variation during 100  $\mu\text{M}$   $\text{H}_2\text{O}_2$  stimulation on MCF7 cells in various metabolic condition: overexpression (OV) of G6PDH, GAPDH or TKT, knock down (KD) of GAPDH activity. Wild type (WT) is the reference control

How GAPDH modulation can influence the flux of G6P to oxidative PPP? GAPDH is controlling both the upper and lower glycolysis flux, connecting the reversible reaction between the two. It has a crucial role in regulating the amount of energy necessary for cell function. Moreover, it is involved in recycling the carbon source to support the scavenging system. It has been reported that  $H_2O_2$  has inhibitory effect on GAPDH activity. In this scenario GAPDH will mediate the G3P production which will be converted to G6P. It will be used in PPP oxidative phase, increasing in consequence the NADPH amount. This way the antioxidants can be maintained in their active form, thus protecting biomolecules against external stress. However, varying the glucose import or the gatekeepers enzymes into PPP and lower glycolysis, G6PDH respectively GAPDH levels does not allow observing the complete system involved in the negative feedback orchestrated in cell cytosol.

Transketolase enzymes are involved in carbon shuffling reactions thus maintaining also the reducing power of the cell. They are converting pentose into hexoses by recycling carbons process. The reversibility of reactions involved in non-oxidative PPP is providing independency by glycolysis flux and is connected with glycolysis via F6P and G3P sugars. They can be directed to lower or upper glycolysis, depending by the cellular metabolic needs.

Overexpressing GAPDH enzymatic activity leads, most probably, to the inhibition of lower glycolysis, thus promoting the antioxidant creation in oxidative PPP branch. The decrease of basal  $H_2O_2$  level is suggesting the particular glycolysis rerouting and the antioxidant role that GAPDH plays in cytosol [170]. Interestingly, the basal level of NAD(P)H is lowered in both GAPDH overexpression and silencing.  $H_2O_2$  has inhibitory effect on GAPDH activity [137]. Under stress conditions, the glucose metabolism is directed to produce NADPH. While more carbon source is needed in the oxidative PPP, it will be distributed in the opposite direction of upper glycolysis, being recycled as G6P. This reaction product will be than after used as substrate in NADPH production. It is used by glutathione and thioredoxins as reduction agent after  $H_2O_2$  decomposition in nontoxic compounds. Interestingly, higher GAPDH amount improves the adaptation behavior under stress conditions, as can be observed in the NAD(P)H signals.

Previously has been described the main possible route of glucose metabolism as an interplay between glycolysis and oxidative PPP. This way the cell is able to produce energy and

building blocks, maintaining an active antioxidant pool. In oxidative stress conditions, the flux through oxidative PPP can be increased also by recycling the carbons. Using the transketolase enzymes substrates of G6PDH and GAPDH can be increased. However, the main negative feedback in redox homeostasis perturbation is regulated by PPP via G6PDH modulation.

### 3.7 Conclusions and discussions

The aim of our study is to link molecular architecture of redox homeostasis and adaptation properties. The cell death is a consequence of cell incapacity to maintain the redox homeostasis during stress (see Chapter 2). Under small extracellular changes, the cell is regulating the internal pathways maintaining the homeostasis. However, under mild stimuli, adaptation process occurs, shifting the cellular homeostasis permanently to a new level often by changing a certain intracellular function [171]. Evidences have been reporting rapid re-routing of metabolic fluxes upon external ROS perturbation as a first defense to oxidative stress. In the adaptation of  $H_2O_2$  degradation rate to  $H_2O_2$  excess the glucose metabolism is directly involved. Negative regulatory feedback as response to  $H_2O_2$  stress is often observed in cellular cytoplasm. Increasing the NAD(P)H production rate for ROS scavenging, the glucose flux from downstream glycolysis is rerouted to Pentose Phosphate Pathway. The redox homeostasis plasticity allows thus perfect adaptation or adaptive hormesis to occur [125,137,141].

In a first step a fast regulation process is observed by monitoring the NAD(P)H kinetics during  $H_2O_2$  stimulation. The 10 minutes timescales of NAD(P)H restoring have been already noticed in another studies where endpoint measurements have been performed [125]. The response is here monitored in mammalian living cells and statistically processed by following the molecular dynamics in single cells. Visualizing the glutathione redox potential variation using Grx1-roGFP2, a slower regulation mechanism occurring in 20-30 min is for the first time here noticed to occur during stress. One hypothesis is that after 30 min, the cell trying to adapt to the stressful condition initiating *de novo* synthesis of antioxidants, thus increasing the scavenging pool in cell cytoplasm. Similar timescales are noticed with HyPer when monitoring both the  $H_2O_2$  and pH dynamics in the same stress conditions. Interestingly, after removing the stimulus,

HyPer is showing a specific gap restoring in time. In perspective, the HyPer signal will be quantified, trying to distinguish the pH by  $H_2O_2$  dynamics.

The cell is a reacting system, initiating defensive mechanisms to protect its vital functions. Both adaptations kinetic identified are coherent with the PPP rerouting flux process in a negative feedback. Modulating the glucose input and exposing the cells to  $H_2O_2$  stimulation is noticed that the defensive main source in cell is supported by carbon sources. The two conditions experienced by MCF7 cells, G+ and G-, confirmed that the glucose is involved in the regulation of a negative feedback dependent pentose phosphate pathway metabolic flux.

To identify the main metabolic routes involved in redox homeostasis restoring process, the PPP flux is monitored when modulating the input and output of it. Perfect adaptation signs are observed when modulating the G6PDH activity. Increasing the GAPDH amount, the adaptation features are improved, comparing to wild type conditions but they are not able to maintain during stress. The TKT modulation is not key regulator in oxidative stress defense. The results are highlighting that the PPP is the main soil feedback, but not the only one. Together with pH modulation, we do observe signs of alternative routes activated during the external  $H_2O_2$  stimulation which are involved in the negative feedback. Despite of low experimental reproduction of data in PPP modulation, we did notice that on higher amplitude of redox homeostasis perturbation, the negative feedback regulated in cell cytoplasm is stronger.

---

## Conclusions and Perspectives

Cellular stress response is the framework of this study, focusing, in particular, on identifying the link between molecular architecture of redox homeostasis and adaptive properties. Redox adaptation dynamics have been already studied in unicellular organisms [137,141,172,173] and plants [174]. It has been noticed occurring at different timescales, maintaining the change even over generations [172]. Few studies have been made to observe this adaptation in mammalian cells and recently the short time adaptation under acute  $\text{H}_2\text{O}_2$  stimulation (10 min) has been observed [125,137]. Here we present a single cell approach, where the dynamics of redox is monitored, during pre-stimulus, stress and post-stimulation conditions, following it in cytoplasm of the same cell. Longer mechanism occurring 30 min during acute stimulation has been observed, controlled by the enzymatic system of the cell involved in  $\text{H}_2\text{O}_2$  scavenging.

The motivation of our work comes from the fact that cellular adaptive response to stress can favor metabolic dysregulations leading to diseases progression as cancer [175]. One of anticancer therapies strategies is to kill cancer cells, without damaging the normal ones around tumor, by increasing the intracellular level of ROS [6]. The main assumption of this strategy is that cancerous cells divide faster than non-cancerous ones, thus having a higher ROS level regulating cellular processes. This mechanism might be an adaptation of a non-cancerous cell to a new metabolic state, which, upon prolonged stress, becomes genetically controlled, leading to pathophysiological consequences [175]. Quantifying the redox balance restoring in temporal scales from minutes to hours, days to generations is a starting point for understanding how cells regulate networks and initiate transcriptions to adapt to changes and how those processes are influencing the cellular fate decisions.

Our study presents an experimental approach where the interplay between metabolic flux and oxidative stress is studied in short time-scales, during a one hour perturbation of redox homeostasis. In a first step, we are interested on controlling the  $\text{H}_2\text{O}_2$  stimulus that will be used as a tool to modulate intracellular redox homeostasis. We want to apply stabile concentration of  $\text{H}_2\text{O}_2$  on breast cancer (MCF7) cells during one hour. The addition and the removal of the stress have to occur in short timescales in order to observe adaptive behaviors. The most common technique used in oxidative stress experiments is bolus addition. Dose response experiments

highlighted that this method has significant drawbacks that are not compatible with the observation of adaptation behavior we are targeting here. Moreover, cellular consumption of  $\text{H}_2\text{O}_2$  in a bolus delivery leads to gradual stimulation, not to a steady state temporal pattern. A new stimulation system has been thus designed, allowing creating controlled temporal stress on mammalian cells. It consists of a rectangular seeding place for adherent cells, maintaining physiological conditions. It is assembled as a fluidic chamber with parallel plates whose design is inspired from Ibidi [176]. The pre/post-stimulus and stimulus are delivered to cells under flow constantly maintained by a syringe pump. Cells are attached by glass transparent bottom and can be monitored in a time-lapse microscopy experiment.

Defining the delivery dose as the integral of stimulus concentration times duration, corrections have been suggested for results found in literature where stimulation is performed by bolus addition. The corrected dose responses are overlapping our data, obtained by quantifying cell death and survival of cell populations. Modulating the duration of stress exposure, we notice that longer exposure is increasing the lethality of cells. However, when the metabolic conditions of cells are changed, the death behavior changes too [177]. While in glucose starvation conditions the cells seem to be more resistant to oxidative stress [178], inhibiting pentose phosphate pathway leads to increased vulnerability to lower doses [179]. Those results motivate us to exploit the cellular sensitivity by modulating the PPP flux controlling enzymes, thus perturbing the main scavenging power in the cell.

In a second step, external  $\text{H}_2\text{O}_2$  stimulation is applied on living cells, therefore disturbing their internal redox balance. For this purpose, experiments have been designed and performed using microfluidics, following the molecular dynamics at the single cell level. The cellular response to stress is quantified by targeting key molecules regulating the redox homeostasis. Given that, the dynamics of NADPH and glutathione potential are visualized using time-lapse fluorescence microscopy in cellular cytoplasm of living cells. The limitations and specificity of fluorescent probes have been discussed. Here we conclude that pH is a key parameter, changing during metabolic modulation and observed while using two different  $\text{H}_2\text{O}_2$  sensitive probes, HyPer and Grx1-roGFP2. Monitoring single cells is observed the cell-to-cell variability of response upon  $\text{H}_2\text{O}_2$  stimulation, which could be attributed to the cell line heterogeneity or different cell-cycle phases [180,181].

Upon H<sub>2</sub>O<sub>2</sub> stimulation, various adaptation features are identified. Controlled temporal stimulation (cells for 1h under 100 μM H<sub>2</sub>O<sub>2</sub>) allowed observation of two adaptive mechanisms. The first one is concerning the fast recovery of NADPH upon stimulation and have been already reported [125,137]. Here we do observe the same behavior: in the first 10 minutes during stress, NADPH level is disturbed, fast restoring to the basal level, during stimulation. This suggests a rapid metabolic response, favoring the increase of G6PDH activity in PPP, thus producing increased amount of NADPH. It is necessary to restore the GSH which in turn is contributing to convert the oxidized Grx into reduced form. Grx is directly responsible of protecting the proteins by oxidation. The second mechanism is for the first time reported during such a stimulation and is highlighting that Grx1-roGFP2 is slowly recovering, process occurring in the first 30 min during stimulation. One can ask why this behavior has not been observed in other studies? Few experimental particularities might contribute to the detection of this degradation process. First of all, controlling the H<sub>2</sub>O<sub>2</sub> stimulation method plays an important role in our study. Another studies where we suspect that this mechanism could be detected [125], used bolus method, which present some drawbacks when making this kind of study. We note that, depending by the cell type and by the permeability of cell membrane, H<sub>2</sub>O<sub>2</sub> can be faster or slower consumed by cells, an important inconvenience while performing bolus stimulation. In lack of details to compare the 2 methods we can only speculate that, in case that H<sub>2</sub>O<sub>2</sub> stimulus is not at steady state performed during 1h, this mechanism could not be observed, perhaps due to gradual stimulation leading to gradual adaptation also. Another aspect to consider is that this adaptation pattern is detected following the redox potential dynamics in cytoplasm of single cells. We notice-first this behavior using a pH sensitive probe, HyPer, which gives us the advantage of noticing a stronger change in the signal highlighting the sign of the second adaptation pattern. This change has not confirmed an adaptation behavior while using a more specific probe, Grx1-roGFP2. Taking in account the cell-to-cell variability we observe, we speculate that endpoint detection on cell population might hide this longer adaptation pattern. Single cell detection allows indeed the observation of longer adaptation mechanism. Although the mean response to stress is showing signs of this negative feedback, near perfect adaptation can be observed only in some single cell. Population analysis can therefore hide this mechanism, its detection being biased by the response of most of the cells.

As pointed in Chapter 2 (see section Cell death), the cellular response to stress is depending on the cell type. MCF7 cancerous cells exhibit high activity of PPP, comparing with

their non-cancerous counterparts MCF10A [182]. We do not have information concerning the heterogeneity between the cell lines used in the two studies to compare the response of our study with another where different cell types have been used (skin keratinocytes and fibroblasts vs. breast cancer cells).

We note that one important consequence of this study is that the way to stimulate is very important. Import rate of external  $H_2O_2$  is regulated by the nutritional apport existing in external cell culture medium leading to faster  $H_2O_2$  consumption in a rich medium when static stimulation is performed. The complexity and direct implication of glucose metabolism in restoring the redox homeostasis is noticed when modulating the glucose input. Faster import rate of  $H_2O_2$  is observed when cells have access to external glucose sources. The lack of glucose is limiting the external  $H_2O_2$  consumption, highlighting not only the role of glucose in supporting cellular scavenging systems, but also the possible role in promoting the active process of  $H_2O_2$  diffusion inside the cell. In presence of glucose, cells are able to show adaptation signs on both short and long term, while in lack of glucose no long-term adaptation is observed. Interestingly, higher amplitude of NADPH restoring is observed in lack of glucose, suggesting that the redox balance is more perturbed when glucose source is limited.

Moreover, modulating the concentration of  $H_2O_2$  exposure during 1h, we notice that the negative feedback supported by PPP becomes stronger with the increase of stimulus intensity. Perfect or near perfect adaptation patterns have been noticed in NADPH dynamics during stimulations lower than  $100 \mu M H_2O_2$ , but NADPH cytosolic pool is not able to regenerate up to it whereas it has not been observed in Grx1-roGFP2 fluorescence ratio where stronger stimulation implies stronger response.

All those results are pointing the direct link between oxidative stress and metabolism. However, one standing question remains: how the dynamics of adaptation response is regulated by cellular metabolism? To answer this question, PPP gatekeepers have been modulated to observe their role in adaptation upon  $H_2O_2$  stress. Increasing the G6P flux toward PPP by overexpressing the G6PDH, strong evidence favoring adaptation mechanism is provided. NADPH pool is faster restored, allowing the glutathione regeneration thus increasing the cellular resistance to  $H_2O_2$  stress. Varying the expression of GAPDH and TKT evidences of allosteric regulation are not clearly observed. The adaptation is not improved, thus their role in fueling the

oxidative PPP by reverse recycling towards G6P is not supported by our experiments. Moreover, their overexpression is decreasing the basal NADPH cytoplasmic level suggesting a downstream to glycolytic activity. We conclude that the G6PDH is a key regulator favoring rapid flux rerouting into oxidative PPP. This mechanism is strongly involved in cellular adaptation upon oxidative stress, regulating the cellular homeostasis *via* negative feedback. G6P is thus controlling the reserve flux capacity sensitive to oxidative stress. Signs of alternative metabolic routes involved in cytosolic defense are observed.

In this work we do confirm the short time regulation of metabolic activity, favoring negative feedback regulation in PPP [125,137]. However, our study is targeting the redox homeostasis dynamics in cytosol being interested to observe short time scales adaptation patterns during 1h stimulation. For longer adaptation patterns as transcription, epigenetics and genomics, molecular dynamics in other compartments as mitochondria should be taken into account. Mitochondria are regulating longer time scales of adaptation which are of interest in tumor progression. Cytoplasmic function is of interest in initiation of tumor genesis, while mitochondria is concerning later stages [175].

Monitoring molecular dynamics in single living cells, targeting a specific compartment and using ratio-metric pH insensitive probes have been possible by creating a new system, starting from wild type cells. The glutathione potential was monitored integrating *via* permanent transfection an unknown number of plasmids producing fluorescent Grx, thus increasing the antioxidant capacity in the cell cytoplasm. We do not have noticed significant cell-to-cell variability when comparing the pre-stimulus basal glutathione potential. However, the transformation of the system using transfection can change the sensitivity of cell to stress.

The impact of redox homeostasis regulation just started to be appreciated in mammalian cells. PPP regulation is observed in short timescales of minutes during acute stress. NADPH dynamics and G6P are involved in this rapid metabolic rerouting process. The main perspective of this work would be to study adaptation on longer timescales. Chronic stimulation can indeed lead to longer adaptation timescales, thus observing the intracellular redox homeostasis regulation by transcription factors. However, for chronic stimulation, our H<sub>2</sub>O<sub>2</sub> delivery protocol has to be improved, cells needing a complex medium to be maintained longer than few hours. Anticancer therapies are exploiting redox homeostasis vulnerability to remove tumors. For this

purpose, estimating intracellular ROS thresholds can provide advantages in removing cancer cells. Knowing that ROS are regulating networks, therapies are exploiting alternative networks regulating redox homeostasis. The impact of other stresses regulating adaptation processes as hypoxia, other ROS, metabolic stress is of interest in this context. Upon stress exposure, adaptation on different timescales can be studied to improve anticancer therapy strategies but also to observe conservation of mechanistic regulation between species and the impact of cellular stress response on cellular fate [137].

## Bibliography

- [1] M.M.J.P.E. Sthijns, A.R. Weseler, A. Bast, G.R.M.M. Haenen, Time in Redox Adaptation Processes: From Evolution to Hormesis, *Int. J. Mol. Sci.* 17 (2016) 1–15. doi:10.3390/ijms17101649.
- [2] E.N. Marieb, K. Hoehn, *Human Anatomy and Physiology*, 9th ed., Pearson, 2013.
- [3] I.R. Cohen, D. Harel, Explaining a complex living system: Dynamics, multi-scaling and emergence, *J. R. Soc. Interface.* 4 (2007) 175–182. doi:10.1098/rsif.2006.0173.
- [4] V. de Oliveira-Marques, L. Cyrne, H.S. Marinho, F. Antunes, A Quantitative Study of NF- B Activation by H<sub>2</sub>O<sub>2</sub>: Relevance in Inflammation and Synergy with TNF-alpha, *J. Immunol.* 178 (2007) 3893–3902. doi:10.4049/jimmunol.178.6.3893.
- [5] H. Sies, Role of metabolic H<sub>2</sub>O<sub>2</sub> generation: Redox signaling and oxidative stress, *J. Biol. Chem.* 289 (2014) 8735–8741. doi:10.1074/jbc.R113.544635.
- [6] D. Trachootham, J. Alexandre, P. Huang, Targeting cancer cells by ROS-mediated mechanisms: A radical therapeutic approach?, *Nat. Rev. Drug Discov.* 8 (2009) 579–591. doi:10.1038/nrd2803.
- [7] B. Perillo, M. Di Donato, A. Pezone, E. Di Zazzo, P. Giovannelli, G. Castoria, A. Migliaccio, ROS in cancer therapy: the bright side of the moon, *Exp. Mol. Med.* 52 (2020) 192–203. doi:10.1038/s12276-020-0384-2.
- [8] H. Selye, A Syndrome produced by Diverse Nocuous Agents, *Nature.* 138 (1936) 32. doi:10.1038/138032a0.
- [9] S. Fulda, A.M. Gorman, O. Hori, A. Samali, Cellular stress responses: Cell survival and cell death, *Int. J. Cell Biol.* 2010 (2010). doi:10.1155/2010/214074.
- [10] M. Chen, S. Xie, Therapeutic targeting of cellular stress responses in cancer, *Thorac. Cancer.* 9 (2018) 1575–1582. doi:10.1111/1759-7714.12890.
- [11] M. Schieber, N. Chandel, ROS function in redox signaling and oxidative stress, *Curr Biol.* 24 (2014) 453–462. doi:10.1016/j.cub.2014.03.034.
- [12] T. Finkel, Signal transduction by reactive oxygen species, *J. Cell Biol.* 194 (2011) 7–15. doi:10.1083/jcb.201102095.
- [13] C.M. Sena, A. Leandro, L. Azul, R. Seiça, G. Perry, Vascular Oxidative Stress: Impact and Therapeutic Approaches, *Front. Physiol.* 9 (2018) 1–11. doi:10.3389/fphys.2018.01668.
- [14] V. Lobo, A. Patil, A. Phatak, N. Chandra, Free radicals, antioxidants and functional foods: Impact on human health, *Pharmacogn. Rev.* 4 (2010) 118. doi:10.4103/0973-7847.70902.
- [15] I. Dalle-Donne, A. Milzani, N. Gagliano, R. Colombo, D. Giustarini, R. Rossi, Molecular

- mechanisms and potential clinical significance of S-glutathionylation, *Antioxidants Redox Signal.* 10 (2008) 445–473. doi:10.1089/ars.2007.1716.
- [16] H. Sies, D. Jones, Oxidative Stress, in: *Encycl. Stress*, 2nd ed., 2007: pp. 45–48. doi:10.1016/B978-012373947-6.00285-3.
- [17] I. Kruk, *Environmental Toxicology and Chemistry of Oxygen Species*, 1998. doi:10.1007/978-3-540-49571-0.
- [18] P. Held, *An Introduction to Reactive Oxygen Species. Measurement of ROS in Cells*, BioTek, 2015.
- [19] M. Jozefczak, T. Remans, J. Vangronsveld, A. Cuypers, Glutathione is a key player in metal-induced oxidative stress defenses, *Int. J. Mol. Sci.* 13 (2012) 3145–3175. doi:10.3390/ijms13033145.
- [20] S. Dey, A. Sidor, B. O'Rourke, Compartment-specific control of reactive oxygen species scavenging by antioxidant pathway enzymes, *J. Biol. Chem.* 291 (2016) 11185–11197. doi:10.1074/jbc.M116.726968.
- [21] K. Das, A. Roychoudhury, Reactive oxygen species (ROS) and response of antioxidants as ROS-scavengers during environmental stress in plants, *Front. Environ. Sci.* 2 (2014) 1–13. doi:10.3389/fenvs.2014.00053.
- [22] F. Anquez, A. Sivéry, I. El Yazidi-Belkourab, Z. Jaouad, P. Suret, S. Randoux, E. Courtade, Production of Singlet Oxygen by Direct Photoactivation of Molecular Oxygen, in: *Compr. Ser. Photochem. Photobiol. Sciences. Singlet Oxyg. Appl. Biosci. Nanosci.*, Royal Soc Of Chemistry, 2016: pp. 75–91.
- [23] M. Nita, A. Grzybowski, The Role of the Reactive Oxygen Species and Oxidative Stress in the Pathomechanism of the Age-Related Ocular Diseases and Other Pathologies of the Anterior and Posterior Eye Segments in Adults, *Oxid. Med. Cell. Longev.* 2016 (2016) 1–23. doi:10.1155/2016/3164734.
- [24] D.R. Zhou, R. Eid, K.A. Miller, E. Boucher, C.A. Mandato, M.T. Greenwood, Intracellular second messengers mediate stress inducible hormesis and Programmed Cell Death: A review, *Biochim. Biophys. Acta - Mol. Cell Res.* 1866 (2019) 773–792. doi:10.1016/j.bbamcr.2019.01.016.
- [25] K.M. Holmstrom, T. Finkel, Cellular mechanisms and physiological consequences of redox-dependent signalling., *Nat. Rev. Mol. Cell Biol.* 15 (2014) 411–21. doi:10.1038/nrm3801.
- [26] D. Gough, T.G. Cotter, Hydrogen peroxide : a Jekyll and Hyde signalling molecule, *Cell Death Dis.* 2 (2011) e213-8. doi:10.1038/cddis.2011.96.
- [27] C. Lin, H. Wang, Short Communication NADPH oxidase is involved in H<sub>2</sub>O<sub>2</sub>-induced differentiation of human promyelocytic leukaemia HL-60 cells, 36 (2012) 391–395. doi:10.1042/CBI20110290.
- [28] F. Goudarzi, A. Mohammadalipour, M. Bahabadi, M. TaghiGoodarzi, A. Sarveazad, I.

- Khodadadi, Hydrogen Peroxide: A Potent Inducer of Differentiation of Human Adipose-Derived Stem Cells into Chondrocytes, *Free Radic. Res.* 5762 (2018). doi:10.1080/10715762.2018.1466121.
- [29] K. Chen, M.T. Kirber, H. Xiao, Y. Yang, J.F.K. Jr, Regulation of ROS signal transduction by NADPH oxidase 4 localization, *J. Cell Biol.* 181 (2008) 1129–1139. doi:10.1083/jcb.200709049.
- [30] R. Caldini, M. Chevanne, A. Mocali, D. Tombaccini, F. Paoletti, Premature induction of aging in sublethally H<sub>2</sub>O<sub>2</sub> treated young MRC5 fibroblasts correlates with increased glutathione peroxidase levels and resistance to DNA breakage, *Mech. Ageing Dev.* 105 (1998) 137–150.
- [31] G.H. Kim, J.E. Kim, S.J. Rhie, S. Yoon, The Role of Oxidative Stress in Neurodegenerative Diseases, *Exp. Neurobiol.* 24 (2015) 325–340. doi:10.5607/en.2015.24.4.325.
- [32] A. Msolly, A. Miled, A. Kassab, Hydrogen Peroxide : an Oxidant Stress Indicator in Type 2 Diabetes Mellitus, 1 (2013).
- [33] T.S. Blacker, M.R. Duchon, Investigating mitochondrial redox state using NADH and NADPH auto fluorescence, *Free Radic. Biol. Med.* 100 (2016) 53–65. doi:10.1016/j.freeradbiomed.2016.08.010.
- [34] M. Gutscher, A.-L. Pauleau, L. Marty, T. Brach, G.H. Wabnitz, Y. Samstag, A.J. Meyer, T.P. Dick, Real-time imaging of the intracellular glutathione redox potential, *Nat. Methods.* 5 (2008) 553–559. doi:10.1038/nmeth.1212.
- [35] D.L. Thomson, The Effect of Hydrogen Peroxide on the Permeability of the Cell, *J. Exp. Biol.* 4 (1928) 252–257. doi:10.1111/j.1744-7348.1927.tb07022.x.
- [36] D.R. Zhou, R. Eid, E. Boucher, K.A. Miller, C.A. Mandato, M.T. Greenwood, Stress is an agonist for the induction of programmed cell death: A review, *Biochim. Biophys. Acta - Mol. Cell Res.* 1866 (2019) 699–712. doi:10.1016/j.bbamcr.2018.12.001.
- [37] N.M. Mishina, Y.A. Bogdanova, Y.G. Ermakova, A.S. Panova, D.A. Kotova, D.S. Bilan, B. Steinhorn, E.S.J. Arnér, T. Michel, V. V. Belousov, Which Antioxidant System Shapes Intracellular H<sub>2</sub>O<sub>2</sub> Gradients? , *Antioxid. Redox Signal.* (2019) 1–18. doi:10.1089/ars.2018.7697.
- [38] A.M. Navale, A.N. Paranjape, Glucose transporters : physiological and pathological roles, *Biophys. Rev.* 8 (2016) 5–9. doi:10.1007/s12551-015-0186-2.
- [39] X. Li, P. Fang, J. Mai, E.T. Choi, H. Wang, X.F. Yang, Targeting mitochondrial reactive oxygen species as novel therapy for inflammatory diseases and cancers, *J. Hematol. Oncol.* 6 (2013) 1–19. doi:10.1186/1756-8722-6-19.
- [40] H.S. Marinho, C. Real, L. Cyrne, H. Soares, F. Antunes, Hydrogen peroxide sensing, signaling and regulation of transcription factors, *Redox Biol.* 2 (2014) 535–562. doi:10.1016/j.redox.2014.02.006.

## Bibliography

---

- [41] N.C. Veitch, Horseradish peroxidase: A modern view of a classic enzyme, *Phytochemistry*. 65 (2004) 249–259. doi:10.1016/j.phytochem.2003.10.022.
- [42] Z.A. Wood, E. Schröder, J.R. Harris, L.B. Poole, Structure, mechanism and regulation of peroxiredoxins, *Trends Biochem. Sci.* 28 (2003) 32–40. doi:10.1016/S0968-0004(02)00003-8.
- [43] B.N. Tripathi, I. Bhatt, K.J. Dietz, Peroxiredoxins: A less studied component of hydrogen peroxide detoxification in photosynthetic organisms, *Protoplasma*. 235 (2009) 3–15. doi:10.1007/s00709-009-0032-0.
- [44] C.S. Sevier, C.A. Kaiser, Formation and transfer of disulphide bonds in living cells, *Nat. Rev. Mol. Cell Biol.* 3 (2002) 836–847. doi:10.1038/nrm954.
- [45] L.V. Papp, J. Lu, A. Holmgren, K.K. Khanna, From Selenium to Selenoproteins: Synthesis, Identity, and Their Role in Human Health, *Antioxid. Redox Signal.* 9 (2007) 775–806. doi:10.1089/ars.2007.1528.
- [46] C.F. Ng, F.Q. Schafer, G.R. Buettner, V.G.J. Rodgers, The rate of cellular hydrogen peroxide removal shows dependency on GSH: Mathematical insight into in vivo H<sub>2</sub>O<sub>2</sub> and GPx concentrations, *Free Radic. Res.* 41 (2007) 1201–1211. doi:10.1080/10715760701625075.
- [47] J.B. Lim, B.K. Huang, W.M. Deen, H.D. Sikes, Analysis of the lifetime and spatial localization of hydrogen peroxide generated in the cytosol using a reduced kinetic model, *Free Radic. Biol. Med.* 89 (2015) 47–53. doi:10.1016/j.freeradbiomed.2015.07.009.
- [48] J.B. Lim, T.F. Langford, B.K. Huang, W.M. Deen, H.D. Sikes, A reaction-diffusion model of cytosolic hydrogen peroxide, *Free Radic. Biol. Med.* 90 (2016) 85–90. doi:10.1016/j.freeradbiomed.2015.11.005.
- [49] D.L. Nelson, M.M. Cox, *Principles of biochemistry*, 2005. doi:10.1007/s11655-011-0820-1.
- [50] W. Ying, NAD<sup>+</sup>/NADH and NADP<sup>+</sup>/NADPH in Cellular Functions and Cell Death: Regulation and Biological Consequences, *Antioxid. Redox Signal.* 10 (2008) 179–206. doi:10.1089/ars.2007.1672.
- [51] R.L. Veech, R. Guynn, D. Veloso, The time-course of the effects of ethanol on the redox and phosphorylation states of rat liver, *Biochem. J.* 127 (1972) 387–397. doi:10.1042/bj1270387.
- [52] D.H. Williamson, P. Lund, H.A. Krebs, The Redox State of Free Nicotinamide-Adenine Dinucleotide in the Cytoplasm and Mitochondria of Rat Liver, *Biochem. Biophys. Res. Commun.* 103 (1967) 514–527. doi:10.1007/BF00527204.
- [53] L.R. Stein, S. Imai, The dynamic regulation of NAD metabolism in mitochondria, *Trends Endocrinol Metab.* 23 (2012) 420–428. doi:10.1016/j.tem.2012.06.005.
- [54] Y. Zhao, Q. Hu, F. Cheng, N. Su, A. Wang, Y. Zou, H. Hu, X. Chen, H.M. Zhou, X. Huang, K. Yang, Q. Zhu, X. Wang, J. Yi, L. Zhu, X. Qian, L. Chen, Y. Tang, J. Loscalzo,

- Y. Yang, SoNar, a Highly Responsive NAD<sup>+</sup>/NADH Sensor, Allows High-Throughput Metabolic Screening of Anti-tumor Agents, *Cell Metab.* 21 (2015) 777–789. doi:10.1016/j.cmet.2015.04.009.
- [55] O. Sallin, L. Reymond, C. Gondrand, F. Raith, B. Koch, K. Johnsson, Semisynthetic biosensors for mapping cellular concentrations of nicotinamide adenine dinucleotides, *Elife.* 7 (2018) 1–32. doi:10.7554/eLife.32638.
- [56] M. Lopez-Lazaro, The Warburg Effect: Why and How Do Cancer Cells Activate Glycolysis in the Presence of Oxygen?, *Anticancer. Agents Med. Chem.* 8 (2008) 305–312. doi:10.2174/187152008783961932.
- [57] J. Feher, ATP Production III, *Quant. Hum. Physiol.* (2017) 241–252. doi:10.1016/b978-0-12-800883-6.00022-7.
- [58] O. Warburg, On the origin of cancer cells, *Science* (80-. ). 123 (1956) 309–314. doi:10.1126/science.123.3191.309.
- [59] J. Da Veiga Moreira, M. Hamraz, M. Abolhassani, E. Bigan, S. Pérès, L. Paulevé, M.L. Nogueira, J.M. Steyaert, L. Schwartz, The redox status of cancer cells supports mechanisms behind the Warburg effect, *Metabolites.* 6 (2016) 1–12. doi:10.3390/metabo6040033.
- [60] C. Riganti, E. Gazzano, M. Polimeni, E. Aldieri, D. Ghigo, The pentose phosphate pathway: An antioxidant defense and a crossroad in tumor cell fate, *Free Radic. Biol. Med.* 53 (2012) 421–436. doi:10.1016/j.freeradbiomed.2012.05.006.
- [61] H.-C. Yang, Y.-H. Wu, W.-C. Yen, H.-Y. Liu, T.-L. Hwang, A. Stern, D.T.-Y. Chiu, The Redox Role of G6PD in Cell Growth, Cell Death, and Cancer, *Cells.* 8 (2019) 1–29. doi:10.3390/cells8091055.
- [62] E.S. Cho, Y.H. Cha, H.S. Kim, N.H. Kim, J.I. Yook, The pentose phosphate pathway as a potential target for cancer therapy, *Biomol. Ther.* 26 (2018) 29–38. doi:10.4062/biomolther.2017.179.
- [63] T. You, P. Ingram, M.D. Jacobsen, E. Cook, A. McDonagh, T. Thorne, M.D. Lenardon, A.P. De Moura, M.C. Romano, M. Thiel, M. Stumpf, N.A.R. Gow, K. Haynes, C. Grebogi, J. Stark, A.J.P. Brown, A systems biology analysis of long and short-term memories of osmotic stress adaptation in fungi, *BMC Res. Notes.* 5 (2012). doi:10.1186/1756-0500-5-258.
- [64] U. Alon, *An introduction to systems biology*, 2007.
- [65] J.E. Ferrell, Perfect and near-perfect adaptation in cell signaling, *Cell Syst.* 2 (2016) 62–67. doi:10.1016/j.cels.2016.02.006.
- [66] J.G. Betts, P. Desaix, E. Johnson, J.E. Johnson, O. Korol, D. Kruse, B. Poe, J.A. Wise, M. Womble, K.A. Young, *Anatomy and Physiology*, OpenStax, 2013. <https://openstax.org/details/books/anatomy-and-physiology>.
- [67] J.J. Tyson, K.C. Chen, B. Novak, Sniffers, buzzers, toggles and blinkers: Dynamics of

- regulatory and signaling pathways in the cell, *Curr. Opin. Cell Biol.* 15 (2003) 221–231. doi:10.1016/S0955-0674(03)00017-6.
- [68] H. Sies, Hydrogen peroxide as a central redox signaling molecule in physiological oxidative stress: Oxidative eustress, *Redox Biol.* 11 (2017) 613–619. doi:10.1016/j.redox.2016.12.035.
- [69] J.T. Hancock, *Cell Signalling*, 3rd ed., OXFORD University Press, 2010.
- [70] E.A. Veal, A.M. Day, B.A. Morgan, Hydrogen peroxide sensing and signaling, *Mol. Cell.* 26 (2007) 1–14. doi:10.1016/j.molcel.2007.03.016.
- [71] H. Wang, S. Schoebel, F. Schmitz, H. Dong, K. Hedfalk, Characterization of aquaporin-driven hydrogen peroxide transport, *BBA - Biomembr.* 1862 (2020) 1–12. doi:10.1016/j.bbamem.2019.183065.
- [72] V. Oliveira-Marques, T. Silva, F. Cunha, G. Covas, H.S. Marinho, F. Antunes, L. Cyrne, A quantitative study of the cell-type specific modulation of c-Rel by hydrogen peroxide and TNF- $\alpha$ , *Redox Biol.* 1 (2013) 347–352. doi:10.1016/j.redox.2013.05.004.
- [73] B.K. Huang, H.D. Sikes, Quantifying intracellular hydrogen peroxide perturbations in terms of concentration, *Redox Biol.* 2 (2014) 955–962. doi:10.1016/j.redox.2014.08.001.
- [74] D.S. Bilan, L. Pase, L. Joosen, A.Y. Gorokhovatsky, Y.G. Ermakova, T.W.J. Gadella, C. Grabher, C. Schultz, S. Lukyanov, V. V. Belousov, HyPer-3: A genetically encoded H<sub>2</sub>O<sub>2</sub> probe with improved performance for ratiometric and fluorescence lifetime imaging, *ACS Chem. Biol.* 8 (2013) 535–542. doi:10.1021/cb300625g.
- [75] O. Lyublinskaya, F. Antunes, Measuring intracellular concentration of hydrogen peroxide with the use of genetically encoded H<sub>2</sub>O<sub>2</sub> biosensor HyPer, *Redox Biol.* 24 (2019) 1–7. doi:10.1016/j.redox.2019.101200.
- [76] D. Labavic, M.T. Ladjimi, Q. Thommen, B. Pfeuty, Scaling laws of cell-fate responses to transient stress, *J. Theor. Biol.* 478 (2019) 14–25. doi:10.1016/j.jtbi.2019.06.014.
- [77] M.S. D’Arcy, Cell death: a review of the major forms of apoptosis, necrosis and autophagy, *Cell Biol. Int.* 43 (2019) 582–592. doi:10.1002/cbin.11137.
- [78] L. Galluzzi, I. Vitale, S.A. Aaronson, J.M. Abrams, D. Adam, P. Agostinis, E.S. Alnemri, L. Altucci, I. Amelio, D.W. Andrews, M. Annicchiarico-Petruzzelli, A. V. Antonov, E. Arama, E.H. Baehrecke, N.A. Barlev, N.G. Bazan, F. Bernassola, M.J.M. Bertrand, K. Bianchi, M. V. Blagosklonny, K. Blomgren, C. Borner, P. Boya, C. Brenner, M. Campanella, E. Candi, D. Carmona-Gutierrez, F. Cecconi, F.K.M. Chan, N.S. Chandel, E.H. Cheng, J.E. Chipuk, J.A. Cidlowski, A. Ciechanover, G.M. Cohen, M. Conrad, J.R. Cubillos-Ruiz, P.E. Czabotar, V. D’Angiolella, T.M. Dawson, V.L. Dawson, V. De Laurenzi, R. De Maria, K.M. Debatin, R.J. Deberardinis, M. Deshmukh, N. Di Daniele, F. Di Virgilio, V.M. Dixit, S.J. Dixon, C.S. Duckett, B.D. Dynlacht, W.S. El-Deiry, J.W. Elrod, G.M. Fimia, S. Fulda, A.J. García-Sáez, A.D. Garg, C. Garrido, E. Gavathiotis, P. Golstein, E. Gottlieb, D.R. Green, L.A. Greene, H. Gronemeyer, A. Gross, G. Hajnoczky, J.M. Hardwick, I.S. Harris, M.O. Hengartner, C. Hetz, H. Ichijo, M. Jäättelä, B. Joseph, P.J. Jost, P.P. Juin, W.J. Kaiser, M. Karin, T. Kaufmann, O. Kepp, A. Kimchi, R.N. Kitsis,

- D.J. Klionsky, R.A. Knight, S. Kumar, S.W. Lee, J.J. Lemasters, B. Levine, A. Linkermann, S.A. Lipton, R.A. Lockshin, C. López-Otín, S.W. Lowe, T. Luedde, E. Lugli, M. MacFarlane, F. Madeo, M. Malewicz, W. Malorni, G. Manic, J.C. Marine, S.J. Martin, J.C. Martinou, J.P. Medema, P. Mehlen, P. Meier, S. Melino, E.A. Miao, J.D. Molkenin, U.M. Moll, C. Muñoz-Pinedo, S. Nagata, G. Nuñez, A. Oberst, M. Oren, M. Overholtzer, M. Pagano, T. Panaretakis, M. Pasparakis, J.M. Penninger, D.M. Pereira, S. Pervaiz, M.E. Peter, M. Piacentini, P. Pinton, J.H.M. Prehn, H. Puthalakath, G.A. Rabinovich, M. Rehm, R. Rizzuto, C.M.P. Rodrigues, D.C. Rubinsztein, T. Rudel, K.M. Ryan, E. Sayan, L. Scorrano, F. Shao, Y. Shi, J. Silke, H.U. Simon, A. Sistigu, B.R. Stockwell, A. Strasser, G. Szabadkai, S.W.G. Tait, D. Tang, N. Tavernarakis, A. Thorburn, Y. Tsujimoto, B. Turk, T. Vanden Berghe, P. Vandenabeele, M.G. Vander Heiden, A. Villunger, H.W. Virgin, K.H. Vousden, D. Vucic, E.F. Wagner, H. Walczak, D. Wallach, Y. Wang, J.A. Wells, W. Wood, J. Yuan, Z. Zakeri, B. Zhivotovsky, L. Zitvogel, G. Melino, G. Kroemer, Molecular mechanisms of cell death: Recommendations of the Nomenclature Committee on Cell Death 2018, *Cell Death Differ.* 25 (2018) 486–541. doi:10.1038/s41418-017-0012-4.
- [79] A. Valencia, J. Morán, Reactive oxygen species induce different cell death mechanisms in cultured neurons, *Free Radic. Biol. Med.* 36 (2004) 1112–1125. doi:10.1016/j.freeradbiomed.2004.02.013.
- [80] Y. Goulev, S. Morlot, A. Matifas, B. Huang, M. Molin, M.B. Toledano, G. Charvin, Nonlinear feedback drives homeostatic plasticity in H<sub>2</sub>O<sub>2</sub> stress response, *Elife.* 6 (2017) 1–33. doi:10.7554/elife.23971.
- [81] J.M. Keegstra, K. Kamino, M.D. Lazova, T. Emonet, T.S. Shimizu, Phenotypic diversity and temporal variability in a bacterial signaling network revealed by single-cell FRET, *Elife.* 6 (2017) 1–33. doi:10.7554/eLife.27455.
- [82] Z. Long, A. Olliver, E. Brambilla, B. Sclavi, M. Cosentino, K.D. Dorfman, Measuring bacterial adaptation dynamics at the single-cell level using a microfluidic chemostat and time-lapse fluorescence microscopy, *Analyst.* 139 (2014) 5254–5262. doi:10.1039/C4AN00877D.
- [83] M. Guilbert, F. Anquez, A. Pruvost, Q. Thommen, E. Courtade, Protein level variability determines phenotypic heterogeneity in proteotoxic stress response, *FEBS J.* (2020). doi:10.1111/febs.15297.
- [84] H. Ryu, M. Chung, M. Dobrzynski, D. Fey, Y. Blum, S.S. Lee, M. Peter, B.N. Kholodenko, N.L. Jeon, O. Pertz, Frequency modulation of ERK activation dynamics rewires cell fate, *Mol. Syst. Biol.* 11 (2015) 1–14. doi:10.15252/msb.20156458.
- [85] M. Putker, J.S.O. Neill, Reciprocal Control of the Circadian Clock and Cellular Redox State - a Critical Appraisal, *Mol. Cells.* 39 (2016) 6–19. doi:10.14348/molcells.2016.2323.
- [86] M. Valko, D. Leibfritz, J. Moncol, M.T.D. Cronin, M. Mazur, J. Telser, Free radicals and antioxidants in normal physiological functions and human disease, *Int. J. Biochem. Cell Biol.* 39 (2007) 44–84. doi:10.1016/j.biocel.2006.07.001.
- [87] R. Vander Velde, N. Yoon, V. Marusyk, A. Durmaz, A. Dhawan, D. Miroshnychenko, D.

- Lozano-peral, B. Desai, O. Balynska, J. Poleszhuk, L. Kenian, M. Teng, M. Abazeed, O. Mian, A.C. Tan, E. Haura, J. Scott, A. Marusyk, Resistance to targeted therapies as a multifactorial, gradual adaptation to inhibitor specific selective pressures, *Nat. Commun.* 11 (2020) 1–13. doi:10.1038/s41467-020-16212-w.
- [88] Sigma-Aldrich, Hydrogen Peroxide 21676, CAS 7722-84-1, (n.d.). <https://www.sigmaaldrich.com/catalog/product/sigald/216763?lang=fr&region=FR>.
- [89] Sigma-Aldrich, Hydrogen Peroxide H1009, CAS 7722-84-1, (n.d.). <https://www.sigmaaldrich.com/catalog/product/sigma/h1009?lang=fr&region=FR>.
- [90] A.R. Giandomenico, G.E. Cerniglia, J.E. Biaglow, C.W. Stevens, C.J. Koch, The importance of sodium pyruvate in assessing damage produced by hydrogen peroxide, *Free Radic. Biol. Med.* 23 (1997) 426–434. doi:10.1016/S0891-5849(97)00113-5.
- [91] H.S. Marinho, L. Cyrne, E. Cadenas, F. Antunes, H<sub>2</sub>O<sub>2</sub> delivery to cells: Steady-state versus bolus addition, *Methods Enzymol.* 526 (2013) 159–173. doi:10.1016/B978-0-12-405883-5.00010-7.
- [92] G. Covas, H.S. Marinho, L. Cyrne, F. Antunes, Activation of Nrf2 by H<sub>2</sub>O<sub>2</sub>: De novo synthesis versus nuclear translocation, *Methods Enzymol.* 528 (2013) 157–171. doi:10.1016/B978-0-12-405881-1.00009-4.
- [93] H. Pichorner, G. Jessner, R. Ebermann, tBOOH Acts as a Suicide Substrate for Catalase, *Arch. Biochem. Biophys.* 300 (1993) 258–264.
- [94] A. Stanoev, A. Mhamane, K.C. Schuermann, H.E. Grecco, W. Stallaert, M. Baumdick, Y. Brüggemann, M.S. Joshi, P. Roda-Navarro, S. Fengler, R. Stockert, L. Roßmannek, J. Luig, A. Koseska, P.I.H. Bastiaens, Interdependence between EGFR and Phosphatases Spatially Established by Vesicular Dynamics Generates a Growth Factor Sensing and Responding Network, *Cell Syst.* 7 (2018) 295-309.e11. doi:10.1016/j.cels.2018.06.006.
- [95] N.M.N. Mishina, P. a Tyurin-Kuzmin, K.N. Markvicheva, A. V Vorotnikov, V. a Tkachuk, V. Laketa, C. Schultz, S. Lukyanov, V. V Belousov, Does cellular hydrogen peroxide diffuse or act locally?, *Antioxid. Redox Signal.* 14 (2011) 1–7. doi:10.1089/ars.2010.3539.
- [96] L. Pollegioni, L. Piubelli, S. Sacchi, M.S. Pilone, G. Molla, Physiological functions of D-amino acid oxidases: From yeast to humans, *Cell. Mol. Life Sci.* 64 (2007) 1373–1394. doi:10.1007/s00018-007-6558-4.
- [97] A. Ishraq, R.E. Haskew-Layton, H. Aleyasin, H. Guo, Rajv R. Ratan, NIH Public Access, *Methods Enzym.* (2014) 251–273. doi:10.1016/B978-0-12-801415-8.00014-X.
- [98] Y.A. Bogdanova, C. Schultz, V. V. Belousov, Local Generation and Imaging of Hydrogen Peroxide in Living Cells, *Curr. Protoc. Chem. Biol.* 9 (2017) 117–127. doi:10.1002/cpch.20.
- [99] C. Mierzwa, R. Rodrigues, A.C.S.C. Teixeira, UV Hydrogen Peroxide Processes, 2018. doi:10.1016/B978-0-12-810499-6.00002-4.

## Bibliography

---

- [100] P.J. Brandhuber, G. Korshin, *Methods for the Detection of Residual Concentrations of Hydrogen Peroxide in Advanced Oxidation Processes*, 2009.
- [101] Sigma, Technical Bulletin. Hydrogen Peroxide Colorimetric Assay CS0270, n.d.
- [102] N. Wang, C.J. Miller, P. Wang, T.D. Waite, Quantitative determination of trace hydrogen peroxide in the presence of sulfide using the Amplex Red / horseradish peroxidase assay, *Anal. Chim. Acta.* 963 (2017) 61–67. doi:10.1016/j.aca.2017.02.033.
- [103] E. Pick, Y. Keisari, A simple colorimetric method for the measurement of hydrogen peroxide produced by cells in culture, *J. Immunol. Methods.* 38 (1980) 161–170. doi:10.1016/0022-1759(80)90340-3.
- [104] E.-F. Grosu, R. Froidevaux, G. Carja, Horseradish peroxidase-AuNP/LDH heterostructures: influence on nanogold release and enzyme activity, *Gold Bull.* (2019). doi:10.1007/s13404-019-00256-y.
- [105] Lumigen, Chemiluminescence, (n.d.). <http://www.lumigen.com/detection-technologies/chemiluminescence/measurement-basics>.
- [106] V.S. Lin, B.C. Dickinson, C.J. Chang, *Boronate-Based Fluorescent Probes: Imaging Hydrogen Peroxide in Living Systems*, 1st ed., Copyright © 2013 Elsevier, Inc. All rights reserved., 2013. doi:10.1016/B978-0-12-405883-5.00002-8.
- [107] L.H. Long, B. Halliwell, Artefacts in cell culture: Pyruvate as a scavenger of hydrogen peroxide generated by ascorbate or epigallocatechin gallate in cell culture media, *Biochem. Biophys. Res. Commun.* 388 (2009) 700–704. doi:10.1016/j.bbrc.2009.08.069.
- [108] Lumigen, Evaluation of Lumigen HyPerBlu technology for high-throughput detection of enzymatically produced hydrogen peroxide, in: 2011. [http://www.lumigen.com/sites/default/files/additional-documents/hyperblu\\_research\\_report.pdf](http://www.lumigen.com/sites/default/files/additional-documents/hyperblu_research_report.pdf) (accessed June 13, 2019).
- [109] D.R. Spitz, W.C. Dewey, G.C. Li, Hydrogen peroxide or heat shock induces resistance to hydrogen peroxide in Chinese hamster fibroblasts, *J. Cell. Physiol.* 131 (1987) 364–373. doi:10.1002/jcp.1041310308.
- [110] H.S. Marinho, L. Cyrne, E. Cadenas, F. Antunes, H<sub>2</sub>O<sub>2</sub> Delivery to Cells: Steady-State Versus Bolus Addition, *Methods Enzymol.* 526 (2013) 159–173. doi:10.1016/b978-0-12-405883-5.00010-7.
- [111] B.M. Kim, Y. Hong, S. Lee, P. Liu, J.H. Lim, Y.H. Lee, T.H. Lee, K.T. Chang, Y. Hong, Therapeutic implications for overcoming radiation resistance in cancer therapy, *Int. J. Mol. Sci.* 16 (2015) 26880–26913. doi:10.3390/ijms161125991.
- [112] T. Bunga, M. Permata, Y. Hagiwara, H. Sato, T. Yasuhara, Base excision repair regulates PD-L1 expression in cancer cells, *Oncogene.* (2019). doi:10.1038/s41388-019-0733-6.
- [113] D.D. Esposti, V.N. Aushev, E. Lee, M.P. Cros, J. Zhu, Z. Herceg, J. Chen, H. Hernandez-Vargas, MiR-500a-5p regulates oxidative stress response genes in breast cancer and predicts cancer survival, *Sci. Rep.* 7 (2017) 1–10. doi:10.1038/s41598-017-16226-3.

- [114] P.K.S. Mahalingaiah, K.P. Singh, Chronic oxidative stress increases growth and tumorigenic potential of MCF-7 breast cancer cells, *PLoS One*. 9 (2014). doi:10.1371/journal.pone.0087371.
- [115] S.-J. Ahn, J.-Y. Bae, R.-A. Lee, W. Han, S.W. Kim, H.-Z. Chae, D.-Y. Noh, Protective Role of Prx (Perodoxin) I and II against H<sub>2</sub>O<sub>2</sub>-Induced Apoptosis of MCF7 Cell Lines, *J Korean Breast Cancer Soc*. 6 (2003) 68–74. doi:10.4048/jkbc.2003.6.2.68.
- [116] S. Alarifi, Assessment of MCF-7 cells as an in vitro model system for evaluation of chemical oxidative stressors, *African J. Biotechnol*. 10 (2011) 3872–3879. doi:10.5897/AJB10.2080.
- [117] S. Weintraub, T. Yarnitzky, S. Kahremany, I. Barrera, O. Viskind, K. Rosenblum, M.Y. Niv, A. Gruzman, Design and synthesis of novel protein kinase R (PKR) inhibitors, *Mol. Divers*. 20 (2016) 805–819. doi:10.1007/s11030-016-9689-4.
- [118] G.P. Kaushal, L. Liu, V. Kaushal, X. Hong, O. Melnyk, R. Seth, R. Safirstein, S. V Shah, Regulation of caspase-3 and -9 activation in oxidant stress to RTE by forkhead transcription factors, Bcl-2 proteins, and MAP kinases, *Am J Physiol Ren. Physiol*. 287 (2004) F1258-68. doi:10.1152/ajprenal.00391.2003.
- [119] S. Chen, Y. Tang, Y. Qian, R. Chen, L. Zhang, L. Wo, H. Chai, Allicin prevents H<sub>2</sub>O<sub>2</sub>-induced apoptosis of HUVECs by inhibiting an oxidative stress pathway, *BMC Complement. Altern. Med*. 14 (2014) 1–8. doi:10.1186/1472-6882-14-321.
- [120] N. Nakamichi, Y. Kambe, H. Oikawa, M. Ogura, K. Takano, K. Tamaki, M. Inoue, E. Hinoi, Y. Yoneda, Protection by exogenous pyruvate through a mechanism related to monocarboxylate transporters against cell death induced by hydrogen peroxide in cultured rat cortical neurons, *J. Neurochem*. 93 (2005) 84–93. doi:10.1111/j.1471-4159.2005.02999.x.
- [121] L.F. Barros, T. Kanaseki, R. Sabirov, S. Morishima, Apoptotic and necrotic blebs in epithelial cells display similar neck diameters but different kinase dependency, *Cell Death Differ*. 10 (2003) 687–697. doi:10.1038/sj.cdd.4401236.
- [122] Q. Chen, M.G. Espey, M.C. Krishna, J.B. Mitchell, C.P. Corpe, G.R. Buettner, E. Shacter, M. Levine, Pharmacologic ascorbic acid concentrations selectively kill cancer cells: Action as a pro-drug to deliver hydrogen peroxide to tissues, *Proc. Natl. Acad. Sci*. 102 (2005) 13604–13609. doi:10.1073/pnas.0506390102.
- [123] R. Gorina, C. Sanfeliu, A. Galitó, À. Messeguer, A.M. Planas, Exposure of glia to pro-oxidant agents revealed selective Stat1 activation by H<sub>2</sub>O<sub>2</sub> and Jak2-independent antioxidant features of the Jak2 inhibitor AG490, *Glia*. 55 (2007) 1313–1324. doi:10.1002/glia.20542.
- [124] A. Joshi, R. Iyengar, J.H. Joo, X.J. Li-Harms, C. Wright, R. Marino, B.J. Winborn, A. Phillips, J. Temirov, S. Sciarretta, R. Kriwacki, J. Peng, A. Shelat, M. Kundu, Nuclear ULK1 promotes cell death in response to oxidative stress through PARP1, *Cell Death Differ*. 23 (2016) 216–230. doi:10.1038/cdd.2015.88.
- [125] A. Kuehne, H. Emmert, R. Lucius, N. Zamboni, A. Kuehne, H. Emmert, J. Soehle, M.

- Winnefeld, F. Fischer, H. Wenck, S. Gallinat, Acute Activation of Oxidative Pentose Phosphate Pathway as First-Line Response to Oxidative Stress in Human Skin Cells Article, *Mol. Cell.* 59 (2015) 359–371. doi:10.1016/j.molcel.2015.06.017.
- [126] V. V. Belousov, A.F. Fradkov, K.A. Lukyanov, D.B. Staroverov, K.S. Shakhbazov, A. V. Terskikh, S. Lukyanov, Genetically encoded fluorescent indicator for intracellular hydrogen peroxide, *Nat. Methods.* 3 (2006) 281–286. doi:10.1038/nmeth866.
- [127] M. Singh, H. Sharma, N. Singh, Hydrogen peroxide induces apoptosis in HeLa cells through mitochondrial pathway, *Mitochondrion.* 7 (2007) 367–373. doi:10.1016/j.mito.2007.07.003.
- [128] C. Dong, L. Zhang, R. Sun, J. Liu, H. Yin, X. Li, X. Zheng, H. Zeng, Role of thioredoxin reductase 1 in dysplastic transformation of human breast epithelial cells triggered by chronic oxidative stress, *Sci. Rep.* 6 (2016) 1–13. doi:10.1038/srep36860.
- [129] F. Hecht, J. Cazarin, C.E. Lima, C.C. Faria, A. Augusto, A.C.F. Ferreira, D.P. Carvalho, R.S. Fortunato, Redox homeostasis of breast cancer lineages contributes to differential cell death response to exogenous hydrogen peroxide, *Life Sci.* 158 (2016) 7–13. doi:10.1016/j.lfs.2016.06.016.
- [130] E. Villa, J.-E. Ricci, How does metabolism affect cell death in cancer?, *FEBS J.* 283 (2016) 2653–2660. doi:10.1111/febs.13570.
- [131] A. King, E. Gottlieb, Glucose metabolism and programmed cell death: an evolutionary and mechanistic perspective, *Curr. Opin.* 21 (2009) 885–893. doi:10.1016/j.ceb.2009.09.009.
- [132] M.J. Mitchell, M.R. King, Computational and Experimental Models of Cancer Cell Response to Fluid Shear Stress, *Front. Oncol.* 3 (2013) 1–11. doi:10.3389/fonc.2013.00044.
- [133] K.A. Gelmon, J. Mackey, S. Verma, Z. Stan, N. Bangemann, P. Klimo, A. Schneeweiss, K. Bremer, D. Soulieres, K. Tonkin, R. Bell, B. Heinrich, D. Grenier, R. Dias, Use of Trastuzumab Beyond Disease Progression : Observations from a Retrospective Review of Case Histories, *Clin. Breast Cancer.* 5 (2004) 52–58. doi:10.3816/CBC.2004.n.010.
- [134] A.J. Genuino, U. Chaikledkaew, D.O. The, T. Reungwetwattana, A. Thakkinstian, Adjuvant trastuzumab regimen for HER2-positive early-stage breast cancer : a systematic review and meta-analysis, *Expert Rev. Clin. Pharmacol.* 12 (2019) 815–824. doi:10.1080/17512433.2019.1637252.
- [135] C. Zhu, W. Hu, H. Wu, X. Hu, No evident dose-response relationship between cellular ROS level and its cytotoxicity - A paradoxical issue in ROS-based cancer therapy, *Sci. Rep.* 4 (2014) 1–10. doi:10.1038/srep05029.
- [136] J. Egea, I. Fabregat, Y.M. Frapart, P. Ghezzi, A. Görlach, T. Kietzmann, K. Kubaichuk, U.G. Knaus, M.G. Lopez, G. Olaso-Gonzalez, A. Petry, R. Schulz, J. Vina, P. Winyard, K. Abbas, O.S. Ademowo, C.B. Afonso, I. Andreadou, H. Antelmann, F. Antunes, M. Aslan, M.M. Bachschmid, R.M. Barbosa, V. Belousov, C. Berndt, D. Bernlohr, E. Bertrán, A. Bindoli, S.P. Bottari, P.M. Brito, G. Carrara, A.I. Casas, A. Chatzi, N.

- Chondrogianni, M. Conrad, M.S. Cooke, J.G. Costa, A. Cuadrado, P. My-Chan Dang, B. De Smet, B. Debelec-Butuner, I.H.K. Dias, J.D. Dunn, A.J. Edson, M. El Assar, J. El-Benna, P. Ferdinandy, A.S. Fernandes, K.E. Fladmark, U. Förstermann, R. Giniatullin, Z. Giricz, A. Görbe, H. Griffiths, V. Hampl, A. Hanf, J. Herget, P. Hernansanz-Agustín, M. Hillion, J. Huang, S. Ilikay, P. Jansen-Dürr, V. Jaquet, J.A. Joles, B. Kalyanaraman, D. Kaminsky, M. Karbaschi, M. Kleanthous, L.O. Klotz, B. Korac, K.S. Korkmaz, R. Koziel, D. Kračun, K.H. Krause, V. Křen, T. Krieg, J. Laranjinha, A. Lazou, H. Li, A. Martínez-Ruiz, R. Matsui, G.J. McBean, S.P. Meredith, J. Messens, V. Miguel, Y. Mikhed, I. Milisav, L. Milković, A. Miranda-Vizueté, M. Mojović, M. Monsalve, P.A. Mouthuy, J. Mulvey, T. Münzel, V. Muzykantov, I.T.N. Nguyen, M. Oelze, N.G. Oliveira, C.M. Palmeira, N. Papaevgeniou, A. Pavićević, B. Pedre, F. Peyrot, M. Phylactides, G.G. Pircalabioru, A.R. Pitt, H.E. Poulsen, I. Prieto, M.P. Rigobello, N. Robledinos-Antón, L. Rodríguez-Mañas, A.P. Rolo, F. Rousset, T. Ruskovska, N. Saraiva, S. Sasson, K. Schröder, K. Semen, T. Seredenina, A. Shakirzyanova, G.L. Smith, T. Soldati, B.C. Sousa, C.M. Spickett, A. Stancic, M.J. Stasia, H. Steinbrenner, V. Stepanić, S. Steven, K. Tokatlidis, E. Tuncay, B. Turan, F. Ursini, J. Vacek, O. Vajnerova, K. Valentová, F. Van Breusegem, L. Varisli, E.A. Veal, A.S. Yalçın, O. Yelisyeyeva, N. Žarković, M. Zatloukalová, J. Zielonka, R.M. Touyz, A. Papapetropoulos, T. Grune, S. Lamas, H.H.H.W. Schmidt, F. Di Lisa, A. Daiber, European contribution to the study of ROS: A summary of the findings and prospects for the future from the COST action BM1203 (EU-ROS), *Redox Biol.* 13 (2017) 94–162. doi:10.1016/j.redox.2017.05.007.
- [137] D. Christodoulou, A. Kuehne, A. Estermann, T. Fuhrer, P. Lang, Reserve Flux Capacity in the Pentose Phosphate Pathway by NADPH Binding Is Conserved across Kingdoms Reserve Flux Capacity in the Pentose Phosphate Pathway by NADPH Binding Is Conserved across Kingdoms, *IScience.* 19 (2019) 1133–1144. doi:10.1016/j.isci.2019.08.047.
- [138] E. Panieri, M.M. Santoro, ROS homeostasis and metabolism: a dangerous liason in cancer cells, *Cell Death Dis.* 7 (2016) e2253. doi:10.1038/cddis.2016.105.
- [139] H. Sies, D.P. Jones, Reactive oxygen species (ROS) as pleiotropic physiological signalling agents, *Nat. Rev. Mol. Cell Biol.* 21 (2020) 363–383. doi:10.1038/s41580-020-0230-3.
- [140] C. Lennicke, J. Rahn, R. Lichtenfels, L.A. Wessjohann, B. Seliger, Hydrogen peroxide – production , fate and role in redox signaling of tumor cells, *Cell Commun. Signal.* 13 (2015) 1–19. doi:10.1186/s12964-015-0118-6.
- [141] D. Christodoulou, H. Link, T. Fuhrer, K. Kochanowski, L. Gerosa, U. Sauer, Reserve Flux Capacity in the Pentose Phosphate Pathway Enables Escherichia coli’s Rapid Response to Oxidative Stress, *Cell Syst.* 6 (2018) 569-578.e7. doi:10.1016/j.cels.2018.04.009.
- [142] S. Neumann, N. Vladimirov, A.K. Krembel, N.S. Wingreen, V. Sourjik, Imprecision of Adaptation in Escherichia coli Chemotaxis, *PLoS One.* 9 (2014) 1–6. doi:10.1371/journal.pone.0084904.
- [143] A. Llamosi, A.M. Gonzalez-Vargas, C. Versari, E. Cinquemani, G. Ferrari-Trecate, P. Hersen, G. Batt, What Population Reveals about Individual Cell Identity: Single-Cell Parameter Estimation of Models of Gene Expression in Yeast, *PLoS Comput. Biol.* 12 (2016) 1–18. doi:10.1371/journal.pcbi.1004706.

- [144] E. Malucelli, A. Procopio, M. Fratini, A. Gianoncelli, A. Notargiacomo, L. Merolle, A. Sargenti, S. Castiglioni, C. Cappadone, G. Farruggia, M. Lombardo, S. Lagomarsino, J.A. Maier, S. Iotti, Single cell versus large population analysis: cell variability in elemental intracellular concentration and distribution, *Anal. Bioanal. Chem.* 410 (2018) 337–348. doi:10.1007/s00216-017-0725-8.
- [145] N.M. Mishina, K.N. Markvicheva, D.S. Bilan, M.E. Matlashov, M. V. Shirmanova, D. Liebl, C. Schultz, S. Lukyanov, V. V. Belousov, Visualization of intracellular hydrogen peroxide with HyPer, a genetically encoded fluorescent probe, in: *Methods Enzymol.*, 1st ed., Copyright © 2013 Elsevier, Inc. All rights reserved., 2013: pp. 45–59. doi:10.1016/B978-0-12-405883-5.00003-X.
- [146] O. Shimomura, F.H. Johnson, Y.O. Saiga, Extraction, Purification and Properties of Aequorin, a Bioluminescent Protein from the Luminous Hydromedusan, *Aequorea*, *J. Cell. Comp. Physiol.* 59 (1962) 223–239. doi:10.1002/jcp.1030590302.
- [147] K.A. Lukyanov, V. V. Belousov, Genetically encoded fluorescent redox sensors, *Biochim. Biophys. Acta - Gen. Subj.* 1840 (2014) 745–756. doi:10.1016/j.bbagen.2013.05.030.
- [148] V. V. Belousov, A.F. Fradkov, K.A. Lukyanov, D.B. Staroverov, K.S. Shakhbazov, A. V. Terskikh, S. Lukyanov, Genetically encoded fluorescent indicator for intracellular hydrogen peroxide, *Nat. Methods.* 3 (2006) 281–286. doi:10.1038/nmeth866.
- [149] Y.A. Bogdanova, C. Schultz, V. V. Belousov, Local Generation and Imaging of Hydrogen Peroxide in Living Cells, *Curr. Protoc. Chem. Biol.* 9 (2017) 117–127. doi:10.1002/cpch.20.
- [150] K.A. Lukyanov, V. V. Belousov, Genetically encoded fluorescent redox sensors, *Biochim. Biophys. Acta.* 1840 (2014) 745–756. doi:10.1016/J.BBAGEN.2013.05.030.
- [151] D.S. Bilan, L. Pase, L. Joosen, A.Y. Gorokhovatsky, Y.G. Ermakova, T.W.J. Gadella, C. Grabher, C. Schultz, S. Lukyanov, V. V. Belousov, HyPer-3: A genetically encoded H<sub>2</sub>O<sub>2</sub> probe with improved performance for ratiometric and fluorescence lifetime imaging, *ACS Chem. Biol.* 8 (2013) 535–542. doi:10.1021/cb300625g.
- [152] Y.G. Ermakova, D.S. Bilan, M.E. Matlashov, N.M. Mishina, K.N. Markvicheva, O.M. Subach, F. V. Subach, I. Bogeski, M. Hoth, G. Enikolopov, V. V. Belousov, Red fluorescent genetically encoded indicator for intracellular hydrogen peroxide, *Nat. Commun.* 5 (2014) 1–9. doi:10.1038/ncomms6222.
- [153] K. Huang, J. Caplan, J.A. Sweigard, K.J. Czymmek, N.M. Donofrio, Optimization of the HyPer sensor for robust real-time detection of hydrogen peroxide in the rice blast fungus, *Mol. Plant Pathol.* 18 (2017) 298–307. doi:10.1111/mpp.12392.
- [154] B.K. Huang, S. Ali, K.T. Stein, H.D. Sikes, Interpreting Heterogeneity in Response of Cells Expressing a Fluorescent Hydrogen Peroxide Biosensor, *Biophys. J.* 109 (2015) 2148–2158. doi:10.1016/j.bpj.2015.08.053.
- [155] D. Poburko, J. Santo-domingo, N. Demarex, Dynamic Regulation of the Mitochondrial Proton Gradient during Cytosolic Calcium Elevations, *J. Biol. Chemistry.* 286 (2011) 11672–11684. doi:10.1074/jbc.M110.159962.

- [156] M.A. Keller, A. Zylstra, C. Castro, A. V Turchyn, J.L. Griffin, M. Ralser, Conditional iron and pH-dependent activity of a non-enzymatic glycolysis and pentose phosphate pathway, (2016).
- [157] S.K. Parks, J. Chiche, J. Pouysségur, Disrupting proton dynamics and energy metabolism for cancer therapy, *Nat. Publ. Gr.* 13 (2013) 611–623. doi:10.1038/nrc3579.
- [158] P. Swietach, What is pH regulation , and why do cancer cells need it ?, (2019) 5–15.
- [159] A.H. Lee, I.F. Tannock, Heterogeneity of Intracellular pH and of Mechanisms That Regulate Intracellular pH in Populations of Cultured Cells, *Cancer Res.* 58 (1998) 1901–1908.
- [160] D.S. Bilan, V. V Belousov, HyPer Family Probes : State of the Art, *Antioxid. Redox Signal.* 24 (2016) 731–751. doi:10.1089/ars.2015.6586.
- [161] R. V Benjaminsen, H. Sun, J.R. Henriksen, N.M. Christensen, K. Almdal, T.L. Andresen, Evaluating Nanoparticle Sensor Design for Intracellular pH Measurements, *ACS Nano.* 5 (2011) 5864–5873. doi:10.1021/nm201643f.
- [162] L.P. Roma, J. Duprez, H.K. Takahashi, P. Gilon, A. Wiederkehr, J.-C. Jonas, Dynamic measurements of mitochondrial hydrogen peroxide concentration and glutathione redox state in rat pancreatic  $\beta$  -cells using ratiometric fluorescent proteins : confounding effects of pH with HyPer but not roGFP1, *Biochem. J.* 441 (2012) 971–978. doi:10.1042/BJ20111770.
- [163] A.J. Meyer, T.P. Dick, Fluorescent protein-based redox probes, *Antioxidants Redox Signal.* 13 (2010) 621–650. doi:10.1089/ars.2009.2948.
- [164] A.J. Meyer, T.P. Dick, Fluorescent Protein-Based Redox Probes, *Antioxid. Redox Signal.* 13 (2010) 621–650. doi:10.1089/ars.2009.2948.
- [165] G.H. Patterson, S.M. Knobel, O. Thastrup, D.W. Piston, Separation of the glucose-stimulated cytoplasmic and mitochondrial NAD(P)H responses in pancreatic islet cells, *PNAS.* 97 (2000) 5203–5207. doi:10.1073/pnas.090098797.
- [166] T.S. Blacker, Z.F. Mann, J.E. Gale, M. Ziegler, A.J. Bain, G. Szabadkai, M.R. Duchon, Separating NADH and NADPH fluorescence in live cells and tissues using FLIM, *Nat. Commun.* 5 (2014) 1–9. doi:10.1038/ncomms4936.
- [167] P. Swietach, R.D. Vaughan-jones, A.L. Harris, A. Hulikova, The chemistry , physiology and pathology of pH in cancer, *Phylosophical Trans. R. Soc. B.* 369 (2014) 1–9. doi:10.1098/rstb.2013.0099.
- [168] S.M. Jeon, N.S. Chandel, N. Hay, AMPK regulates NADPH homeostasis to promote tumour cell survival during energy stress, *Nature.* 485 (2012) 661–665. doi:10.1038/nature11066.
- [169] S.H. Almagadam, A. Trentini, M. Maritati, C. Contini, G. Rugna, T. Bellini, M.C. Manfrinato, F. Dallochio, S. Hanau, Influence of 6-aminonicotinamide (6AN) on *Leishmania* promastigotes evaluated by metabolomics: Beyond the pentose phosphate

- pathway, *Chem. Biol. Interact.* 294 (2018) 167–177. doi:10.1016/j.cbi.2018.08.014.
- [170] D. Peralta, A.K. Bronowska, B. Morgan, É. Dóka, K. Van Laer, P. Nagy, F. Gräter, T.P. Dick, A proton relay enhances H<sub>2</sub>O<sub>2</sub> sensitivity of GAPDH to facilitate metabolic adaptation, *Nat. Chem. Biol.* 11 (2015) 156–163. doi:10.1038/nchembio.1720.
- [171] F. Ursini, M. Maiorino, H.J. Forman, Redox homeostasis: The Golden Mean of healthy living, *Redox Biol.* 8 (2016) 205–215. doi:10.1016/j.redox.2016.01.010.
- [172] Y. Goulev, S. Morlot, A. Matifas, B. Huang, M. Molin, M.B. Toledano, G. Charvin, Nonlinear feedback drives homeostatic plasticity in H<sub>2</sub>O<sub>2</sub> stress response, *Elife.* 6 (2017) 1–33. doi:10.7554/eLife.23971.
- [173] P.I. Nikel, T. Fuhrer, M. Chavarría, A. Sánchez-Pascuala, U. Sauer, V. de Lorenzo, Redox stress reshapes carbon fluxes of *Pseudomonas putida* for cytosolic glucose oxidation and NADPH generation, *BioRxiv.* (2020) 1–31. doi:10.1101/2020.06.13.149542.
- [174] F.J. Cejudo, V. Ojeda, V. Delgado-Requerey, M. González, J.M. Pérez-Ruiz, Chloroplast Redox Regulatory Mechanisms in Plant Adaptation to Light and Darkness, *Front. Plant Sci.* 10 (2019) 1–11. doi:10.3389/fpls.2019.00380.
- [175] J.D. Hayes, A.T. Dinkova-Kostova, K.D. Tew, Oxidative Stress in Cancer, *Cancer Cell.* 2 (2020) 1–31. doi:10.1016/j.ccell.2020.06.001 ll.
- [176] Ibidi, sticky-Slide I Luer | Self-Adhesive Underside | ibidi, (n.d.). <https://ibidi.com/sticky-slides/63-sticky-slide-i-luer.html> (accessed June 21, 2019).
- [177] D.R. Green, L. Galluzzi, G. Kroemer, Metabolic control of cell death, *Science* (80-. ). 345 (2014) 1–24. doi:10.1126/science.1250256.
- [178] L. Wang, Z. Shang, Y. Zhou, X. Hu, Y. Chen, Y. Fan, X. Wei, L. Wu, Q. Liang, J. Zhang, Z. Gao, Autophagy mediates glucose starvation-induced glioblastoma cell quiescence and chemoresistance through coordinating cell metabolism, cell cycle, and survival, *Cell Death Dis.* 9 (2018) 1–17. doi:10.1038/s41419-017-0242-x.
- [179] L. Mele, F. Paino, F. Papaccio, T. Regad, D. Boocock, P. Stiuso, A. Lombardi, D. Liccardo, G. Aquino, A. Barbieri, C. Arra, C. Coveney, M. La Noce, G. Papaccio, M. Caraglia, V. Tirino, V. Desiderio, A new inhibitor of glucose-6-phosphate dehydrogenase blocks pentose phosphate pathway and suppresses malignant proliferation and metastasis in vivo, *Cell Death Dis.* 9 (2018) 1–12. doi:10.1038/s41419-018-0635-5.
- [180] S.L. Goldman, M. Mackay, E. Afshinnekoo, A.M. Melnick, S. Wu, C.E. Mason, The Impact of Heterogeneity on Single-Cell Sequencing, *Front. Genet.* 10 (2019) 1–8. doi:10.3389/fgene.2019.00008.
- [181] S. Chakrabarti, A.L. Paek, J. Reyes, K.A. Lasick, G. Lahav, F. Michor, Hidden heterogeneity and circadian-controlled cell fate inferred from single cell lineages, *Nat. Commun.* 9 (2018) 1–13. doi:10.1038/s41467-018-07788-5.
- [182] A.P. Drabovich, M.P. Pavlou, A. Dimitromanolakis, E.P. Diamandis, Quantitative Analysis of Energy Metabolic Pathways in MCF-7 Breast Cancer Cells by Selected

## Bibliography

---

- Reaction Monitoring Assay, *Mol. Ans Cell. Proteomics*. 11 (2012) 422–434. doi:10.1074/mcp.M111.015214.
- [183] B. Csóka, G. Nagy, Determination of diffusion coefficient in gel and in aqueous solutions using scanning electrochemical microscopy, *J. Biochem. Biophys. Methods*. 61 (2004) 57–67. doi:10.1016/j.jbbm.2004.03.001.
- [184] P.O. Gendron, F. Avaltroni, K.J. Wilkinson, Diffusion coefficients of several rhodamine derivatives as determined by pulsed field gradient-nuclear magnetic resonance and fluorescence correlation spectroscopy, *J. Fluoresc.* 18 (2008) 1093–1101. doi:10.1007/s10895-008-0357-7.